MOLECULAR PATHOGENESIS OF T LYMPHOBLASTIC LYMPHOMAS IN AN ATM-DEFICIENT MOUSE MODEL

by

Peggy Pui Chi Wong

A thesis submitted in conformity with the requirements

for the degree of Doctor of Philosophy

Graduate Department of Medical Biophysics

University of Toronto

Molecular Pathogenesis of T Lymphoblastic Lymphomas in an ATM-deficient Mouse Model

Peggy Pui Chi Wong
Doctor of Philosophy
Department of Medical Biophysics
2013

GENERAL ABSTRACT

T lymphoblastic lymphoma/leukemia (T-LL) represent malignant disease of T-cell progenitors. Dysregulation of Notch1 and IL-7R pathways promotes T-LL, however the timing of these events remains unclear. Furthermore, the spectrum of *Notch1* mutations has not been fully characterized in T-LL models. Chapter 2 demonstrated 3 T-LLs classified based on activated Notch1 (ICN1) expression that arose spontaneously in mice lacking ataxia telangiectasia mutated (ATM) protein. One group expressed truncated forms of ICN1 (T-ICN1) resulting from frame-shifting PEST mutations. T-LL cells but not normal thymocytes expressed a proteoglycan, syndecan 1 (SDC1). $SDC1^+$ blasts were detected in thymi with normal cellularity from clinically healthy mice, thus representing the earliest discernible stage of T-LL progression. T-ICN1 and IL-7Rα were both aberrantly expressed at this early T-LL stage. Therefore, these data suggest that *Notch1* mutations, aberrant expression of IL-7Rα and SDC1 arise early during T-LL progression. Chapter 3 demonstrated a paucity of HD mutations, yet T-LL cells proliferated in a Notch ligand-independent fashion. Analysis of $ICN1^+$ T-LLs revealed truncated *Notch1* mRNAs lacking ligand-binding domain and part of negative regulatory region. All truncated transcripts contained the intramembranous methionine that has previously been shown to serve as the translational start site. Collectively, our data identify truncated *Notch1* mRNAs in T-LLs

that likely encode for polypeptides undergoing ligand-independent activation. The third group lacked ICN1 expression (UD-ICN1). Chapter 4 revealed that UD-ICN1 T-LLs expressed low levels of Notch targets and proliferated independently of Notch signal. Gene set enrichment analyses of genes differentially expressed between UD-ICN1 and T-ICN1 T-LLs revealed higher levels of transcription factor *krüppel-like factor 9* (*Klf9*) and other transcriptional regulators associated with the highly proliferative pre-DP stage of normal T-cell development. siRNA knockdown experiments demonstrated that *Klf9* promoted proliferation of UD-ICN1 T-LL cells. Although further studies are warranted, the findings in this thesis reveal oncogenic activation of Notch1 as an early event in $Atm^{-/-}$ T-LL progression, and truncated *Notch1* transcripts likely represent a novel mode of ligand-independent Notch1 activation. On the other hand, *Klf9* promotes proliferation of Notch-independent T-LLs and may represent a potential therapeutic target for this T-LL group.

ACKNOWLEDGEMENTS

Somewhere ages and ages hence:
Two roads diverged in a wood, and I,
I took the one less traveled by,
And that has made all the difference.

-Robert Frost

I had the good fortune of interacting with a number of people who have made my Ph.D. training an enriching experience. I am grateful to my supervisors, Dr. Jayne Danska and Dr. Cynthia Guidos for their advice, guidance and support. A giant dose of thanks to my supervisory committee members Dr. Jane McGlade and Dr. Dwayne Barber for their generosity with time and ideas. My sincere gratitude to members of my examination committee for their time and insightful comments: Dr. Andrew Weng, Dr. Sean Egan, Dr. Mark Minden and Dr. Jack Greenblatt.

I am indebted to my mentors Dr. Amira Klip, Dr. Hans Hitzler, Dr. Meredith Irwin, Dr. David Malkin and Dr. Victor Blanchette for their wise counsel and faith in me. Their doors are always open and they never hesitate to give me a boost over brick walls. I greatly appreciate the advice and support of my Canadian Child Health Clinician-Scientist Program mentors Dr. Thierry Lacaze and Dr. Sylvain Chemtob.

My thesis would not be complete without extensive bioinformatic and statistical support. I would like to thank Dr. Daniele Merico for his bioinformatic expertise and Ms. Vicki Ling and Dr. Shaheena Bashir for their statistical analyses and teaching. I am grateful to Dr. Bertrand Montpellier, Dr. Irina Matei, Dr. Paul Kowalski, Mr. Greg Chang, Ms. Queenie Cheung, Mr. Stevan Lauriault, Mr. Goce Bogdanoski, Ms. Ildiko Grandal and the late Janet Ellis for their experimental input and scientific discussion.

I have learned a lot from my fellow students and post-docs including Ms. Tatiana Perova, Ms. Sujeetha Rajakumar, Dr. Claudia Pfrommer, Dr. Jes Adams, Ms. Eniko Papp, Dr. Sara Suliman, Dr. Radia Johnson and Mr. Alan Kraguljac.

I would also like to thank Ms. Alexandra Ho, Ms. Naomi Strobach, Ms. Chau Dang and Ms. Merle Casci for their administrative support.

I thank the Terry Fox Foundation, National Cancer Institute of Canada, Canadian Child Health and Clinician Scientist Program, the Division of Hematology/Oncology at the Hospital for Sick Children and the Christopher Brundage Leukemia Research Endowment Fund for their financial support.

I have been fortunate to become close friends to Dr. Philaretos Kousis, Dr. Aleksandra (Ola) Kowalczyk, soon-to-be Dr. Andrea Wong and Dr. Ioana Visan. Their determination to

pursue science as a career is inspirational to me. Phil has also been my running buddy and together we have trained for numerous running events including half and full marathons. I greatly appreciate his encouragement and support both on and off the running course. I have known Ola through Phil and she is as close to a "Dutch Uncle" as one can get. I can always count on her for her honest feedback.

I have definitely won the "parent lottery," if I may borrow the phrase from the late Randy Pausch. My parents moved halfway across the world to make sure that my brother and I have the best opportunities to achieve our dreams. They have taught me the importance of integrity, hard work, perseverance, loyalty and positive thinking. Mom and Dad, thank you for your love and guidance. My brother is a testament that "brick walls are there for a reason. They give us a chance to show how badly we want something." He has turned his disability into a source of inspiration for his research. Anyone who can turn an adversity into a positive life experience is a hero in my book.

TABLE OF CONTENTS

LIST OF FIGURES

Chapter 1: Introduction

Chapter 2: Aberrant Notch1 activation occurs early in *Atm*$^{-/-}$ T lymphoblastic lymphoma transformation

Chapter 3: Identification of truncated *Notch1* transcripts in Notch-dependent *Atm*$^{-/-}$ T-LLs

Chapter 4: Krüppel-like factor 9, *Klf9*, promotes proliferation of Notch-independent T lymphoblastic lymphomas

LIST OF TABLES

LIST OF ABBREVIATIONS

ADAM	a disintegrin and metalloproteinase
ANK	ankyrin repeats
APC	allophycocyanin
AT	ataxia telangiectasia
Atm	ataxia telangiectasia mutated
BTD	b-trefoil domain
CIP	calf intestine alkaline phosphatase
CS	calf serum
CSL	CBF1/Su(H)/Lag-1
CTD	C-terminal domain
DL	delta-like
DN	CD4/CD8 double negative
DOS	Delta and OSM-11-like
DP	CD4/CD8 double positive
DSL	Delta, Serrate, Lag2
Dtx	Deltex
EGF	epidermal growth factor
ETP	early T-cell-lineage progenitor
Fbw7	F-box and WD repeat domain-containing 7
FITC	fluorescein isothiocyanate
GSI	γ-secretase inhibitor
HD	heterodimerization domain
ICN	intracellular Notch
IL	interleukin
ISP	CD8 immature single positive
Jag	Jagged
JME	juxtamembrane expansion
kD	kilo-Dalton
Klf	krüppel-like factor
Lfng	Lunatic fringe
LNR	lin12-Notch repeat
MAML	mastermind-like
Mfng	Manic fringe
MHC	mature histocompatibility complex
Mib	Mindbomb
MINT	Msx2-interacting nuclear target
Nct	nicastrin
NEC	extracellular domain of Notch
Neur	Neuralized
NEXT	Notch extracellular truncation
NLS	nuclear localization sequence
Nrarp	Notch-regulated ankyrin repeat protein
NRR	negative regulatory region

NT	non-truncated
NTD	N-terminal domain
NTM	transmembrane domain of Notch
ORF	open reading frame
PCR	polymerase chain reaction
PE	phycoerythrin
PEST	region rich in proline, glutamic acid, serine and threonine
PI-3K	phosphotidylinositol-3-kinase
Psen	Presenilin
PTEN	phosphatase and tensin homolog
PVDF	polyvinylidene difluoride
RACE	rapid amplification of cDNA ends
RAM	RBP-Jk association module
RBPJ	recombination signal binding protein for immunoglobulin kappa J region
Rfng	Radical fringe
RSS	recombination signal sequence
SDC	syndecan
SDS-PAGE	sodium dodecyl sulfate polyacrylamide gel electrophoresis
shRNA	small hairpin RNA
siRNA	small interfering RNA
SM	staining media
SP	single positive
T	truncated
TACE	TNFα converting enzyme
TAD	transcriptional activation domain
TAP	tobacco acid pyrophosphatase
TCR	T-cell receptor
T-LL	T lymphoblastic leukemia and lymphoma
TMD	transmembrane domain
UD	undetectable
WT	wildtype

Chapter 1:

INTRODUCTION

1. INTRODUCTION

T lymphoblastic leukemia and lymphoma (T-LL) represent a malignancy of the immature T precursors that affects adults and children. T-LL often manifests clinically with a mediastinal mass causing respiratory and cardiovascular distress, low blood counts and fever[1]. Current therapy includes intensive, multi-agent chemotherapy with or without cranial or mediastinal irradiation. The five-year event-free survival rates are 70-90% and 50-60% for children and adults, respectively[2,3]. Relapses in the central nervous system, bone marrow and mediastinum are frequent causes of treatment failure[1,4]. Moreover, treatment-related toxicity can cause significant long-term morbidity or death. Further improvement in clinical outcome is hampered by a lack of prognostic markers that can be used to stratify treatment intensity according to risk of relapse, as well as a lack of molecular targets for design of safe therapy. These barriers can only be overcome by a more comprehensive understanding of T-LL pathogenesis.

T-LL arises as a result of accumulation of genetic hits that cause T-cell differentiation arrest, as well as enhanced survival and proliferation by co-opting developmental pathways. One such pathway is Notch signaling, whose activation relies on interaction with Notch ligands, and plays an instructive role in launching the T-cell maturation program[5]. Gain-of-function *NOTCH1* mutations occur in 60% of human and animal models of T-LL, which are frequently associated with Notch-dependence for survival and proliferation[6-10]. In contrast, less is known about the remaining 40% of T-LL cases harboring wildtype *NOTCH1* that include a subgroup of Notch-independent T-LL. This thesis aimed to gain molecular insights into Notch-dependent and -independent T-LL, thereby identifying potential molecular targets for T-LL treatment.

1.1 T-cell Development

1.1.1 Overview of αβ T-cell development

Mammalian T-cell development begins when multipotent hematopoietic progenitors migrate from the bone marrow or fetal liver to the thymus. The thymus provides an essential micro-environment to induce and sustain T-cell differentiation, which necessitates progenitors to gain T-cell specific functions (referred to as specification), while gradually losing alternative lineage potential in a process called T-lineage commitment[5]. Both processes progress over distinct phenotypic stages characterized by different surface markers (Fig. 1.1). The most immature cells can be divided into four CD4/CD8 double negative (DN1-4) phases according to their cell surface expression of CD117 (c-Kit) and CD25. Development from the early T-cell-lineage progenitor (ETP or DN1) stage to the DN3 stage occurs independently of T-cell receptor (TCR) signaling. ETP and DN2 cells proliferate extensively until reaching DN3 stage, when proliferation ceases and rearrangement at the TCRβ locus occurs. Only thymocytes that successfully rearrange the *TCRβ* gene are allowed to proceed beyond DN3 stage via a process known as β-selection[11]. The nascent TCRβ chain pairs with an invariant pre-TCRα (pTα) protein and CD3 proteins to form a pre-TCR complex. Pre-TCR signals cell-autonomously to induce the β-selected DN3 cells to survive, proliferate and differentiate into CD8 immature single positive (ISP), then CD4/CD8 double positive (DP) thymocytes[12]. DP thymocytes exit the cell cycle and rearrange *TCRα* gene segments. Expression of cell surface TCRαβ heterodimers is required to allow MHC-mediated positive selection. Less than 5% of DPs survive this selection process to mature as single positive (SP) CD4 or CD8 T cells and exit the thymus to form

the peripheral T cell repertoire[13,14]. During early T-cell development, Notch signaling is essential in orchestrating the T-cell-lineage specification, commitment and proliferation of early thymic precursors[15]. In the subsequent sections, I review Notch signaling (section 1.1.2) and then examine its role in T-lineage commitment (section 1.1.3), and β-selection (section 1.1.4).

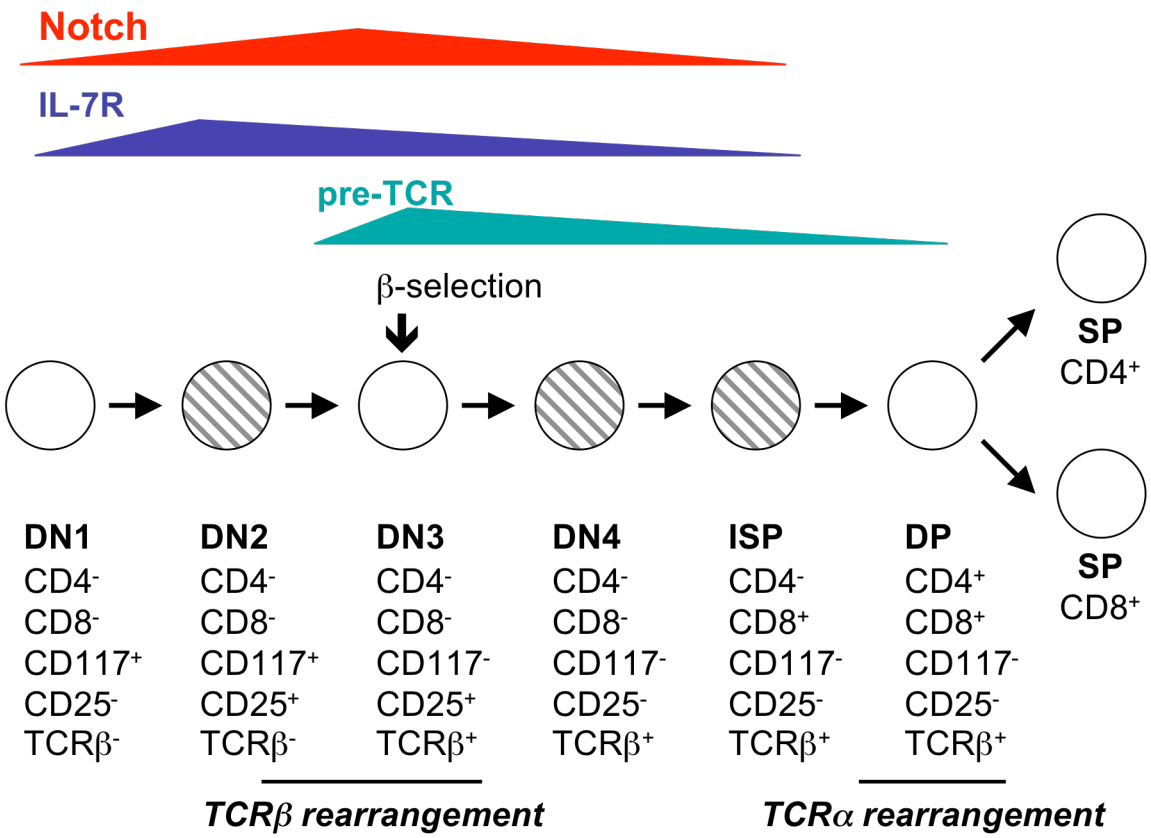

Figure 1.1 Overview of murine thymocyte development. Hematopoietic progenitors seed the thymus and intrathymic differentiation proceeds sequentially through CD4/CD8 double-negative (DN), immature single positive (ISP), CD4/CD8 double-positive (DP) and CD4 or CD8 single-positive (SP) stages. The DN cells are subdivided based on their cell surface expression of CD117 (c-Kit) and CD25: DN1, $CD117^{+}CD25^{-}$; DN2, $CD117^{+}CD25^{+}$; DN3, $CD117^{-}CD25^{+}$; DN4, $CD117^{-}CD25^{-}$. β-selection occurs at DN3 stage and only cells that express a productively rearranged TCRβ chain on their cell surface proceed to DN4 and proliferate extensively. Notch signaling is essential for T-cell fate commitment and efficient β selection during DN to DP transition. The IL-7 receptor signaling ensures survival and expansion of DN2 cells. The pre-TCR complex signals cell-autonomously and mediates survival, proliferation and differentiation of β-selected cells. Hatched circles indicate cellular expansion.

1.1.2 Notch signaling

In 1917, Thomas H. Morgan first reported the 'notch' mutant phenotype in fruit flies characterized by serration of the distal wing[16]. Almost seventy years later, a partial loss-of-function mutation in the *Drosophila Notch* gene was identified as the cause of the mutant phenotype[17,18]. Soon after, human and mouse homologs of *Drosophila Notch*[19,20] were identified. Notably, a translocation involving the human *NOTCH1* gene was implicated in T-cell acute lymphoblastic leukemia[21]. This puts Notch on the map for those studying malignant and normal T-cell biology.

The Notch receptor is a single-pass transmembrane protein that is cleaved by furin convertase at site S_1 soon after its synthesis [22,23], giving rise to a heterodimeric receptor–comprised of extracellular (N^{EC}) and transmembrane (N^{TM}) domains–at the cell surface. Binding of ligand to N^{EC} displaces the Lin12-Notch repeats (LNR) from an S_2 cleavage site located in the extracellular portion of N^{TM}, allowing for proteolysis by ADAM metalloprotease[24] (Fig. 1.2). The resulting membrane-tethered truncated receptor, called NEXT (Notch extracellular truncation), is cleaved at an intramembranous S_3 site by γ-secretase complex, which releases Notch intracellular region (ICN) to the cytosol. ICN then enters the nucleus and recruits transcription co-activators such as Mastermind-like protein (MAML) to a DNA-binding transcription factor CSL (CBF1/Su(H)/Lag-1), thus activating target gene transcription. Notch signaling therefore requires 3 events: 1) interaction between Notch ligand and receptor; 2) receptor activation; and 3) assembly of a transcription activation complex. I will first introduce the different elements of the Notch pathway and then review the 3 steps involved in Notch signal transduction.

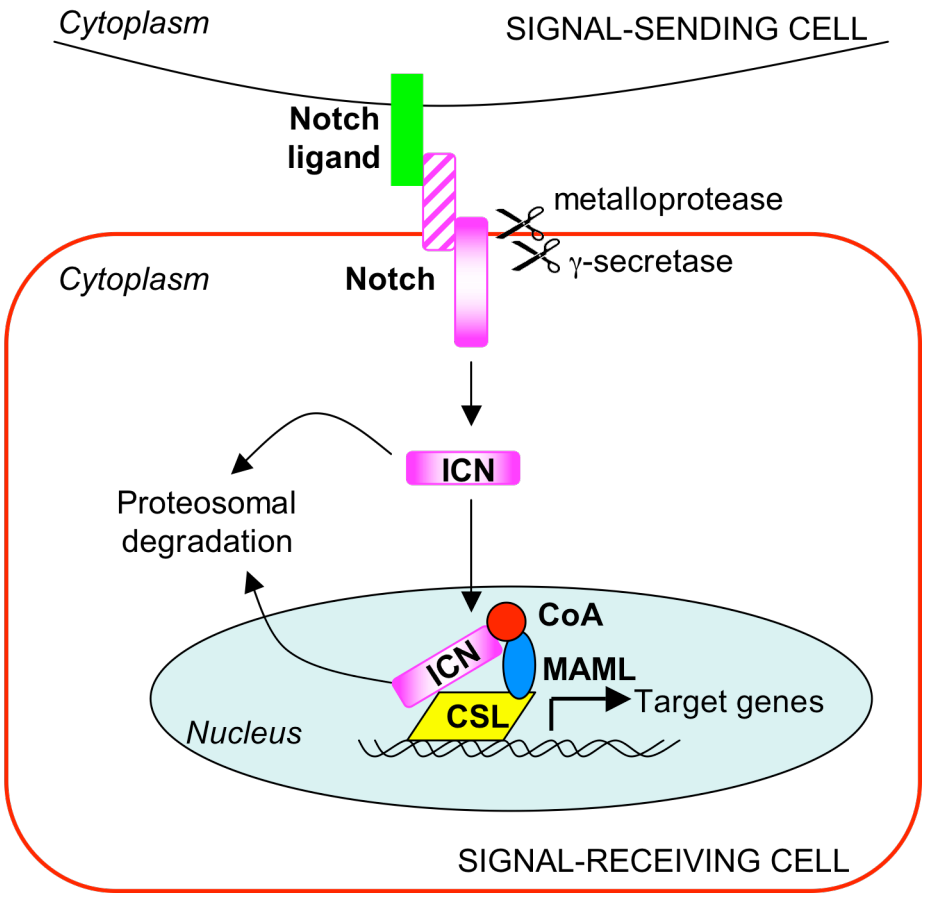

Figure 1.2 The Notch signaling pathway. After synthesis, Notch preproprotein is cleaved by furin convertase at site S1, and the extracellular and intracellular portions are non-covalently linked to form a mature heterodimeric protein localized at the cell surface. Binding of Notch with its ligand activates 2 proteolytic events, first by metaolloprotease at S2, followed by γ-secretase at S3, which releases ICN (intracellular Notch) from the membrane. ICN then translocates to the nucleus. ICN binds to its nuclear effector CSL and recruits transcription coactivator MAML. The ICN-CSL-MAML ternary complex in turn recruits additional coactivators to initiate transcription of target genes. Phosphorylated serine residues in the PEST domain at the Notch C-terminus is recognized by Fbw7, an ubiquitin ligase, which targets ICN for proteosomal degradation, thus concluding the Notch signal.

1.1.2.1 Core components of the Notch pathway

Notch receptors

Notch receptors are synthesized as 300-350 kDa type I single-pass transmembrane proteins. The fly *Drosophila melanogaster* has 1 Notch receptor, the worm *Caenorhabditis elegans* has 2 (LIN-12 and GLP-1) and mammals have 4 (Notch1-4). Structures of mammalian Notch1-4 differ in the number of epidermal growth factor (EGF)-like repeats and in the length of transcriptional activation domain (TAD). The extracellular domain of mammalian Notch proteins contains 29-36 EGF-like repeats[20,25-28], some of which facilitate ligand interaction (Fig. 1.3). Specifically, EGF-like repeats 11 and 12 are necessary and sufficient for receptor-ligand interaction between two cells (trans-interaction)[29,30]; whereas, EGF-like repeats 24-29 mediate cis-inhibition by ligands expressed on the same cell[31]. These EGF-like repeats can bind Ca^{2+} that mediates ligand interaction. In particular, mutation of calcium-binding residue in EGF-like repeat 12 of human Notch1 abrogates binding to Delta-like 1[32].

Within the extracellular domain, EGF-like repeats are followed by three LNR modules that are part of the negative regulatory region (NRR). Each LNR module is made up of 35-40 amino acids, contains 3 disulfide bonds among 6 cysteine residues, and acidic and polar amino acids that coordinate a calcium ion to ensure proper folding and stability of LNR[33]. Two 6-10-residue linkers separate 3 LNR modules[34]. Point mutations in LNR domain of worm Notch receptor *Lin12* lead to gain-of-function phenotypes[35]. Similarly, deletion of LNRs results in activation of Notch signaling in reporter assays[36]. These data suggest an important role for LNR modules in preventing premature activation of Notch signaling.

The Notch receptor is synthesized as a single-chain transmembrane precursor that is cleaved by furin convertase at extracellular site S_1[22,23]. The resulting protein fragments are held together at the heterodimerization domain (HD) by non-covalent interactions between the C-terminal ~100 residues of N^{EC} and the extracellular ~70 residues of N^{TM} [37]. HD contains the S_2 metalloprotease cleavage site (located ~12 residues before the transmembrane domain) that serves as a receptor activation switch[38]. The LNR modules keep the switch in an 'OFF' state in the absence of ligand, hence both HD and LNR constitute what is known as the negative regulatory region (NRR)[39]. Following the HD domain, a stretch of ~25 hydrophobic residues spans the membrane (transmembrane domain - TMD), which harbors the γ-secretase cleavage site (S3) between glycine 1743 and valine 1744 of mouse Notch1. Release of ICN from the plasma membrane occurs only after γ-secretase cleavage[40]. The ICN contains several functional domains important for association with the CSL (CBF1/RBP-Jκ/Su(H)/Lag-1) DNA-binding protein, MAML and other transcription factors. These include (from N- to C-terminus) the RAM domain (RBP-Jk association module), seven iterative ankyrin (ANK) repeats, and the transcription activation domain (TAD). Both RAM and ANK domains are sufficient and necessary for interaction with CSL[41,42]. The ANK domain is flanked by two nuclear localization sequences (NLS). Finally, located at the C-terminus of N^{TM} are PEST sequences (a region rich in proline, glutamic acid, serine, and threonine) that regulate ICN turnover[43,44]. Collectively, ligand binding triggers regulated intramembrane proteolysis of Notch, liberating ICN to activate a CSL transcription factor complex in the nucleus.

Notch ligands

Notch ligands are type I transmembrane proteins with the extracellular domain characterized by an N-terminal (NT) domain, a DSL (Delta, Serrate, Lag2) domain and variable number of EGF-like repeats[45-47] (Fig. 1.3). Mammalian Notch ligands are categorized as either Delta-like (Dll1, Dll3 and Dll4) or Serrate-like (Jagged1 and Jagged2) based on their homology to orthologs in *Drosophila*[24]. The NT and DSL domains of *Drosophila* Delta are necessary and sufficient to mediate binding to Notch[48]. Following the DSL domain, a conserved motif known as DOS (Delta and OSM-11-like proteins) is found in some mammalian Notch ligands such as Dll1, Jagged1 and Jagged2 but not in Dll3 and Dll4. The DOS motif cooperates with DSL to activate Notch signaling[49]. The intracellular sequences of Notch ligands are highly divergent[50] but most ligands, except Dll3, contain intracellular lysine residues that are potential sites for ubiquitination. Indeed, RING-containing E3 ligases, Neuralized (Neur) and Mind bomb (Mib) have been implicated in regulating ligand signaling activity by ubiquitination[51-56]. While fruit fly Neur and Mib appear to serve similar roles in Notch signaling, mammalian Neur and Mib E3 ligases have evolved to perform non-redundant functions. For instance, removal of Mib1 produces embryonic lethal phenotypes similar to *Notch1* null mice[53,57]; whereas *Neur1*, *Neur2* and *Mib2* genes are dispensable for normal development[58]. Our knowledge on the structure and function of Notch ligands is evolving, which will undoubtly enhance our understanding of Notch receptor activation.

CSL transcription factor

All Notch signals ultimately cause changes in gene expression through activation of CSL-dependent transcription. A highly conserved core region in CSL (~420 amino acids) contains an N-terminal domain (NTD), followed by a β-trefoil domain (BTD) and a C-

terminal domain (CTD)[59] (Fig. 1.3). CSL binds DNA as a monomer[41]. The consensus DNA sequence for CSL-binding is –C/tGTGGGAA-[60]; however, more recent studies question the selectivity of some residues[61]. The NTD and BTD form an extensive electropositive surface that contacts DNA: the NTD specifically recognizes the -GGGA- base pairs whereas the BTD recognizes the –C/tG- residues. Notably, the BTD and CTD domains of CSL interact with the RAM and ANK domains of ICN, respectively[62].

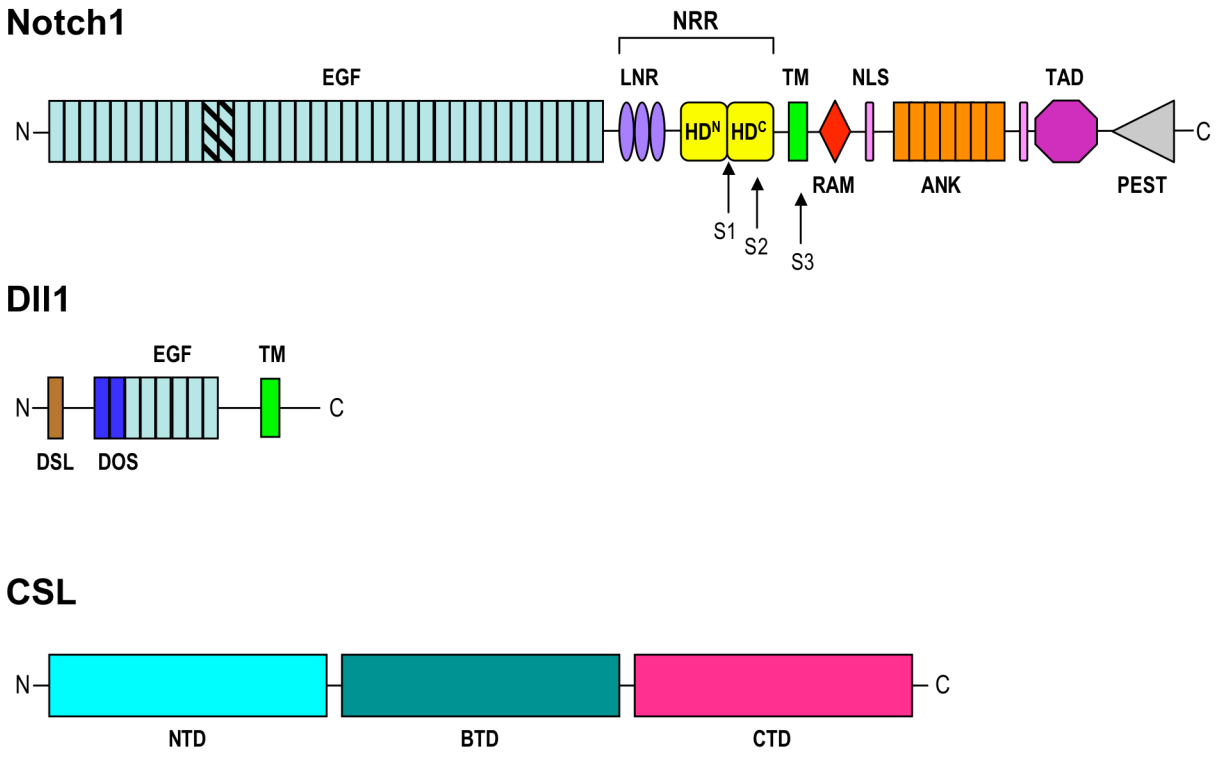

Figure 1.3 Functional domains of the core components of Notch pathway. Notch1 is a heterodimeric type I transmembrane protein. The extracellular portion consists of 36 EGF-like repeats, of which repeats 11 and 12 (hatched) are necessary and sufficient for ligand binding. These are followed by NRR comprised of 3 LNR (Lin12-Notch repeats) and HD (heterodimerization domain). Following the transmembrane domain, the intracellular portion of Notch1 consists of RAM (RBP-J associated molecule), followed by the first NLS (nuclear localization signal), 7 ankyrin repeats, a second NLS, TAD (transactivation domain) and PEST (proline, glutamate, serine, and threonine) domain. Notch ligand, Dll1, is also a type I transmembrane protein that comprises extracellularly of DSL (Delta/Serrate/LAG-2), DOS (Delta and OSM-11-like) and 6 EGF repeats. The CSL transcription factor is a DNA-binding protein comprised of 3 functional domains as indicated. Both NTD and BTD bind to DNA; whereas the BTD and CTD interact with RAM and ANK of Notch1, respectively.

1.1.2.2 Notch receptor-ligand interactions

Activation of Notch signaling normally requires binding of a ligand expressed on the signal-sending cell to a Notch receptor on the signal-receiving cell (Fig. 1.2). Post-translational modifications of Notch proteins regulate ligand-receptor interaction[24]. O-linked glycosylation of Notch receptor is essential for Notch signaling in mammals and flies although it has yet to be confirmed in *C. elegans*[63,64]. O-fucosyltransferase (O-fut1 in *Drosophila* and POFUT1 in mammals) adds an O-fucose to serine or threonine residues on EGF repeats containing the consensus sequence $C_2XXX(A/G/S)(S/T)C_3$ (X indicates any amino acid)[63-65]. There are 13 evolutionarily conserved O-fucosylation sites in mammalian Notch1[66]. Of these, homozygous mutation of T466A in EGF repeat 12 in mice results in reduced binding to Dll1 and Notch signaling, which impairs thymocyte maturation[67]. Moreover, pairing of this mutant allele with a *Notch1* null allele resulted in embryonic lethality. These data suggest that the T466A mutation is hypomorphic and that O-fucosylation in the ligand-binding domain regulates interaction between Notch1 on T cells and Dll1[67]. The O-fucose at EGF repeats is a substrate for further sugar modification by Fringe glycosyltransferase, which catalyzes addition of N-acetylglucosamine (GlcNAc) to O-fucose[68,69]. In *Drosophila*, Fringe enhances responsiveness of Notch to Delta and inhibits responsiveness to Serrate[70]. Furthermore, *in vitro* studies using purified Fringe, Notch and its ligands indicate that Fringe glycosylates Notch and addition of N-acetylglucosamine to O-fucose on EGF domain of Notch is sufficient to enhance binding to Delta and inhibit binding to Serrate[71]. In mammals, the effect of Fringe on Notch-ligand interaction is complicated by the numerous receptors, ligands and Fringe glycosyltransferases (Lfng,

lunatic fringe; Mfng, manic fringe; and Rfng, radical fringe) involved[24]. In the case of Notch1 in T cells, Lfng enhances Notch signaling via interaction with Delta but not Jagged ligands[72]. However, the effect of Lfng differs among Notch paralogs. For example, Lfng actually potentiates both Jag1- and Dll1-mediated Notch2 signaling[73]. The explanation for receptor-specific response to ligands will likely require crystal structures for each receptor-ligand complex. Current data support a role for Notch glycosylation in modulating receptor-ligand affinity and Notch signal strength[24].

1.1.2.3 Notch activation

The critical event regulating Notch activation is proteolysis by metalloprotease at S2, which generates a substrate for subsequent γ-secretase-mediated release of ICN from the membrane (Fig. 1.2). Earlier studies indicate that the extracellular domain of *Drosophila* and mouse Notch negatively regulates its activity[30,74]. More recent findings have established that LNR modules are responsible for preventing premature proteolysis at S2, whereas the HD holds N^{EC} and N^{TM} together in a stable complex via non-covalent interactions. These properties are conserved among mammalian Notch proteins[37]. Importantly, the basis for autoinhibition lies in the three-dimensional structure of LNR and conformation of this region relative to site S2 within HD. Gordon *et al*. solved the NRR structure from human NOTCH2 and NOTCH1, which exhibit remarkable similarity. Notably, the three LNR modules form a cap-like structure over the HD domain, which is stabilized by extensive interactions between HD and linker connecting the first 2 LNRs (LNR-AB linker), LNR-B and LNR-C. A hydrophobic plug that lies in LNR-AB linker sterically occludes S2 [75,76]. Deletion of the first 2 LNRs and their linker region is necessary and sufficient for ligand-

independent Notch activation as shown in a cell-based reporter assay, consistent with the structural findings that LNR-AB linker and LNR-B provide key protection for S2.

A key question remains: how does ligand interaction overcome autoinhibition when the ligand binding region lies over 1000 amino acids N-terminal to S2? The autoinhibited conformation of NRR predicts that a substantial conformational movement is required to expose S2 [76]. Prevailing models that attempt to explain how ligand interaction transduces its signal long-range to overcome an autoinhibited state at S2 are mechanotransduction-based[24]. One of these proposes that trans-endocytosis of the Notch ectodomain into the ligand-expressing cell provides mechanical force that lifts at least 2 of 3 LNR modules away from HD and allows metalloprotease to access S2 – a model referred to as "lift and cut"[76]. A second model suggests that mechanical force from trans-endocytosis dissociates N^{EC} and N^{TM}, which, in turn, results in exposure of S2 [77]. Evidence against this latter model comes from studies on *Drosophila* Notch that is not processed by furin convertase, hence it exists as a single transmembrane polypeptide without HD region. Yet ligand interaction can activate Notch, whereas soluble ligands without the ability to lift LNR modules fail to induce receptor activation[78]. The findings in *Drosophila* suggest that heterodimer dissociation is not an essential prerequisite for Notch activation; thus the "lift and cut" is a more consistent model.

Metalloprotease-mediated proteolysis of Notch at S2 sheds the ectodomain and generates NEXT with shortened extracellular domain[39]. Both ADAM 10 and ADAM17/TACE (TNFα converting enzyme) have been implicated in S2 cleavage *in vitro*[79,80]. However, while *Adam10* knockout mice display a phenotype similar to Notch1 null mice, Adam17 null mice do not[81]. The short extracellular domain (< 30 amino acids) in

NEXT becomes a substrate for intramembranous proteolysis by γ-secretase complex[82,83]. The efficiency of proteolysis inversely correlates to the length of extracellular domain[83]. Consistent with this idea, inhibition of metalloproteases greatly reduces γ-secretase-dependent ICN production and target gene expression[77]. The γ-secretase complex contains four proteins Psen (presenilin), Nct (nicastrin), Aph-1 (anterior pharynx defective 1) and Pen-2 (presenilin enhancer 2)[84]; of which, presenilin forms the catalytic active component[40,85,86]. Following ectodomain shedding, γ-secretase cleaves the transmembrane domain of NEXT sequentially at multiple positions starting from S3, close to the cytoplasmic border of the membrane, and ending at S4 near the middle of TMD[87]. Cleavage at S3 releases ICN from the membrane intracellularly[40]; whereas S4-cleavage generates Nβ peptide, which is released to the extracellular space[87,88]. ICN translocates to the nucleus to activates target gene transcription via CSL[89].

1.1.2.4 Assembly of a CSL transcription activation complex

Once ICN translocates to the nucleus, it activates target gene transcription via DNA-binding protein CSL[90] (Fig. 1.2). Whether CSL represses or activates transcription depends on its interaction with corepressors or coactivators, respectively. CSL functions as a transcription repressor was first reported in cultured mammalian cells[91,92]. Subsequent experiments demonstrated that mammalian ICN1 binds CSL and this interaction converts CSL from a repressor to an activator[93]. A number of corepressors that interact with CSL have been identified. The two best characterized are Hairless in flies[94] and MINT (Msx2-interacting nuclear target protein) in mammals[95].

Hairless interacts with and antagonizes the *Drosophila* CSL ortholog, Suppressor of Hairless (Su(H))[94,96] by recruiting co-repressor proteins Groucho and CtBP[97]. Despite its

conservation in insects, mammalian Hairless counterparts have not been identified. However, studies have suggested that MINT might be a functional homolog of Drosophila Hairless[95,98]. MINT competes with ICN for binding to CSL and represses Notch-mediated transcription activation. Consistent with this biochemical findings, MINT deficiency enhances Notch-dependent marginal zone B lymphocyte differentiation in mouse spleen[95] and early mouse fetal thymocyte differentiation[98]. These data support the idea that Hairless and MINT as important repressors of Notch target gene transcription.

Structural analyses and binding assays demonstrate that RAM and ANK domains of ICN are sufficient and necessary for CSL binding[41,42]. The RAM domain of ICN shows high-affinity binding to the BTD domain of CSL; whereas the ANK domain interacts weakly with the CTD region[99,100]. Once ICN is bound to CSL, this complex is able to interact with transcription activator MAML protein[101,102]. Interestingly, MAML can form a ternary complex with ICN and CSL but not a binary complex with either. In this ternary complex, MAML binds to the interface created by CTD of CSL and ANK of ICN as well as the NTD of CSL[62,103]. Assembly of this transcription activation complex occurs in a stepwise manner. First, high-affinity binding of RAM domain of ICN to CSL promotes association of ANK to CSL, which in turn dissociates co-repressor proteins. Second, the ANK-CTD interface recruits coactivator MAML. Third, the ICN-CSL-MAML ternary complex recruits histone acetyltransferases complexes such as p300-PCAF at the target gene promoter to facilitate transcription activation[24,90]. Notch regulates differentiation, apoptosis and proliferation by activating transcription of target genes including transcription repressor *Hes/Hey* genes; T-cell genes such as *Il2ra*, *Ptcra*, and *Gata3*; proliferation gene *Myc*; components of the Notch pathway such as *Notch1*, *Notch3*, ubiquitin ligase *Dtx1*; and Notch

inhibitor *Nrarp* [104-110]. Notch regulates some of its targets both positively and negative, a process known as incoherent network logic. One example is *Pten*, which is directly induced by CSL/Notch complex but also repressed by Hes1[111,112].

Since Notch regulates important developmental processes such as T-cell differentiation, the duration of its signal must be precisely controlled. Failure to do so, as in the case of gain-of-function mutations in the PEST domain of human *NOTCH1*, leads to T-cell acute lymphoblastic leukemia/lymphoma[10]. In normal Notch signaling, while the ICN-CSL-MAML ternary transcription activation complex is assembling, a process that leads to ICN degradation has been initiated. MAML recruits Cyclin C:Cdk8 complex, which phosphorylates Notch at serine residues, S^{2514}, S^{2517} and S^{2538} within the PEST domain[43,113]. Fbw7, an E3 ubiquitin ligase, then recognizes the phosphorylated PEST domain and targets ICN for proteasomal degradation[43]. The destruction of ICN ends the Notch signal. Notch signal regulates critical development processes such as T-cell lineage commitment (section 1.1.3) and maturation (section 1.1.4), hence its activity must be tightly controlled as noted above.

1.1.3 Notch Signaling in T-cell Lineage Commitment

When a hematopoietic progenitor enters the thymus, it has access to different cell fates including myeloid, dendritic (DC), natural killer (NK), B as well as T cell[114]. Therefore to become a T cell, the thymic seeding progenitor must lose alternative developmental fates prior to T-lineage commitment, which occurs at DN1/ETP and DN2, a process that is induced by Notch signaling. Notch1 loss of function mediated by conditional inactivation of *Notch1* or transcription factor *CSL* results in a small thymus that lacks T cells, and instead contains B cells[115,116], demonstrating a role for Notch in B-lineage

suppression. Indeed, Notch signaling rapidly extinguishes B-cell potential irreversibly at the ETP/DN1 stage[117]. By late DN2 stage, referred to as DN2b, myeloid, NK and DC potentials disappear, hence completing T-cell commitment[118,119]. Both the induction of alternative fate potentials and their repression are regulated by a number of transcription factors. For example, EBF-1 and Pax5 are essential for B-cell development[120], and suppression of B-cell fate is coordinated by 2 T-cell-specific transcription factors GATA-3 and TCF-1[121]. TCF-1 expression is upregulated by Notch signaling[122]. Moreover, Notch signaling can also block B-cell development *in vitro* in a GATA-3-independent manner[123]. Therefore, Notch1, TCF-1 and GATA-3 direct the B-cell exclusion program at the ETP stage. GATA-3 and TCF-1 also block PU.1[124,125], a key factor in myeloid and DC development[126,127]. In addition, Runx1/CBFb complexes and Gfi1 repress PU.1 through its cis-regulatory elements[128,129]. In addition to PU.1, C/EBPα also promotes myeloid development[127] and Notch signaling antagonizes C/EBPα activity possibly through Hes1[130,131]. The final stage of T-lineage commitment involves suppression of NK potential that is achieved by T-lineage specific transcription factor Bcl11b[132-134]. Bcl11b represses NK-specific regulatory gene *Zfp105* and *Il2rb* among others to shut off NK cell development. Thus Notch signaling cooperates with other regulators such as GATA-3, TCF-1, Runx and Bcl11b to sequentially exclude alternative potentials in order to achieve T-cell commitment.

In addition to commitment, the ETP to DN2 stage is marked by a wave of IL-7R and Notch-dependent cellular expansion[135] (Fig. 1.1). Mice deficient in IL-7 or IL-7R demonstrated a block in T-cell development at DN stage, which can be rescued by Bcl-2 overexpression[136], suggesting a pro-survival effect of IL-7 signaling on T precursors. The IL-7R is a heterodimer comprised of the IL-7Rα and common γ (γc) chains. Expression of

IL-7Rα rises from ETP to DN2 stage, then declines steadily, is absent at DP stage and re-expressed at SP stage[137-140]. This variable IL-7Rα expression is in contrast to constitutive expression of γc chain. Binding of IL-7 leads to activation of the Janus kinases Jak1 and Jak3 that are associated with IL-7Rα and γc chains, respectively[141-143]. The Jak kinases phosphorylate IL-7Rα cytoplasmic tyrosine residues in order to trigger phosphotidylinositol-3-kinase (PI-3K)/Akt and STAT5 signaling pathways[144-146]. Downstream target genes include *Bcl2*, *Mcl1*, *Cycd1*, *Socs1* and *Myc*[147]. Therefore, IL-7R signaling supports the survival and clonal expansion of T-lineage committed DN2 progenitors[148-150].

1.1.4 Notch Signaling in β-selection

Once the T-lineage committed DN2b cells reach the DN3 stage, they stop proliferation and begin TCRβ rearrangement: first, with Dβ gene segments rearranging to Jβ gene segments, followed by Vβ gene segments to DJβ gene segments[151,152]. A successful in-frame rearrangement in DN3 cells generates a TCRβ chain that can complex with pre-Tα and CD3 to produce a pre-TCR, which signals in a ligand-independent fashion[153,154]. Pre-TCR signaling prevents DN3 cell death, and promotes clonal expansion and differentiation into DP cells in a process known as β-selection[12,15]. Cooperation between pre-TCR and Notch signaling is required for effective β-selection (Fig. 1.1). For example, conditional deletion of *Notch1*[155] or its transcriptional mediator *CSL*[156] at the DN2 stage results in a partial block in DP development. However, it is unclear if Notch1 activation lies upstream or downstream of pre-TCR signaling. Using an *in vitro* OP9 stromal co-culture system, Ciofani *et al*. showed that in the absence of Notch1 activation, DN3 cells were blocked in

their differentiation, failed to proliferate and died despite the presence of a pre-TCR[157]. Maillard *et al*. showed similar results in mice that conditionally expressed a dominant-negative form of transcription co-activator MAML (DN-MAML), which prevented Notch activation at DN2[158]. DN-MAML$^+$ DN3 cells failed to grow, proliferate and differentiate into DP despite relatively normal TCRβ expression, suggesting a requirement for Notch activation independent of pre-TCR signaling during β-selection. Finally, Ciofani and Zuniga-Pflucker demonstrated that trophic and anti-apoptotic effects of Notch signaling were Akt-dependent[159], and possibly involved Notch-mediated *Pten* downregulation[111]. These findings therefore suggest a pre-TCR independent role of Notch in promoting metabolism, survival, proliferation and differentiation of DN3 cells undergoing β-selection. Interestingly, T-LL cells frequently arrest at DN3 to DP stages that mark the β-selection checkpoint, suggesting that thymic progenitors may co-opt developmental pathways such as Notch in order to undergo malignant transformation.

1.2 T lymphoblastic leukemia and lymphoma (T-LL)

1.2.1 Clinical features of T-LL

T lymphoblastic lymphoma and leukemia (T-LL) represent a malignancy of T-cell precursors that affect children and adults. The incidence of T lymphoblastic leukemia is 0.8 and 0.3 per 100,000 children and adults, respectively; whereas the incidence of T lymphoblastic lymphoma is 0.2 per 100,000 children and 0.3 per 100,000 adults[160]. With intensive, high-dose, multi-agent chemotherapy, the five-year event-free survival rates for T-LLs are 70-90% and 50-60% for children and adults, respectively[2,3]. Relapses in the central nervous system, bone marrow and mediastinal compartments are common causes of

treatment failure. Further improvement in clinical outcome has been hampered by a lack of clinical or laboratory prognostic markers that can predict risk of relapse and guide treatment modification. The heterogeneity in T-LL biology and the relative low disease incidence contribute to the difficulty in identifying reliable prognostic factors[161]. Currently, only early treatment response evaluated by minimal residual disease quantification is predictive of T-LL relapse risk[162]. Providing a long-term cure for those patients who develop a relapse remains a challenge[4,163,164]. There is a need for more specific and less toxic therapeutic agents designed to improve overall clinical outcomes. An understanding of how genetic lesions result in aberrant activation of developmental pathways and contribute to the malignant transformation of T-cell progenitors is a prerequisite to design such agents.

1.2.2 Cytogenetic subgroups of T-LL

Much of our current knowledge of T-LL molecular biology reflects studies on recurrent cytogenetic aberrations, mutations and gene expression profiles. Chromosomal translocations occur in ~ 50% of T-LL cases, although each type of aberration accounts for a small fraction of disease. Chromosomal abnormalities can be categorized into three groups. First, rearrangements of transcription factors *TAL1*, *LYL1*, *LMO1*, *LMO2*, *TLX1*, *TLX3* and the *HOXA* cluster, downstream of promoter or enhancer elements of T-cell receptor (TCR) loci on chromosome 7 (*TCRB* and *TCRG*) or chromosome 14 (*TCRA* and *TCRD*), leading to transcription factor gene overexpression. While some transcription factors, such as Lyl-1[165], Tal-1[166], and HoxA[167], function in normal T-cell development or hematopoiesis, others are ectopically expressed by transformed T-cells. Rearrangements of *LMO1*, *LMO2* and *TAL1* are observed in 3-9% of patients; whereas rearrangments of *TLX1* and *HOXA* are found in 10% and 4% of patients, respectively[161]. The oncogenic potential of TAL1 and LMO

proteins is likely due to their inhibitory effect on E2A transcriptional activity[168-170]. Second, chromosomal translocations generate fusion genes coding for novel chimeric proteins or leading to dysregulated expression of one gene under transcriptional regulatory elements of another. Examples include *SIL-TAL1* (10-25% of T-LL patients), *TLX3-BCL11B* (20%), *CALM-AF10* (8%) and *NUP214-ABL1* (5%)[161]. Bcl11b plays a critical role in T-lineage commitment[171]. *TLX3-BCL11B* translocation results in aberrant TLX3 expression through regulatory elements downstream of *BCL11B*[172]. *CALM-AF10* fusion leads to upregulation of specific *HOXA* cluster genes and disrupts normal hematopoietic differentiation[173,174]. The *NUP214-ABL1* fusion encodes for a constitutively activated tyrosine kinase that is sensitive to the tyrosine kinase inhibitor imatinib[175]. Lastly, the third group of chromosomal translocations juxtapose *MLL1* gene to different partner genes, accounting for 5-10% of T-LL cases. Characterization of these translocations has increased our knowledge of T-LL translocations; unfortunately, none of the translocations has provided a clinically useful prognostic marker.

1.2.3 Gene expression profiles of T-LL

Gene expression profiling studies in T-LL have been instrumental in defining the transcriptional networks that distinguish disease subgroups, in particular those lacking known cytogenetic abnormalities. These profiling studies have identified at least 5 major subgroups of T-LLs including *HOX11/TLX1*, *HOX11L2/TLX3*, *TAL1/LMO*, *HOXA*, and *LYL1*[173,176,177] (Fig. 1.4). These subgroups are associated with arrest at specific stages of T-cell differentiation. For example, *HOX11/TLX1*-positive T-LLs express *CD1A* and *CD10*, reflecting differentiation arrest at early cortical CD4/8 DP stage[176]. Furthermore, these T-LLs express genes that can be targeted by drugs such as inhibitors of dihydrofolate reductase

(methotrexate), topoisomerase IIa (anthracyclines) or glucocorticoid receptor (corticosteroids), which may explain their better clinical outcome[178-181]. In contrast, T-LLs expressing *HOX11L2/TLX3*, a gene similar to *HOX11*, are arrested a different stage of differentiation and show a poor outcome in some[176,182] but not in all[178] studies. Similarly, the expression profile of *TAL1/LMO*$^+$ T-LL suggest two subgroups arrested either at a late cortical DP or mature SP stage[173]. The *HOXA*-positive group includes T-LLs that ectopically express *HOXA* genes by CALM-AF10, SET-NUP214, MLL fusion proteins or rearrangements to the TCR loci[173,174,177,183]. The association between this T-LL group and stage of T-cell differentiation has not been clearly established. A poor outcome is associated with *CALM-AF10*, but prognosis remains unknown for patients with *HOXA*$^+$ T-LL. CALM-AF10, SET-NUP214 and MLL-AF10 T-LLs aberrantly express *HOXA* genes via recruitment of H3-K79 methyltransferase DOT1L, to *HOXA* promoter region[177,184,185]. This finding is clinically relevant because a DOT1L inhibitor targeting MLL leukemias[186] is currently in a phase I trial. This inhibitor may also be a useful treatment for *HOXA*$^+$ T-LL (up to 15% of T-LL patients), if recruitment of DOT1L to the *HOXA* promoter represents a common mechanism used by this group.

The *LYL1*$^+$ T-LL group expresses early differentiation marker *CD34* and *LMO2* but lacks CD3/4/8 expression, suggestive of a DN stage block in T-cell development[176]. The signature of *LYL1*$^+$ cases resembles the expression profile seen in immature T-LL cases, which includes high expression of *LYL1*, *CD34* and *LMO2* as well as frequent expression of myeloid markers *CD13* and *CD33*[173]. Coustan-Smith and colleagues further characterized the biology of this immature T-LL group. Using genes that distinguish early T-cell precursors (ETP) from more mature T-cell subsets, they identified 13% of T-LL cases

showing ETP features[187]. ETP leukemic cells lack CD1a and CD8, express either myeloid (CD13, CD33, CD11b, CD65) or stem cell markers (CD34, CD117), and weakly express T-cell antigen CD5. The ETP T-LL cases have elevated *LYL1*, *ERG* and *LMO1* expression and contain higher number of genomic DNA copy number changes when compared to non-ETP T-LLs, reflecting their genomic instability; however, no particular chromosomal abnormality is associated with ETP T-LL. ETP T-LLs portend a poor prognosis in children[187-189] but not in adults[190]. Gain-of-function mutations in genes regulating cytokine and RAS signaling are common in T-LL (67% of cases; *IL7RA, FLT3, JAK3, JAK1, NRAS* and *KRAS*) as are inactivating mutations in histone-modifying genes (*EZH2, SUZ12, EED, SETD2* and *EP300*) particularly in ETP T-LL samples[191] suggesting inhibitors targeting these pathways may be therapeutic. In summary, most T-LL cases can be classified using their gene expression profiles into 5 major subgroups, which tend to occur in a mutually exclusive fashion[161]. There are early indications of prognostic significance associated with some subgroups; however, these associations need confirmation from larger patient cohorts treated with different protocols before using the information in a clinical setting. Gene expression profiling studies have also increased our understanding of the biology of different subgroups, e.g. ETP and *HOXA*$^{+}$ cases, and revealed potential molecular targets for novel therapeutic strategies.

1.2.4 Common mutations in T-LL

In contrast to the mutually exclusive nature of most chromosomal rearrangements, recurrent mutations are often found in multiple molecular subgroups of T-LL. These mutations affect various cellular functions and developmental pathways including loss of cell cycle inhibitors (*CDKN2A* and *CDKN2B*)[192-195], activation of cytokine receptor

signaling (*IL7RA, JAK1, JAK3, PTEN, PI3K* and *AKT*)[196-199], dysregulation of T-cell differentiation (*BCL11B*)[200,201] and activation of Notch signaling (*NOTCH1* and *FBW7*)[10,202,203]. In this section, I will discuss *CDKN2A*, *CDKN2B*, *BCL11B* and *IL7RA* mutations (Fig. 1.4). Activating mutations of the NOTCH1 pathway will be reviewed in the following section.

CDKN2A and *CDKN2B* are two neighbor genes located on chromosome 9p21 that are most frequently inactivated in T-LL (up to 95%)[204]. *CDKN2A* encodes p16 and p14 that are transcribed from different promoters, have first exons, but share exons 2 and 3. *CDKN2B* encodes p15. Inactivation of p16 and p15, which prevent cyclinD/CDK4-mediaed G1/S phase progression[205], occurs by deletion, mutation and methylation. Biallelic and monoallelic deletion of 9p21 frequently involves both genes[192,193]. Point mutations and promoter hypermethylation are additional mechanisms that result in CDKN2A/B inactivation[194,195,206]. In *TAL1xLMO1* transgenic mice, where expression of *TAL1* and *LMO1* was driven by *SIL* and *LCK* promoters, respectively, all developed T-LL by 7 months of age[207]. Enforced expression of $p16^{INK4A}$ driven by *LCK* promoter prolonged the latency (13 months) and reduced the incidence (35%) of T-LL. Furthermore, T-LL that developed in $p16^{INK4A}$*xTAL1xLMO1* transgenic mice frequently lost *p16* expression, indicating that $p16^{INK4A}$ inactivation is a critical event in human and murine T-LL development.

BCL11B is located on chromosome 14q32.2 and codes for 3 zinc-finger transcription factors: α, β and γ. Only Bcl11b-α and -β are highly expressed in the thymus[208]. The gene was first discovered when mutations and deletions were identified in irradiation-induced mouse thymic lymphomas[209]. In normal T-cell development, Bcl11b is expressed starting at the DN2 stage and it suppresses the alternative lineage choice (natural killer cells) and

terminates self-renewal of DN2 cells prior to commitment[114,171]. Heterozygous deletions and inactivating mutations (frameshift and missense) of *BCL11B* have been reported in 16% of *TLX1*-positive T-LL[200]. In a cohort of unselected T-LL patients, 9% harbor monoallelic *BCL11B* lesions, which co-exist with all major molecular subtypes of T-LL[201]. Loss of one copy of *Bcl11b* accelerates thymic lymphoma development in *Trp53*$^{+/-}$ mice or after γ-irradiation, suggesting that *Bcl11b* haploinsufficiency causes T-LL[210]. These findings also suggest that Bcl11b may be a tumor suppressor in T-LL. Based on its function in T-cell progenitors, it is reasonable to speculate that loss of Bcl11b may allow T-LL cells access to a self-renewal program at the DN2 stage to facilitate clonal expansion.

IL-7 promotes proliferation of up to 70% of human T-LL samples *in vitro*[211] and affects their growth in xenograft models[212]. Notably, activating mutations of *JAK1* and *JAK3*, protein tyrosine kinases that bind IL-7Rα and γc, respectively, have been identified in T-LL cases[191,196,213]. For example, in ~10% of pediatric T-LLs, gain-of-function in-frame insertions or insertions-deletions are found in an exon coding for the extracellular juxtamembrane-transmembrane region of IL-7Rα [198,199]. A majority of these mutations result in unpaired cysteines that promote disulfide bond formation between mutant IL-7Rα, thereby activating downstream signaling via JAK1 in an IL-7 independent manner[199]. *IL7R* mutations are often found in *TLX3*$^{+}$ and *HOXA*$^{+}$ T-LL subgroups. Notably, mutant IL-7Rα-expressing primary T-LL cells are sensitive to JAK-STAT pathway inhibition[199].

In summary, recurrent mutations contribute to the malignant phenotype of T-LL. A block in normal T-cell differentiation by inactivating a critical transcription factor *BCL11B* results in differentiation arrest as well as self-renewal capacity of transformed thymocytes. Furthermore, inactivation of cell cycle inhibitors such as *CDKN2A/B*, and acquisition of

cytokine-independent growth by *IL7R* mutations ensure survival and proliferation of T-LL cells. Importantly, constitutive activation of IL-7R signaling provides a novel therapeutic approach to target downstream effectors such as JAK1 and STAT5 for this group of T-LL.

1.2.5 Oncogenic Notch pathway mutations in T-LL

Gain-of-function mutations in the Notch pathway are the second most frequent group of recurrent mutations, occurring in about 60% of T-LL cases[10,202,203]. A role of NOTCH1 in T-LL pathogenesis was first proposed in 1991 when a rare balanced translocation t(7;9)(q34;q34.3) placed intracellular *NOTCH1* coding sequence downstream of the *TCRβ* locus, aberrantly activating expression of a truncated protein[21]. Importantly, enforced expression of truncated form of NOTCH1 (ICN1) transformed mouse bone marrow progenitors and induced T-LL in 50% of transplanted animals, thus demonstrating the oncogenic potential of ICN1 specifically in immature T-cell precursors[214]. Aberrant Notch signaling was later found to occur more frequently than thought.

Most *NOTCH1* mutations cluster in two hotspots: the HD and C-terminal PEST domains[10] (Fig. 1.3). Mutations in the HD domain occur in 44% of human T-LL, which are more frequently detected than PEST mutations (30%). Moreover, about 12% of samples harbor both mutations on the same allele. The HD mutations consist of missense mutations as well as small in-frame insertions or deletions. Biochemical studies of mutant NRR region suggest that these mutations destabilize the heterodimer to varying degrees, hence increasing its susceptibility to metalloprotease cleavage at S2. Rarely, a mutation increases susceptibility to metalloprotease by displacing the protective LNR away from the S2 site without altering stability of the heterodimer[215]. Structural studies on NOTCH1 NRR confirmed the above findings and revealed that HD mutations mainly locate to the

hydrophobic core harboring metalloprotease cleavage site, S2. Furthermore, these mutations increase the susceptibility of S2 by destabilizing NRR and/or increasing exposure of S2 [75]. Notably, all HD mutant NOTCH1 proteins retain their dependence on γ-secretase for receptor function, hence validating γ-secretase inhibitor as a rational therapeutic strategy for Notch-dependent T-LL[10,215].

NRR mutations outside of the HD domain rarely occur in T-LL[75]. The H1545P missense mutation in LNR-C modestly affects stability of the heterodimer. Thus it is postulated that this amino acid substitution disrupts the Ca^{2+}-binding site in LNR-C and induces a conformation change extensive enough to allow for access of the metalloprotease to S2, independent of ligand interaction. Another type of mutation (~3% T-LL) occurs in the extracellular juxtamembrane region causing juxtamembrane expansion (JME)[216]. *NOTCH1* JME mutants contain in-frame insertions of 11 or more amino acids that displace NRR away from the membrane without affecting stability of the heterodimer. The activity of JME mutants remains dependent on metalloprotease and γ-secretase proteolysis but independent of ligand interaction. The mechanism of increased metalloprotease susceptibility resulting from JME mutations remains unclear.

NOTCH1 mutations also occur within sequences coding for the C-terminal PEST domain. The PEST region targets proteins for proteolytic degradation[44]. Mutations scatter across the last *NOTCH1* exon and consist of nonsense mutations, insertions or deletions resulting in a premature stop codon[10]. Mutant ICN1 proteins lack at least 42 amino acids in the C-terminus (residues 2515-2556) that contains serine phosphorylation sites critical for protein degradation, e.g. S^{2517} and S^{2538} by CycC:CDK8 complex[43,113]. One degradation mechanism requires Fbw7, an E3 ubiquitin ligase that targets nuclear ICN1 for proteasomal

degradation[217-219]. Supporting the idea that FBW7 negatively regulates Notch, inactivating mutations in substrate-binding WD40 repeats of *FBW7* occur in 9-16% of human T-LL and lead to ICN1 accumulation, thus increase Notch activity[202,203]. Mutant FBW7 proteins fail to bind a degron in ICN1 containing phosphorylated T^{2512}, S^{2514} and S^{2517} and target it for destruction. Homozygous inactivation of *Fbw7* in DN2 T-lineage progenitors is oncogenic in mice[220]. Therefore FBW7 loss-of-function mutants and NOTCH1 gain-of-function PEST mutants aberrantly sustain intracellular NOTCH1 stability and contribute to T-LL development. Studies have shown that *NOTCH1* gain-of-function mutations commonly found in human T-LL impart different signal strength and leukemogenic potential[221]. PEST mutations alone confer a weak NOTCH signal and fail to initiate T-LL when expressed in mouse bone marrow progenitors. This likely reflects the limited amount of NOTCH ligand available in the microenvironment to activate mutant NOTCH1 proteins. Consistent with this explanation, expression of PEST and HD mutations in *cis* synergistically increases Notch activity enough to initiate T-LL.

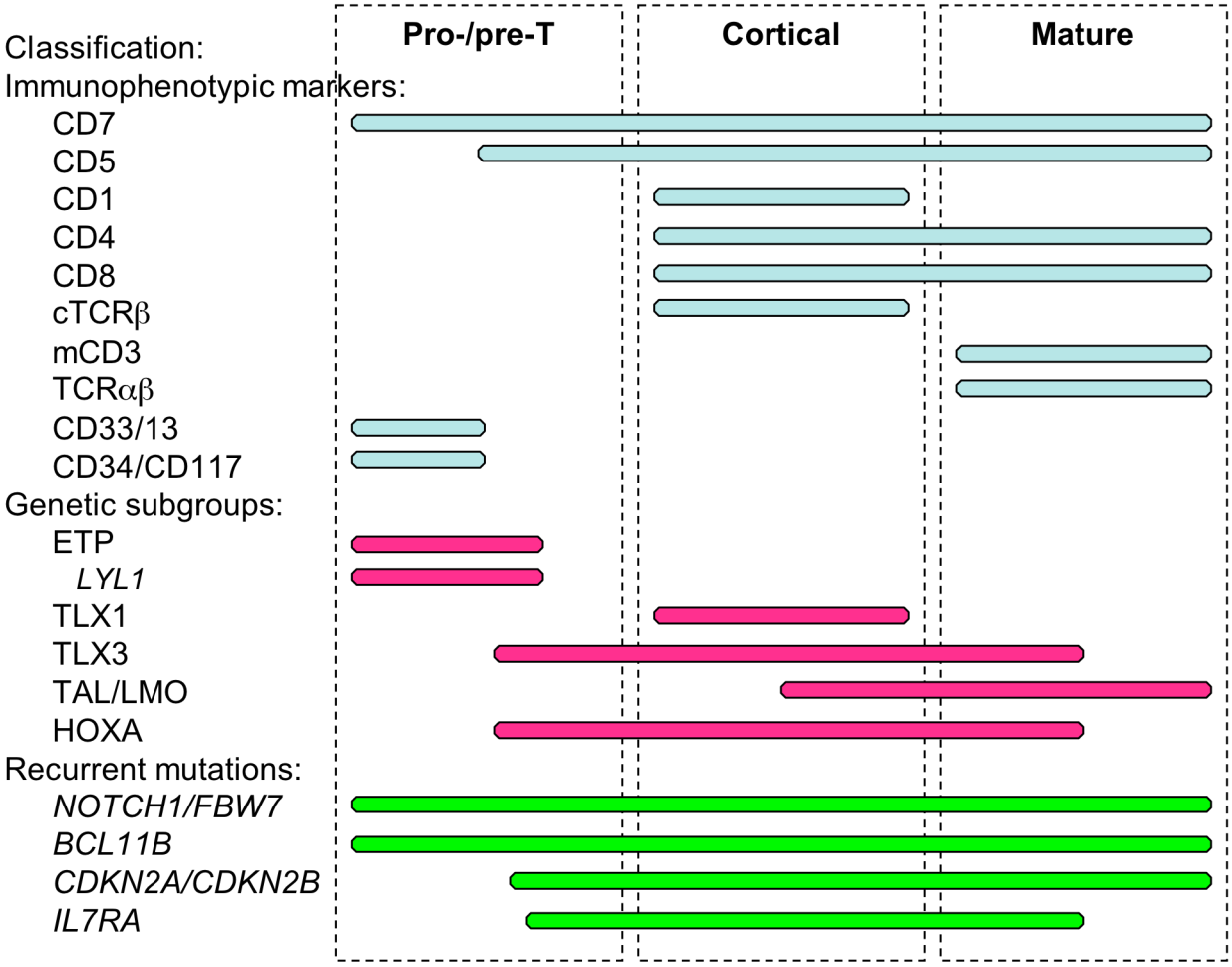

Figure 1.4 Overview of genetic subgroups of T-LL. The genetic subgroups are defined by cytogenetic abnormalities or associated gene expression profiles in relation to their stage of T-cell differentiation arrest. Recurrent mutations found in different genetic subgroups are also indicated. (This figure is modified from ref. [222]).

1.2.5.1 *Notch1* mutations in murine T-LL models

In mice, PEST mutations are commonly found in T-LLs arising from a variety of genetic contexts such as dysregulated expression of Tal1[9] or Lmo[8]; deficiency of E2A[223] or Ikaros[224]; constitutive activation of K-ras[7]. Surprisingly, HD mutations occur infrequently in these mouse T-LL models, suggesting that mechanisms for aberrant Notch1 activation are yet to be uncovered. The first clue came from retrovirus insertional mutagenesis studies that identified frequent integration sites in the *Notch1* gene[225-228]. Specifically, insertion sites cluster around exon 26 and intron 26 (NRR domain), resulting in truncated Notch1 proteins that lacked most if not all of their ectodomain. Our second clue came from studies on radiation-induced lymphomas arising in scid or Atm-deficient mice, where genomic rearrangements of *Notch1* were detected. These often involved deletions at the 5' end, however the consequence of deletions was unclear[229-231]. In some cases, the deleted regions were flanked by recombination signal sequences (RSS), indicating that Rag-dependent illegitimate V(D)J recombination was likely involved. These studies suggest that disruption of NRR frequently occur in mouse T-LL models and involve diverse mechanisms.

Two recent studies further characterize the mechanisms and consequences of genomic rearrangements involving the 5' end of *Notch1* in different T-LL-prone mouse strains. Ashworth *et al*. identified two types of 5' deletions of *Notch1*[232]. Type 1 deletions, the more common type, likely resulted from illegitimate Rag-mediated recombination and were previously described by Tsuji *et al*. The deletions removed exon 1 and its promoter, and transcription initiated at a cryptic promoter within exon 25. In contrast, Type 2 deletions retained exon 1 and a region comprised of exon 2 to exon 26-28 was deleted instead. These deletions appeared to be Rag-independent and possibly resulted from other

non-homologous end-joining mechanisms. Even though the aberrant *Notch1* transcripts originated from distinct mechanisms, they nonetheless shared the same fate: translation initiated at methionine 1727 within the transmembrane domain, and upstream of γ-secretase cleavage site, S3. Hence these 5'-deleted transcripts coded for truncated Notch1 proteins devoid of extracellular domain sequences, which underwent ligand-independent, yet γ-secretase-dependent activation.

In another study, conditional deletion of the *Notch1* promoter and exon 1 hastened T-LL development in Ikaros-deficient mice[233]. These T-LL cells used a cryptic intragenic promoter at exon 25 in a similar fashion as those harboring type 1 deletions mentioned above. Ikaros is a transcription factor that associates with negative chromatin-remodelling factors such as histone deacetylases to regulate early T-cell differentiation[234-236]. Therefore, loss of Ikaros and deletion of *Notch1* promoter reprogrammed the epigenetic landscape at the *Notch1* locus and facilitated accumulation of active chromatin marks at the intragenic cryptic promoter. In contrast, 5' *NOTCH1* deletion has only been described in one case of human T-LL[237], suggesting HD mutations as the main contributor to aberrant activation of NOTCH1 signaling in human T-LL.

In summary, 5' deletions of the *Notch1* locus lead to disruption of NRR and ligand-independent activation of Notch1. These deletions are found in various T-LL-prone mouse models and may represent a predominant mechanism for ligand-independent Notch1 activation since HD mutations are rare. Genomic rearrangements of *Notch1* have been described in Atm-deficient T-LLs but their impact has not been examined; hence we studied their consequence in chapter 3.

1.2.5.2 Notch1 targets in T-LL

Following activation, ICN1 translocates to the nucleus to activate CSL by recruiting co-activator MAML[101,102]. The formation of ICN1-CSL-MAML ternary complex is critical in upregulating target gene transcription[24,238]. These target genes promote survival, proliferation and growth of T-LL cells. Notable direct transcriptional targets of Notch in this context include *Hes1*[106], *Myc*[108-110], and *Il7r*[239].

Hes1, a transcription repressor belonging to the basic helix-loop-helix (bHLH) family, is an evolutionarily conserved direct Notch target and its expression has often been used as a surrogate for Notch signaling[240]. There are 7 mammalian *Hes* genes (*Hes1-7*), of which *Hes1*, *Hes5* and *Hes7* are regulated by Notch[241]. Hes1 and Hes5 are expressed in T cells and hematopoietic stem cells[242,243]. Hes1 represses transcription by recruiting corepressors such as histone deacetylases or Groucho (mammalian homologs: TLE1-4) and/or sequestering other bHLH transcription factors through dimerization[241]. ICN1-induced T-LL in mouse bone marrow progenitors strongly upregulated *Hes1*[244]. However, overexpression of *Hes1* or *Hes5* in bone marrow progenitors failed to induce T-LL, suggesting that Hes proteins are insufficient for T-LL initiation. Recently, Wendorff *et al*. re-examined the role of Hes1 in T-LL induction using conditional Hes1-deficient mice. These mice were crossed to mice that conditionally expressed an oncogenic form of ICN1, and Hes1-deleted ICN1-expressing offspring failed to develop T-LL[245]. Furthermore, this group demonstrated a critical role for Hes1 in maintenance of ICN1-induced T-LL. Similarly, shRNA-mediated knockdown of Hes1 in a human T-LL cell line impaired cell growth and induced apoptosis. Taken together, these findings suggest that Hes is necessary for Notch-mediated T-LL induction and maintenance, but insufficient to initiate T-LL.

Notch regulates a number of key signaling pathways including PI3K-Akt[111,159]. Notch1-induced Hes1 represses transcription of lipid phosphatase *PTEN*, which antagonizes PI3K action; hence Notch1 strengthens PI3K-Akt signaling in human and murine T-LL[111]. Palomero *et al*. further demonstrated that PTEN loss conferred resistance to Notch inhibition by GSI, at least in established human T-LL cell lines. Medyouf *et al*. recently challenged the generalizability of this phenomenon to all T-LL cases since they observed no correlation between PTEN status and GSI sensitivity in primary human T-LL samples[246]. Notch1 also directly activates transcription of *IL7R*[239], which upon binding to ligand triggers downstream signaling including PI3K-Akt in thymocytes and T-LL cells[211,247]. Hence, cross-talk between Notch1 and PI3K-Akt signaling occurs at several levels. Although mutational activation of Notch1 can be an initiating or early event in T-LL development[8,214,224], it is unclear whether other potentially cooperating pathways such as IL-7R signaling are also activated early in T-LL progression. This question will be addressed in chapter 2. This may have clinical implications since drugs targeting of initiating events could well eradicate cancer-propagating clone and achieve a durable remission[248].

Another notable direct Notch1 target is *Myc*[108-110]. c-Myc drives cell growth and proliferation of most if not all cells[249] including thymocytes and T-LL. Without c-Myc, pre-TCR-expressing immature DN3 and DN4 thymic precursors fail to undergo clonal expansion and subsequent differentiation into DP cells[250]. Similarly, c-Myc stimulates T-LL cell growth and proliferation[108-110]. These findings posit Notch1 as a master transcriptional regulator of cell growth and proliferation of normal and malignant thymocytes.

1.2.5.3 *NOTCH1* mutations as a prognostic marker

Since gain-of-function *NOTCH1* mutations occur in more than 50% of human T-LL cases, several groups have studied whether mutation status correlates with treatment outcome. The results of this analysis are inconsistent and depend on treatment protocol[161,251]. Specifically, protocols such as ALL-BFM 2000 that included cranial radiation (CRT) as central nervous system (CNS) prophylaxis observed a favorable outcome associated with *NOTCH1* pathway mutations[251-254]; whereas regimens without cranial irradiation did not[255-259]. For instance, the largest study (301 patients) of the ALL-BFM 2000 protocol reported a better 5-year event-free survival for *NOTCH1*-mutated vs. -wildtype patients ($p = 0.005$)[251]. This result may indicate that the *NOTCH1*-mutated disease is particularly sensitive to BFM-type treatment strategy. A better understanding of the biology of *NOTCH1*-wildtype disease may help facilitate design of novel targeted treatment to improve outcome for this patient group.

A mechanistic link between aberrant Notch1 activation and CNS dissemination has recently been proposed from mouse T-LL studies[260]. Buonamici *et al*. demonstrated that ICN1-driven T-LL upregulated chemokine receptor *Ccr7* that was necessary and sufficient to target T-LL cells to the CNS. In light of this, one could speculate that CRT effectively prevented CNS relapse that are frequently associated with *NOTCH1*-mutated T-LL, thus a more favorable outcome was only seen for this disease group treated when regimen included CRT. Consistent with this idea, another study reported a higher incidence of CNS relapse in *NOTCH1*-mutated vs. *NOTCH1*-wildtype high-risk patients (high-risk group defined by poor response to early treatment determined within the first 10 weeks by blast count in peripheral blood or minimal residual disease; BCR-ABL$^+$ or MLL-AF4$^+$ disease)[255].

In contrast, CNS relapses were rarely found in patients treated with BFM-type therapy[251]. It will be interesting to determine whether CNS relapses are associated with a higher incidence of $CCR7^+$ T-LL cases. Controversies exist regarding the use of prophylactic CRT for children with T-ALL, the findings presented here identify a subgroup of patients, those harboring *NOTCH1* mutations and responding poorly to early treatment, who may benefit from CRT prophylaxis.

Aberrant NOTCH1 activation occurs in 60% in human T-LLs, making this pathway an attractive therapeutic target. Early clinical trials using γ-secretase inhibitor MK-0752 in patients with relapsed T-LL were met with dose-limiting severe gut toxicity[261]. Recently, intermittent rather than continuous daily dosing of GSI dramatically improves toxicity profile for children and adults with solid tumors[262,263]. Future trials should assess the toxicity profile and efficacy of intermittent dosing regimen of γ-secretase inhibitors in treatment of T-LL. Finally, less is known about biology of T-LL without aberrant Notch activation as found in 40% of T-LL patients. These patients fare worse in some treatment protocols, hence warranting further studies to identify novel therapeutic targets. Since studies on identifying signaling pathways in Notch-independent T-LLs are lacking, we examined their biology in chapter 4.

1.2.6 Atm-deficient mice as a model for human T-LL

The mouse is a key model organism for studying molecular mechanisms of human disease. Our laboratory has studied $Atm^{-/-}$ mice since a majority developed T-LL before 5 months of age[264-266]. Atm, a PI3K-like protein kinase, regulates DNA damage surveillance and repair[267,268]. $Atm^{-/-}$ mice share similar phenotypes to humans suffering from ataxia telangiectasia (AT) including immunodeficiency, genomic instability, a high incidence of

leukemia/lymphoma, and radiation hypersensitivity[269]. AT patients have 70 to 250-fold increased risk of developing leukemia/lymphoma, particularly of the immature phenotype[270]. We have studied the molecular and developmental basis of T cell deficiency and susceptibility to T-LL in *Atm*-deficient mice. Similar to AT patients, $Atm^{-/-}$ mice show thymic hypoplasia, reflecting a paucity of mature single-positive ($CD4^+$ or $CD8^+$) thymocytes and nearly all develop aggressive pre-T-ALL between 2-5 months of age[264-266]. These murine T-LL blasts display predominantly an immature CD8 ISP and/or DP phenotype that is similar to the leukemic blasts seen in human T-LL[271]. Thus, $Atm^{-/-}$ mice provide an animal model for studying T-LL development.

1.3 Rationale and Hypothesis

Mutation-based aberrant Notch1 activation contributes frequently to T-LL oncogenesis, however the timing of their occurrence has not been clearly defined. Furthermore, the rarity of HD mutations observed in mouse T-LL models relative to humans suggests additional mechanisms may confer ligand-independent Notch1 activation in mice. Less is known about the subgroup of T-LL containing low/absent Notch1 expression, yet according to some treatment protocols this subgroup portends a less favorable prognosis. Using $Atm^{-/-}$ mice as a tool to understand T-LL pathogenesis, the specific aims of this thesis are as follows: 1) to determine the timing of occurrence of *Notch1* mutations during T-LL progression (chapter 2); 2) to characterize the mechanisms of Notch1 activation in Notch-dependent T-LL (chapter 3); and 3) to identify proliferation and survival signal in Notch-independent T-LL (chapter 4).

CHAPTER 2:

ABERRANT NOTCH1 ACTIVATION OCCURS EARLY IN *ATM*$^{-/-}$ T LYMPHOBLASTIC LYMPHOMA TRANSFORMATION

Peggy P. C. Wong[1,3,5], Irina R. Matei[1,5], Jayne S. Danska[1,2,5], and Cynthia J. Guidos[2,4]

[1]Department of Medical Biophysics, [2]Department of Immunology, University of Toronto, Toronto ON M5G 2M9
[3]Division of Haematology/Oncology, Department of Paediatrics, the Hospital for Sick Children, Toronto ON M5G 1X8
[4]Program in Developmental and Stem Cell Biology, the Hospital for Sick Children, Toronto ON M5G 1L7
[5]Program in Genetics and Genome Biology, the Hospital for Sick Children, Toronto ON M5G 1L7

Author contributions:
All experiments and data analysis in this chapter were performed by P. Wong with the following exceptions: Genomic DNA was prepared by I. Matei; sequencing of HD and PEST mutations from some samples and heteroduplex assay were performed by I. Matei. P. Wong and I. Matei both contributed to the immunophenotyping of T-LL and pre-malignant thymocytes.

2. ABERRANT NOTCH1 ACTIVATION OCCURS EARLY IN *ATM*$^{-/-}$ T-CELL LYMPHOBLASTIC LYMPHOMA TRANSFORMATION

2.1 Abstract

T-cell lymphoblastic lymphoma/leukemia (T-LL) is a malignant disease of lymphoid precursors that affects children and adults. Both Notch1 and interleukin-7 receptor (IL-7R) activation contributes to T-LL development. Gain-of-function *NOTCH1* mutations and aberrant IL-7R expression are frequently detected in human and murine T-LL yet the relative timing of their occurrence in T-LL progression is unclear. Using a spontaneous mouse model of T-LL due to a deficiency of ataxia telangiectasia mutated (ATM), we identified 3 groups of T-LL stratified by active Notch1 (ICN1) expression: truncated ICN1 (T-ICN1, 63%); non-truncated ICN1 (17%); and undetectable ICN1 (UD-ICN1, 20%). Truncated ICN1 resulted from frameshift mutations at the PEST domain, and infrequently HD mutations (9%). In order to study early events in T-LL progression, we identified a proteoglycan, syndecan 1 (SDC1), that is highly expressed on T-LL cells but not normal thymocytes. We screened a cohort of young clinically healthy *Atm*$^{-/-}$ mice and identified an abnormal SDC1^{+} blast subset in mice that otherwise had normal thymic cellularity. We also detected truncated ICN1 and aberrant IL-7R expression in these samples. Collectively, these data suggest that *Notch1* mutations as well as aberrant SDC1 and IL-7R expression arise early during T-cell lymphomagenesis in *Atm*$^{-/-}$ mice, promoting abnormal survival and proliferation.

2.2 Introduction

T lymphoblastic lymphoma/leukemia (T-LL) is a malignancy of lymphoid precursors. The overall incidence of T-cell lymphoblastic leukemia is 0.8 and 0.3 per 100,000 children and adults, respectively. The incidence of T-cell lymphoblastic lymphoma is 0.2 per 100,000 children and 0.3 per 100,000 adults[160]. With conventional multi-agent chemotherapy, the five-year event-free survival rates are 70-90% and 40-60% for children and adults respectively[2,3]. Further improvement in clinical outcome has been hampered by a lack of prognostic markers that can effectively predict at diagnosis the patients who are at high risk of disease relapse so that treatment can be intensified. Moreover, providing long-term cure for those patients who develop a relapse remains a challenge. There is a need for more specific and less toxic therapeutic agents designed to improve overall clinical outcomes. An understanding of how aberrant activation of developmental pathways contributes to the malignant transformation of T-cell progenitors is a prerequisite to design such agents.

Notch signaling plays a critical role in intra-thymic T-cell development and pathological activation of the pathway results in T-LL. There are four mammalian Notch proteins, Notch1-4. Loss-of-function and overexpression of Notch1 suggests its unique requirement in T-lineage specification, commitment and maturation[115,158,272,273]. Notch1 is a transmembrane receptor that, after cleavage by furin-like convertase at the S1, appears as a heterodimer on the cell surface[22,23]. Binding of its extracellular domain to Notch ligands triggers proteolytic events by metalloprotease[38,80] and γ-secretase complex[40], which release the intracellular part of Notch1 (ICN1) from the membrane. ICN1 then translocates to the nucleus, binds to a transcription factor known as recombination signal binding protein for

immunoglobulin kappa J (RBP-J, also known as CSL) to activate transcription of target genes such as *Hes1* and *Dtx1*[90]. Notch signaling is necessary for T-lineage specification and commitment during CD4/8 double negative-1 (DN1), DN2 and DN3 stages. Moreover, Notch signaling promotes proliferation and differentiation of thymocytes in transit from DN3 to CD4/8 double positive (DP), during a process called β-selection [157,158,274]. Collectively, Notch signaling plays an inductive role in intra-thymic early T-cell differentiation.

Interestingly, gain-of-function mutations in the *NOTCH1* gene have been frequently detected in human and mouse T-LLs. Most are clustered in two regions of *NOTCH1*: the heterodimerization (HD) domain and the C-terminal PEST domain[10]. The HD domain together with Lin12-Notch repeats (LNR) form the negative regulatory region (NRR), which normally prevents ligand-independent proteolytic release of ICN1[37]. On the other hand, the PEST domain, which is subjected to ubiquitination by Fbw7 ubiquitin ligase, regulates the half-life of ICN1[43]. Hence, HD and PEST mutations result in ligand-independent release of ICN1 and prolonged intracellular ICN1 stability, respectively[10]. However, it remains unclear whether these mutations promote initiation or maintenance of T-LL.

Interleukin-7 receptor (IL-7R) signaling is required for early T-cell development and aberrant expression of IL-7 and IL-7R contributes to T-LL progression. The IL-7R comprises IL-7R alpha-chain (IL7Rα) and common cytokine receptor γ-chain (γc). Upon ligand binding, IL7Rα and γc heterodimerize[275] and activate downstream signaling, mainly JAK/STAT and PI3K/AKT pathways[247]. In normal T-cell development, IL-7Rα is expressed at the DN2-DN4 stages, absent at the DP stage, and re-expressed in SP cells[138]. Dysregulated expression of IL7Rα in thymic progenitors of AKR/J mice was associated

with spontaneous thymic lymphoma[276]. Furthermore, human T-LL cells frequently express IL-7R and their proliferation can be induced by exogenous IL-7[211,277-279]. Our laboratory has recently demonstrated aberrant expression of IL7Rα by Atm-deficient T-LL cells[280]; however, when this aberration occurs during T-LL development remains to be determined. The answer to this question may have clinical implications, since drugs targeting initiating events are more likely to provide a durable remission by eradicating cancer-propagating clone(s)[248].

In order to study kinetics of *Notch1* mutations and aberrant expression of IL-7Rα in T-LL, we studied a genetically sensitized mouse model involving targeted disruption of *Atm* (ataxia telangiectasia mutated)[264,267]. In order to study early stages of T-LL development, we sought a marker of early transformation. Our previous gene expression profile of $Atm^{-/-}$ T-LLs revealed ectopic expression of *Sdc1* (syndecan-1), a transmembrane heparan-sulfate-bearing proteoglycan. We validated SDC1 expression on the surface of T-LL blasts. Both SDC1 and IL7Rα were detected on thymocytes at the earliest discernible stage of lymphomatous progression, demonstrating only an increased frequency of blasts in clinically healthy $Atm^{-/-}$ mice. Interestingly, thymocytes at this earliest stage of transformation expressed truncated ICN1 resulting from PEST mutations. Therefore, *Notch1* mutations and aberrant IL-7Rα and SDC1 expression can be early events in $Atm^{-/-}$ T-lymphomagenesis.

2.3 Materials and Methods

2.3.1 Mice

129S6/SvEvTac-*Atm*^{tm1Awb}/J heterozygotes[264] (Jackson Laboratory, Bar Harbor, ME) were mated to generate *Atm*$^{-/-}$, *Atm*$^{+/-}$ and *Atm*$^{+/+}$ progeny. B6.129S6-*Rag2*^{tm1Fwa} (*Rag2*$^{-/-}$) mice were purchased (Taconic Farms, Germantown, NY). All mice were housed under pathogen-free conditions at the Toronto Centre for Phenogenomics (Toronto, ON). Pre-malignant thymocytes were harvested from *Atm*$^{-/-}$ mice at 4-6 weeks of age. Thymocytes harvested from moribund *Atm*$^{-/-}$ mice with enlarged thymi were the source of primary T-LL samples, and thymocytes from *Atm*$^{+/+}$ littermates were used for comparisons. All procedures met the requirements set forth by the Guidelines and Policies of the Canadian Council on Animal Care.

2.3.2 Genomic DNA extraction

High molecular weight genomic DNA was prepared from T-LL single cell suspensions by proteinase K digestion, followed by phenol-chloroform extraction[281]. Briefly, 1x10^7 cells were digested in 800 µl of buffer containing 10mM Tris-Cl (pH 8.0), 25 mM EDTA (pH 8.0), 100 mM NaCl, 0.5% SDS and 0.1 mg/ml proteinase K (Invitrogen) for 12-18 hours at 50 ^{o}C. DNA was extracted sequentially with equal volume of phenol (pH 8.0), 25:24:1 (v/v/v) phenol:chloroform:isoamyl alcohol and chloroform. At each extraction step, the top aqueous phase was transferred to a clean tube. After chloroform extraction, DNA was precipitated by increasing the NaCl concentration to 200 mM and adding 2 volumes of ice-cold 100% ethanol. DNA was spooled onto an end-sealed 5-3/4 inch glass pipette and

washed successively in 70% and 100% ethanol, air dried for 5′, resuspended in Tris buffer (pH 8.0) and stored at 4 °C.

2.3.3 Notch1 *mutation analysis*

The following primers were used to amplify exons 26, 27 and 34a of mouse *Notch1* from genomic DNA (45 ng) by phenol-chloroform extraction[281]: HD1_fwd, GCTGAGTTTCTTTAGAGTC; HD1_rev, CCTCCCCTGAGGTTACACCT; HD2_fwd, GAGTGTCCCATTGCGGGGCT; HD2_rev, TGCAGAGGTCAGAAAGTGTT; PEST1_fwd, GCTCCCTCATGTACCTCCTG; PEST1_rev, TGCTGGGTCTGCACCAGGTGA; PEST2_fwd, TACCAGGGCCTGCCCAACAC; PEST2_rev, GCCTCTGGAATGTGGGTGAT. PCR cycling conditions were: 94 ^{o}C for 2'; 35 cycles of 94 ^{o}C for 15", 62 ^{o}C for 30" and 72 ^{o}C for 1'; 72 ^{o}C for 10'. PCR products were purified with QIAquick PCR purification kit (QIAGEN, Toronto, ON) and sequenced at the Toronto Centre of Applied Genomics facility (TCAG, Hospital for Sick Children). In some cases, heteroduplex analysis was used to detect PEST mutations[282]. 5'-FAM-conjugated PEST2_fwd & PEST2_rev primers were used to amplify part of exon 34a where PEST mutations frequently clustered. Amplified products were denatured at 95 ^{o}C for 10 min and then gradually cooled to 40 ^{o}C to form mismatch heteroduplexes in mutated samples. These samples were incubated with CEL I (a mismatch-specific endonuclease) at 40 ^{o}C for 1 h followed by analysis of the fragments with ABI Prism Model 3100 capillary electrophoresis machine and GeneMapper software (Applied Biosystems, Carlsbad, CA).

2.3.4 Western blotting

T-LL cells and thymocytes were lysed in modified RIPA buffer supplemented with phosphatase inhibitor cocktail and protease inhibitor cocktail (Thermo Scientific, Rockford, IL), according to Millipore technical publication mcproto402 (www.millipore.com). Protein concentration was determined by Lowry assay (Bio-rad, Missisauga, ON). Whole cell lysates (15-20 μg) were separated by 8% SDS-PAGE, transferred onto PVDF membrane, which was incubated first with rabbit polyclonal antibody against cleaved Notch1, or rabbit monoclonal antibody against β-actin (Cell Signaling Technology, Danvers, MA), followed by horseradish peroxidase-conjugated secondary goat anti-mouse or anti-rabbit antibodies (Santa Cruz Biotechnology, Santa Cruz, CA). Blots were developed by chemiluminescence using ECL reagents (GE Healthcare).

2.3.5 Flow cytometry

Live single-cell suspensions were prepared from thymi. Once harvested from euthanized mice, thymi were placed in cold staining media (SM: Hank's Balanced Salt solution (HBSS) (Invitrogen, Burlington, ON), 2% calf serum (Wisent, Inc, QC), 10 mM HEPES, pH 7.2 (Wisent, Inc, QC)). Thymi were processed on ice by cutting with non-serrated scissors into small pieces, followed by gentle pressing through 100 um wire mesh with a 3-ml plunger. Cell suspension was then filtered through 70-mm Nitex nylon screen prior to centrifugation at 400 xg for 5 min at 4 ^{o}C. Cell pellets were washed with 20 ml of SM and cells collected by centrifugation. An aliquot of resuspended cells was stained with Trypan blue (Sigma Aldrich,Oakville, ON; 1/4 dilution of stock in 1xPBS, with 2 mM NaN_3) and live cells (unstained) were counted using a hemocytometer (Hausser Scientific, Horsham, PA). 1-2 x

10^6 cells were resuspended in 50 μl of SM containing a saturating amount (pre-determined by titration experiments) of antibodies raised against the following proteins: CD4 (RM4-5), CD8α (53-6.7), CD25 (7D4) and TCRβ (H57-597), CD127(A7R34), CD138 (281-2). These antibodies were conjugated to FITC, PE or APC. All antibodies were purchased from BD Bioscience, eBioscience, or the Sunnybrook and Women's Hospital Research Institute (SWRI) Antibody Core Facility. After incubating for 30 min on ice, cells were washed with 10 volumes of SM, underlaid with 5 volumes of calf serum (CS) and collected by centrifugation. The pellets were resuspended in 500 μl of SM containing 1 μg/ml of propidium iodide (Sigma Aldrich, Oakville, ON) to exclude dead cells. Unstained cells were used for comparison. Stained cells were analyzed by LSR II cytometer (BD) and FlowJo software (Tree Star, Ashland, OR).

2.4 Results

2.4.1 Spontaneous T lymphoblastic lymphomas in $\mathbf{Atm^{-/-}}$ *mice exhibit a spectrum of Notch1 activity*

ATM deficiency resulting in genomic instability that leads to T lymphoblastic lymphoma (T-LL) development may serve as a relevant model for human T-LL[283]. A majority of $Atm^{-/-}$ mice (83%, n=36) died from respiratory failure resulting from thymic lymphomas as reported in prior studies[230,264] (Fig. 2.1A). The median age of disease onset was 17 weeks (range = 9–32 weeks), all $Atm^{+/+}$ or $Atm^{+/-}$ mice remained disease free at 36 weeks of age. We first determined if $Atm^{-/-}$ T-LLs expressed activated Notch1 by Western blotting lysates from 35 primary *ex vivo* samples using an antibody that recognizes an epitope created by γ-secretase-mediated cleavage of Notch1. In wildtype mice, this cleavage generates a ~110 kD ICN1 fragment. As expected from other studies on $Atm^{-/-}$ mice [230,283,284], many T-LLs (63% in this cohort) expressed high levels of truncated ICN1 due to mutations in the C-terminal PEST domain (Fig. 2.1B, Table 2.1). We found PEST mutations in 70% of cases (n=16). In 9 cases, PEST mutations were identified by sequencing genomic PCR products and included missense, as well as nonsense (1756), insertion and deletion mutations that altered reading frame (Table 2.1). Alignment of translated PEST domain sequences showed frame shifts that lead to premature translational stop codons, explaining truncated ICN1 (Fig. 2.2). Importantly, all truncated proteins lacked the degron sequence targeted by Fbw7 for proteasomal degradation[43,202,203], thereby stabilizing ICN1. We identified PEST mutations in the remaining 7 cases using a heteroduplex assay[282], which detects mismatch between mutated and wildtype sequences. In

contrast to the high frequency of PEST mutations, HD mutations were identified in only 2/23 cases (9%), and were thus infrequent, as seen in other murine T-LL models. HD mutations were found in samples also containing PEST mutations (1756 and 6106; Table 2.1). It seems likely that both mutations were present on the same *Notch1* allele in these samples, since 18% of human T-LLs contain compound mono-allelic HD+PEST mutations. Both HD mutations are located in the C-terminal portion of HD. The missense L1668P mutation found in sample 1756 and identified in other murine T-LL models[8,9] and human T-LLs [10], increased susceptibility to ligand-independent metallopreotease cleavage thereby activating a Notch signal[215]. The missense A1710P mutation found in 6106 was novel. Alanine 1710 and valine 1711 span metalloprotease cleavage site, S2, suggesting that this missense mutation might also mediate ligand-independent Notch activation[80].

We detected ICN1 protein with the same apparent molecular weight as wild-type ICN1 in samples that lacked mutations in HD and PEST sequences (Table 2.1). Thus, in these samples with non-truncated (NT-ICN1), Notch1 signaling was activated in the absence of "hotspot" mutations. Finally, other samples lacked detectable ICN1 protein, and were designated undetectable ICN1 (UD-ICN1). Thus, we identified 3 groups of T-LLs based on ICN1 expression that modeled the spectrum of ICN1 expression in human immature T-cell malignancy[285].

2.4.2 Atm$^{-/-}$ T-LLs arrest at an immature stage of T-cell development and aberrantly express syndecan 1

Human T-LLs are frequently arrested at pre-T and cortical thymocyte stages of development[286]. These features are also common in T-lineage leukemias and lymphomas

found in children with ataxia-telangiectasia[287]. We analyzed CD4 and CD8 expression in 40 *Atm*$^{-/-}$ T-LL samples to determine if they exhibited a similar maturation arrest to the human disease. Thymi from mice with T-LL cells contained excessive proportions of large cells with high forward scatter (blasts) than normal thymocytes (Fig. 2.3, panel i) and commonly displayed one of three abnormal immunophenotypic profiles: 1) DP; 2) CD8 single positive (SP); and 3) mixture of DP and CD8 SP (Fig. 2.3, Table 1). Furthermore, these lymphoblasts exhibited low to intermediate level of TCRβ on the cell surface (Fig. 2.3), consistent with their previously documented defect in TCRα rearrangement[271,288,289]. Therefore, similar to human T-LL, *Atm*$^{-/-}$ T-LLs were arrested at CD8 ISP and DP stages of thymocyte differentiation.

A previous gene expression microarray study revealed that syndecan-1 (*Sdc1*) was highly expressed in *Atm*$^{-/-}$ T-LL cells but not normal thymocytes[280]. SDC1 (CD138) is a transmembrane heparan sulfate proteoglycan that binds cytokines[290] and regulates cell adhesion[291]. We validated cell surface expression of SDC1 in all T-LL samples by flow cytometry (Fig. 2.3, panel iv; Table 1). SDC1 was present on T-LL cells with variable CD4/8 profiles, suggesting that it was a useful a marker of malignant transformation in Atm-deficient thymocytes.

2.4.3 SDC1 and IL7Rα expression during T-LL development

We next examined a cohort of apparently healthy 10-17 week-old *Atm*$^{-/-}$ mice for immunophenotypes suggestive of early stages in T-LL development. SDC1 was not expressed in any of the samples lacking features of transformation, i.e. thymic enlargement, abnormal thymocyte numbers[292] (mean = $74x10^6$), increased blast frequency (≤ 15%), or

abnormal CD4/8 profiles (Table 2.2). In contrast, SDC1 was expressed in all samples that displayed these features (Table 2.2); e.g. in mice that were entirely populated by cells at late stages of malignant transformation, as evidenced by increased thymic cellularity (>100 $x10^6$) and cell size (>90% blasts). However, 8 samples had normal thymic cellularity (mean = $77x10^6$) but had notably increased numbers of blasts (mean = 58%). Furthermore, 6 of these showed an abnormal DP and/or CD8 ISP immunophenotype (Table 2.2). The remaining 2 samples (7546 & 7826) showed increased blast fractions (>15%) and abnormal SDC1 expression as the only abnormalities and thus representeding the earliest stage of disease detectable in our cohort. IL7Rα expression mirrored to a great extent that of SDC1 in these cohort samples. IL-7Rα is normally expressed on DN and mature SP subsets but not DP cells[138,139]. Similar to SDC1, IL-7Rα was not detected in DP cells of all 12 samples that lacked other evidence of malignant transformation (Table 2.2). One of the 2 samples that showed the earliest sign of transformation (#7826), i.e. increased blast frequency, expressed IL-7Rα in the DP subset. IL-7Rα was aberrantly expressed in all 8 samples that displayed abnormal CD4/8 profiles. Therefore, both SDC1 and IL7Rα were atypically expressed in early stages of lymphoma progression.

We compared immunophenotypic profiles of thymocytes from *Atm*$^{-/-}$ mice representing distinct stages of lymphoma progression (Fig. 2.4A). Mouse #7833 displayed no evidence of transformation, whereas #7826 demonstrated increased blasts (47%) including SDC1$^+$ (Fig. 2.4A, panel iii) and IL7Rα$^+$ (Fig. 2.4A panel iv) sub-populations despite a relatively normal CD4/8 profile (Fig. 2.4A panel ii). The SDC1$^+$ blasts were arrested at the DP stage (Fig. 2.4A panel v). Samples #7618 and #7465 represented later disease phases evident by higher blast frequency (Fig. 2.4A panel i), and abnormal CD8 ISP

and/or DP thymocyte accumulation (Fig. 2.4A panel ii). Our findings suggested that both SDC1 and IL7Rα were aberrantly expressed at an early stage of lymphoma progression.

2.4.4 Truncated ICN1 marks early stages of lymphoma progression

Since PEST mutations resulting in expression of T-ICN1 occurred frequently in *Atm*$^{-/-}$ T-LLs, we assessed ICN1 expression during different stages of lymphoma progression in thymocytes from a cohort of 23 apparently healthy *Atm*$^{-/-}$ mice. Six of the 8 thymi with normal thymocyte numbers but increased blast frequency also expressed T-ICN1 (Table 2.2). Three out of four samples expressed T-ICN1 (Fig. 2.4B). Importantly, sample 7826 expressed markers of the earliest stage of disease expressed T-ICN1. Therefore, aberrant Notch1 activation occurs at an early stage of T-LL progression in this mouse model.

Table 2.1 Summary of CD4/8 profiles, ICN1 and SDC1 expression, HD and PEST domain mutation status of 41 T-LL samples. Nucleotide position corresponds to *Notch1* coding DNA reference sequence (NM_0087714.3). Amino acid substitutions resulting from missense HD mutations are indicated. *PEST mutations were detected by heteroduplex assay. HD=heterodimerization domain; WT=wildtype sequence; ND=not determined. ICN1 was detected by Val1744 antibody: T=truncated; NT=non-truncated; UD=undetectable.

Mouse ID	CD4/8 profile	HD mutation	PEST mutation	ICN1 status	SDC1 expression
10	CD8 ISP, DP	WT	c.7544_7545insC	ND	ND
1124	CD8 ISP	ND	ND	T	Y
1178	DP	ND	ND	UD	Y
1536	DP	ND	ND	T	ND
1690	CD8 ISP, DP	WT	c.7082delinsCCC	T	ND
1752	CD8 ISP	ND	ND	T	ND
1755	DP	WT	WT	UD	ND
1756	CD8 ISP	c.5003T>C (p.L1668P)	c.7300C>T	T	ND
1898	DP	ND	ND	UD	ND
1902	DP	ND	ND	T	Y
1910	DP	WT	WT	NT	ND
1927	CD8 ISP	ND	ND	T	Y
1975	DP	WT	Yes*	T	ND
2037	CD8 ISP, DP	WT	Yes*	T	ND
2103	DP	ND	ND	NT	Y
2170	CD8 ISP	WT	Yes*	T	Y
2313	CD8 ISP, DP	WT	c.7195_7196insGG c.7417T>A; c.7437_7438del; c.7442C>T	T	Y
2317	CD8 ISP	ND	ND	T	Y
2490	DP	WT	WT	NT	Y
2612	DP	ND	ND	T	Y
2633	DP	ND	ND	NT	Y
2967	DP	WT	Yes*	T	Y
2971	DP	WT	WT	NT	Y
3157	CD8 ISP	ND	ND	T	Y
3169	CD8 ISP	WT	c7402delinsGC	ND	ND
3496	CD8 ISP	WT	c.7082G>C; c7083_7084insC	T	Y
4299	DP	WT	WT	UD	ND
5052	CD8 ISP	ND	ND	T	Y
5173	DP	WT	Yes*	T	ND
5290	DN, CD8 ISP	ND	ND	T	ND
5759	DN, CD4 SP	ND	ND	NT	Y
6106	CD8 ISP, DP	c.5128G>C (p.A1710P)	Yes*	T	Y
6620	CD8 ISP, DP	WT	c.7352_7364delTGACCACTAC CCA	T	Y
6625	DP, CD4 SP	ND	ND	UD	Y
6652	DP	ND	ND	UD	Y
6658	CD8 ISP, DP	WT	Yes*	T	Y
6924	DP	ND	ND	UD	Y
6925	DP, CD4 SP	WT	c.7082delinsAAAAA	T	Y
8528	DN, CD8 ISP	WT	WT*	ND	ND
8641	CD8 ISP	WT	WT	ND	ND
9000	CD8 ISP, DP	WT	c.7082G>C; c7083_7084insC	ND	ND

Table 2.2 Summary of immunophenotypic profiles, SDC1, IL7Rα and truncated ICN1 expression in thymocytes from 22 *Atm*$^{-/-}$ mice. CD4, CD8, IL7Rα and SDC1 expression was determined by flow cytometry. Detection of truncated ICN1 was determined by immunoblotting of whole cell lysate prepared from thymocytes.

Mouse ID	Age (wk)	No. of live cells (x10^6)	% Blasts	CD4/8 Profile	SDC1 Expression	IL7Rα Expression	Truncated ICN1
D7009	17.5	15	14	Normal	−	−	−
D7016	17	52	11	Normal	−	−	−
D7007	16.5	100	11	Normal	−	−	−
7472	14	127	11	Normal	−	−	−
7531	12.5	76	15	Normal	−	−	−
7532	12.5	83	15	Normal	−	−	−
7535	12.5	88	9	Normal	−	−	−
7543	12.5	88	11	Normal	−	−	−
7664	11	52	13	Normal	−	−	−
7665	11	105	13	Normal	−	−	−
7833	10.5	40	10	Normal	−	−	−
7814	10	70	13	Normal	−	−	−
7546	12	94	53	Normal	+	−	−
7826	10.5	55	47	Normal	+	+	+
7534	12.5	86	36	CD8 ISP, DP	+	+	+
7855	10	29	37	CD8 ISP, DP	+	+	+
7618	12	106	76	CD8 ISP, DP	+	+	+
7835	11	100	90	CD8 ISP, DP	+	+	+
7620	12	86	65	DP	+	+	+
7832	10	59	60	DP	+	+	−
D7145	16	228	94	DP	+	+	+
7465	14	276	98	DP	+	+	+

A.

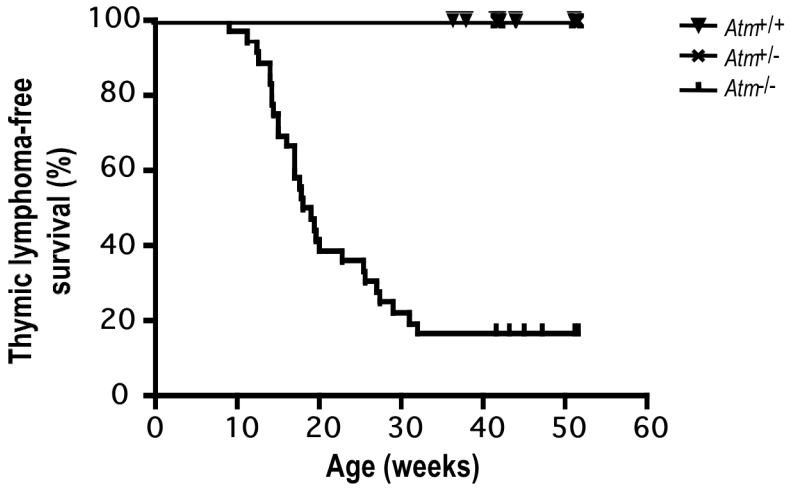

B.

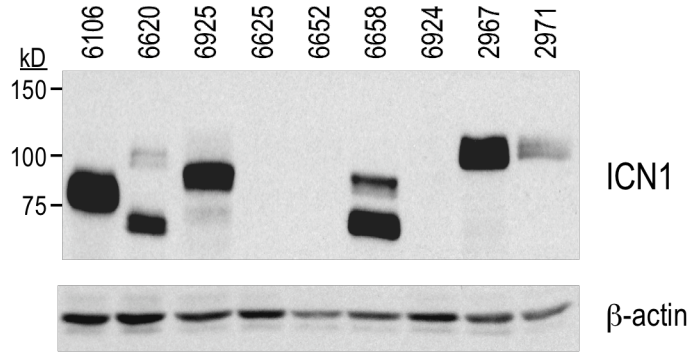

Figure 2.1 Spontaneous T-LL development in *Atm*$^{-/-}$ mice and ICN1 expression in *Atm*$^{-/-}$ T-LLs. (A) Thymic lymphoma-free survival in *Atm*$^{-/-}$ (n=36, |), *Atm*$^{+/-}$ (n=6, ×) and *Atm*$^{+/+}$ (n=6,▼) mice. (B) Western blotting for ICN1 expression in whole cell lysate prepared from 9 T-LL samples. T-LL 2971 contains ICN1 of wildtype size, ~110 kD.

Figure 2.2 Alignment of translated PEST mutations found in 9 T-LL samples. The top sequence represents reference Notch1 protein sequence (NP_032740.3) and numbers indicate amino acid positions. Underlined are amino acid sequences generated by frame-shifting insertions and deletions. * indicates end of sequence due to stop codon. Highlighted in red is Fbw7 degron sequence.

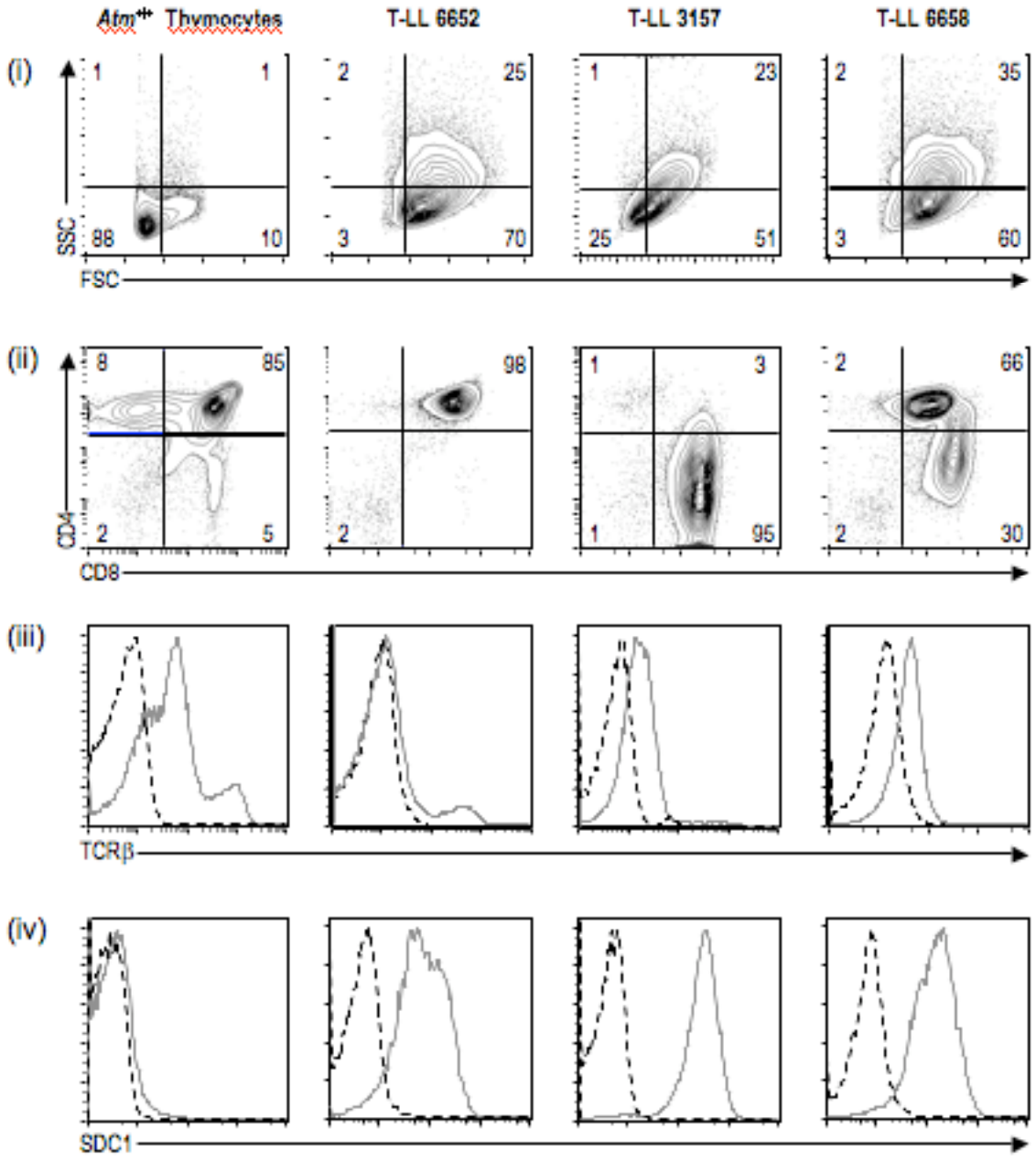

Figure 2.3 Immunophenotypic profiles of T-LL samples. Flow cytometric analysis of *Atm*$^{+/+}$ thymocytes and 3 representative T-LL samples. (i) SSC vs. FSC profiles; (ii) CD4 vs. CD8 staining profiles (number in quadrant gates represent percentage of cells). (iii) TCRβ surface staining; (iv) SDC1 surface staining (dashed line represents isotype control).

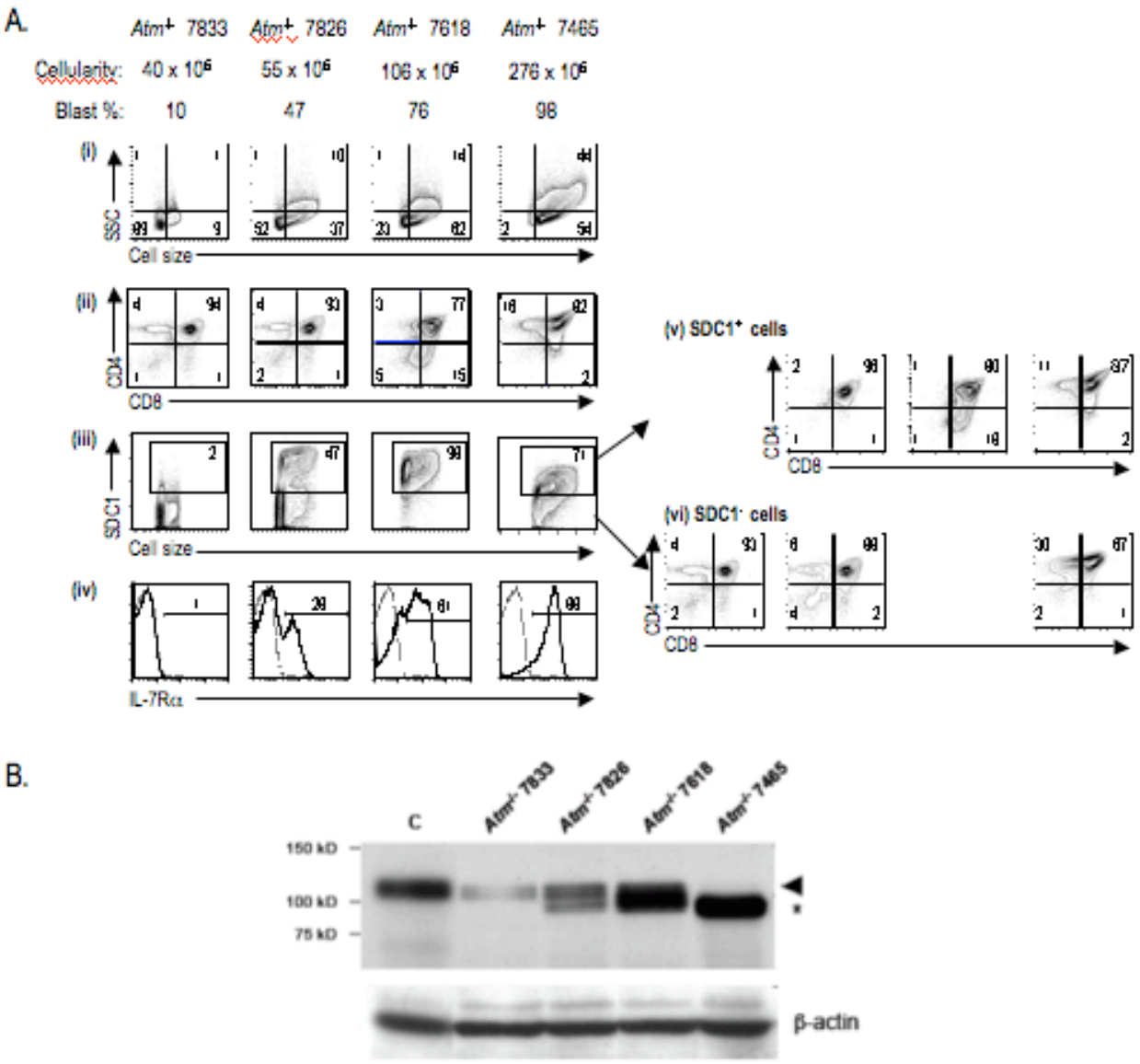

Figure 2.4 Immunophenotypic profiles and ICN1 expression of thymocytes harvested from 4 *Atm*$^{-/-}$ mice (10-14 wks) at different stages of lymphoma development. (A) Flow cytometry phenotypic profiles. (i) Side scatter vs. cell size profiles. (ii) CD4 vs. CD8 profiles. (iii) SDC1 expression vs. cell size (positive gate was set to include 1% of *Atm*$^{+/+}$ thymocytes from littermate control). iv) Expression of IL-7Rα was determined for CD4/CD8 DP subsets of *Atm*$^{-/-}$ 7833 & 7826 and bulk populations of *Atm*$^{-/-}$ 7618 & 7465 (dashed line: IL-7Rα expression by *Atm*$^{+/+}$ DP thymocytes; positive gate was set to include 1% of *Atm*$^{+/+}$ DP cells). (v) CD4 vs. CD8 profiles of SDC1^{+} cells. (vi) CD4 vs. CD8 profiles of SDC1^{-} cells. Numbers in quandrants indicate percentage of subsets. (B) Notch expression at different stages of T-LL progression. Whole cell lysate (WCL) prepared from thymocytes was subjected to immunoblotting for ICN1 (◄indicated non-truncated ICN1; * represents truncated protein). 'C' represents WCL prepared from 4-wk-old *Rag2*$^{-/-}$ thymus. β-actin shown as a loading control.

2.5 Discussion

In this study, we define 3 subgroups of T-LL with different levels of Notch activity that arise spontaneously in mice lacking the *Atm* tumor suppressor. In agreement with prior studies[230,283], we found that most *Atm*$^{-/-}$ T-LLs (63% in our cohort of 35 samples) had HD and/or PEST mutations in *Notch1*, similar to those found in human T-LL. Accordingly, this T-ICN1 subgroup expressed high levels of known *Notch1* target genes and grew in a Notch-dependent fashion. Although most T-ICN1 samples had PEST but not HD mutations, one sample harbored a novel alanine to proline substitution at position 1710 in the HD region. A prior study showed that substituting glutamine for alanine at this position allows ligand-independent ICN1 production[80]. Although it is possible that the proline at position 1710 might impair metalloprotease cleavage, we speculate that this bulky residue likely would nonetheless disrupt conformation of the negative regulatory region to allow ligand-independent γ-secretase cleavage and ICN1 release.

The timing of *Notch1* mutation in T-LL progression may have therapeutic implications since drugs targeting initiating events may eradicate initiating cells that perpetuate the disease, hence achieving a durable remission[248]. In order to study early transformation, we needed a protein marker that distinguished transformed cells from normal thymocytes. Our previous gene expression profiling study of *Atm*$^{-/-}$ T-LL samples suggested ectopic expression of *Sdc1* when compared to pre-malignant *Atm*$^{-/-}$ thymocytes. Here, we validated expression of SDC1 as an early harbinger of T-LL. SDC1 was also detected in thymi with normal CD4/8 profiles and absolute cell numbers harvested from clinically healthy *Atm*$^{-/-}$ mice. The only appreciable abnormality that accompanied SDC1

expression was an increased frequency of blasts likely representing the earliest discernible stage of T-LL transformation. One such sample also had detectable truncated ICN1. Therefore *Notch1* mutations can be an early event in T-LL progression in $Atm^{-/-}$ mice.

Notch1 mutations have also been identified as an early transforming event in other murine T-LL models. TAL1/SCL and LMO (LMO1 or LMO2) are ectopically expressed in 50-60% human T-LLs[176]. Not surprisingly, $SCL^{tg}LMO1^{tg}$ mice[8,293] and a related model, *Tal1/Lmo2* mice[294] develop T-LL which frequently harbor *Notch1* mutations. In the pre-leukemic phase, both models show accumulation of DN3 and DN4 progenitors carrying *Notch1* PEST mutations. In these studies, serial transplantation experiments identified leukemia-initiating potential enriched in DN3 and/or DN4 populations. Notch inhibition decreased leukemia-initiating cell frequency and delayed disease onset[294]. Enforced expression of constitutively active ICN1 at the DN2 stage in $Notch1^{tg}SCL^{tg}LMO1^{tg}$ mice accelerated the onset of leukemia and conferred leukemogenic potential to DN1-4 progenitors from pre-leukemic mice[293]. These findings suggest that aberrant Notch1 activation may occur early and drive T-LL transformation.

In Ikaros-deficient mice, aberrant Notch activation can be observed at different stages of T-LL progression. In hypomorphic Ikaros ($Ik^{L/L}$) expressing mice, upregulation of Notch targets, *Hes1* and *Dtx1* was detected in pre-malignant DP thymocytes[224], however it was not clear whether these abnormalities were linked to gain-of-function *Notch1* mutations. In contrast, in Ikaros-null ($Ikzf1^{-/-}$) mice, accumulation of ICN1 and increased levels of its transcriptional targets were detected only at a late stage of transformation characterized by increased thymic cellularity and an abnormal population of $CD8^{+}TCR\alpha\beta^{int/hi}$ or $CD4^{+}CD8^{+}$ $TCR\alpha\beta^{int/hi}$ blasts[295]. Collectively, these data suggest that *Notch1* mutations can be an early

event that confer disease-initiating potential or, alternatively, may occur later in T-LL progression, suggesting that accumulation of genetic changes rather than the order of their appearance is key to the neoplastic transformation in T-LL[296].

Activating *NOTCH1* mutations have also been reported as an early and possibly initiating event in human T-LL development[297]. Specifically, HD mutation was detected in a neonatal Guthrie blood spot obtained from a patient diagnosed with T-LL at 7 years of age. At diagnosis, both *NOTCH1* HD mutation and a secondary event, a *SIL-TAL1* fusion transcript, were identified. These results suggest the likely prenatal origin of *NOTCH1* mutations and secondary genetic changes acquired postnatally, such as *SIL-TAL1* fusion, are required to complete the transformation process.

The earliest discernible stage of T-LL transformation seen in $Atm^{-/-}$ mice is reminiscent of the pre-leukemic phase seen in adult patients with ataxia-telangiectasia (AT). Unlike children with AT who are prone to develop T-LL, adult AT patients are predisposed to develop mature peripheral T-cell leukemia known as prolymphocytic leukemia (T-PLL). For some patients, the diagnosis of T-PLL can be preceded by 1-15 years of an abnormal circulating T-cell clone marked by translocations. Interestingly, this clone gradually takes over the T-cell compartment without elevating the absolute lymphocyte count[287], similar to the finding reported here that normal thymocyte numbers can be maintained in $SDC1^{+}$ $Atm^{-/-}$ thymi with *Notch1* mutations. Transformation to T-PLL occurs upon acquisition of additional cytogenetic changes, which facilitate elevation of circulating lymphocyte number. Additional oncogenic events are therefore likely required for pre-malignant thymocytes in $Atm^{-/-}$ mice to escape cell number regulation.

IL-7 promotes survival and proliferation of T-LL cells, and dysregulated expression of IL-7 or IL-7R is oncogenic[276,277,279,298]. Surprisingly, enforced expression of IL7Rα throughout T-cell development resulted in a decreased thymocyte number in adult *Il7ra*-transgenic mice, due to competition with DP progeny for a limited supply of endogenous IL-7 in the thymus[137]. Hence, downregulation of IL-7R by DP cells in wildtype thymus has been termed an 'altruistic' act to ensure adequate supply of IL-7 for DN subsets. Indeed, in IL-7- and IL7Rα-deficient mice, αβ T-cell development still occurs, albeit with a dramatic reduction in thymocyte number[299,300], implying a role for IL-7R signaling in controlling thymic size. Our results show aberrant expression of both SDC1 and IL7Rα at an early stage of lymphoma development. SDC1 is a transmembrane proteoglycan that bears heparan sulfate chains that mediate cell adhesion and migration by binding to extracellular matrix[301-303]. One proposed mechanism for syndecan-mediated growth regulation is via the extracellular heparan sulfate (HS) chains, which limit diffusion of growth factors and serve as a reservoir for HS-binding growth factors[304]. Indeed, enzymatic removal of heparan sulfate on SDC1-expressing pro-B cells dramatically reduces binding and responsiveness to IL-7, which is critical for early B-cell development[305]. Therefore SDC1 expression by T-LL may positively regulate IL-7R-driven signal by capturing IL-7 through their HS moieties. Further studies are required to examine whether changes in SDC1 expression alter IL-7 dose responsiveness in T-LL cells.

2.6 Acknowledgements

The authors thank B. Apresto and S. Pullenayegum (at the TCAG, Hospital for Sick Children) for DNA sequencing. This work was supported by the Genome Canada grant to J.S.D. and C.J.G. Salary support for PPCW was provided by the Terry Fox Foundation, Canadian Child Health and Clinician Scientist Program, Christopher Brundage Endowment Fund and the Division of Haematology/Oncology, the Hospital for Sick Children.

CHAPTER 3:

IDENTIFICATION OF TRUNCATED *NOTCH1* TRANSCRIPTS IN NOTCH-DEPENDENT *ATM*$^{-/-}$ T-LLS

Peggy P. C. Wong[1,3,5], Bertrand Montpellier[4], Irina R. Matei[1,5], Stephen G. Chang[4], Queenie C. K. Cheung[4], Jayne S. Danska[1,2,5], and Cynthia J. Guidos[2,4]

[1]Department of Medical Biophysics, [2]Department of Immunology, University of Toronto, Toronto ON M5G 2M9
[3]Division of Haematology/Oncology, Department of Paediatrics, the Hospital for Sick Children, Toronto ON M5G 1X8
[4]Program in Developmental and Stem Cell Biology, the Hospital for Sick Children, Toronto ON M5G 1L7
[5]Program in Genetics and Genome Biology, the Hospital for Sick Children, Toronto ON M5G 1L7

Author contributions:
All experiments and data analysis in this chapter were performed by P. Wong with the following exceptions: Notch1 genomic PCR was performed by B. Montpellier. I. Grandal and P. Wong prepared RNA from T-LL samples. B. Montpellier, S. Chang, Q. Cheung and P. Wong performed GSI *in vitro* culture experiments. I. Matei and P. Wong performed T-LL OP9 coculture experiments.

3. IDENTIFICATION OF TRUNCATED *NOTCH1* TRANSCRIPTS IN NOTCH-DEPENDENT *ATM*$^{-/-}$ T-LLS

3.1 Abstract

Gain-of-function *NOTCH1* mutations have been identified in ~60% of human T-LL and activating HD domain mutations predominate. However, murine T-LL models arising from diverse genetic background reveal a paucity of HD mutations, instead PEST mutations that result in increased intracellular Notch1 stability occur commonly. Recent reports identify two types of intragenic deletions that lead to ligand-independent Notch1 activation. Types 1 and 2 deletions initiate transcription within exon 25 and at exon 1, respectively. Using *Atm*$^{-/-}$ mice as a spontaneous T-LL model, we identified PEST mutations in 70% of T-LLs, of which only 9% of cases concomitantly harbored HD mutations. However, T-LL cells lacking HD mutations proliferate in a Notch-ligand-independent fashion. We hypothesized that these cases harbored intragenic deletions. Yet, we only found Types 1 and 2 deletions in 4% and 13% of T-LL cases respectively. Eight ICN1+ T-LL samples contain truncated *Notch1* mRNA and their sequences initiate either in the middle of exons 25/26 or exon 1a, an exon upstream of exon 1. All truncated transcripts contain the intramembranous methionine M^{1727} that has been shown to be the translation start site for truncated Notch1 proteins in previous studies. Collectively, our data identify truncated *Notch1* transcripts in *Atm*$^{-/-}$ T-LLs that likely encode Notch1 polypeptides that undergo oncogenic activation.

3.2 Introduction

Notch signaling plays critical roles in normal development and disease. There are 4 mammalian Notch proteins, Notch1-4, of which Notch1 is best characterized. Notch1 is synthesized as a precursor type I transmembrane polypeptide that is cleaved by furin convertase at the Golgi, forming a heterodimer. At the cell surface, interaction between the extracellular EGF repeats of Notch1 with ligand leads to displacement of LNR repeats, which shields the S2 cleavage site. Together, the HD and LNR repeats are known as the negative regulatory region (NRR). ADAM metalloprotease-mediated S2 cleavage is a prerequisite for proteolysis at the intramembranous S3 site by γ-secretase complex, which releases the intracellular portion of Notch1 (ICN1) from the membrane. ICN1 translocates to the nucleus and activates target gene transcription via the DNA-binding transcription factor CSL. The Notch signal is shut off when ubiquitin ligase Fbw7 recognizes a phosphorylated degron located in the C-terminal PEST domain, thereby targeting ICN1 for proteosomal degradation[43]. Thus, Notch regulates important developmental processes by activating target gene expression and of its signal duration must therefore be precisely controlled.

Aberrant Notch signal causes cancer. The first clue came from identification of a chromosomal translocation t(7;9)(q34;q34.3), which juxtaposes the intracellular half of *NOTCH1* downstream of the TCRβ joining region, in <1% of human T-LL[21]. Importantly, constitutive expression of a truncated form of NOTCH1 in mouse bone marrow progenitors causes T-LL, hence establishing the oncogenic potential of NOTCH1[214]. Gain-of-function *NOTCH1* mutations were found subsequently in ~60% of human T-LL cases[10]. These

mutations can be categorized into two groups. The first consists of truncating PEST mutations that remove degron sequence hence increasing its stability[202,203]. Mutations that allow ligand-independent NOTCH1 activation form the second group and these include mutations in the NRR that destabilize the HD domain (class 1) or enhance sensitivity to metalloprotease at S2 site (class 2)[215]. PEST and HD mutations are found in 12% and 26% of human T-LLs, respectively; moreover, both mutations occur in 18% of human T-LLs[10]. These *NOTCH1* mutations are identified in all molecular subtypes of T-LLs including *TAL1*$^+$, *LYL1*$^+$, *HOX11*$^+$, *HOX11L2*$^+$, *LMO1*$^+$, *LMO2*$^+$, suggesting aberrant Notch signal as a key contributor to T-LL development[176]. Amino acid insertions that expand the NOTCH1 juxtamembrane extracellular region are functionally similar to class 2 HD mutations and have been identified in 3% of human T-LLs[216]. Survival and proliferation of these T-LLs are dependent on Notch signaling. Hence functional *NOTCH1* mutations frequently occur in human T-LLs.

Mouse models of T-LL also frequently acquire *Notch1* mutations, however the spectrum of mutations differs from that seen in humans. Nonsense and frame-shifting PEST mutations are detected in 30-90% of T-LLs arising from transgenic mice of diverse genetic backgrounds including those with deregulated expression of Tal1[9], Lmo1[8], E2A[223], Ikaros[224] as well as in radiation-[231] or chemical-induced T-LLs[6]. In contrast HD mutations are rarely detected (0-10%) in these T-LL models. Functional studies on *Notch1* mutations suggest that PEST mutations alone weakly activate Notch1 and are not capable of initiating T-LL development[221]. Yet, most of these T-LL cells are sensitive to Notch inhibition by γ-secretase *in vitro*, indicating that their survival and proliferation are dependent on Notch.

Thus, the mechanism of Notch1 activation in mouse T-LL models lacking HD mutations remains unclear.

Two recent studies identify novel activating *Notch1* mutations in murine T-LLs[232,233]. Ashworth and colleagues identify 2 types of intragenic *Notch1* deletions that result in abnormal transcripts lacking the extracellular ligand-binding domain. Both types of transcripts code for truncated Notch1 proteins that undergo ligand-independent but γ-secretase-dependent activation. The 2 types of transcripts differ in their transcription start sites: type 1 transcripts initiate transcription at cryptic sites in the middle of exon 25 due to genomic deletion spanning exon 1 and the normal *Notch1* promoter; whereas, type 2 transcripts begin at exon 1 which is spliced into exons 27/28 as a result of intragenic deletion between intron 1 and exons 26-28. Furthermore, type 1 deletions are flanked by recombination signal sequence (RSS)-like sequences and involve addition of bases consistent with N- and P nucleotides, suggesting that RAG-mediated non-homologous end joining as a likely mechanism for deletion. In a different mouse T-LL model, Jeannet and colleagues deleted exon 1 and *Notch1* promoter, which gives rise to truncated mRNA similar to type 1 transcripts. These findings suggest that ligand-independent Notch1 activation is highly selected for and identify deletion-based mechanisms for oncogenic Notch1 activation.

In this study, we find that 70% of $Atm^{-/-}$ T-LLs contain PEST mutations giving rise to truncated ICN1, whereas only 9% of T-LLs concomitantly harbor HD mutations. ICN1+ T-LL samples are sensitive to Notch inhibition by γ-secretase inhibitor, suggesting that their *in vitro* expansion is Notch-dependent. Yet, proliferation of T-LL cells lacking HD mutation does not require Notch ligand interaction. We hypothesize that these cases harbor Type 1 or

Type 2 deletions[232]. However, we find Type 1 and Type 2 deletions in only 4% and 13% of cases, respectively. Eight ICN1+ T-LL samples contain truncated *Notch1* mRNA and their sequences initiate either in the middle of exons 25/26 or exon 1a, an exon upstream of exon 1. All truncated transcripts contain the intramembranous methionine that has been shown to represent a translation start site for Notch1 proteins in previous studies[232,233]. Collectively, our data identify truncated *Notch1* transcripts in $Atm^{-/-}$ T-LLs that likely code for Notch1 polypeptides with oncogenic potential.

3.3 Materials and Methods

3.3.1 Mice

129S6/SvEvTac-*Atm*^{tm1Awb}/J heterozygotes[264] (Jackson Laboratory, Bar Harbor, ME) were mated to generate *Atm*$^{-/-}$, *Atm*$^{+/-}$ and *Atm*$^{+/+}$ progeny. B6.129S6-*Rag2*^{tm1Fwa} (*Rag2*$^{-/-}$) mice were purchased (Taconic Farms, Germantown, NY). All mice were housed under pathogen-free conditions at the Toronto Centre for Phenogenomics (Toronto, ON). Pre-malignant thymocytes were harvested from *Atm*$^{-/-}$ mice at 4-6 weeks of age. Thymocytes harvested from moribund *Atm*$^{-/-}$ mice with enlarged thymi were the source of primary T-LL samples, and thymocytes from *Atm*$^{+/+}$ littermates were used for comparison. All procedures met requirements set forth by the Guidelines and Policies of the Canadian Council on Animal Care.

3.3.2 T-LL culture

Single cell suspensions were prepared from enlarged thymic masses removed from moribund *Atm*$^{-/-}$ mice under sterile conditions. Live cells were identified by Trypan blue exclusion and resuspended at 2 x 10^6 cells/ml of T-LL media: RPMI 1640 media (Wisent, St-Bruno, QC) containing sodium pyruvate, glutamine, non-essential amino acids, HEPES, 2-mercaptoethanol, penicillin (100 U/ml, Invitrogen), streptomycin (100 μg/ml, Invitrogen), and 10% (v/v) fetal bovine serum (FBS, Invitrogen). Cells were grown in the presence of 10 ng/ml of recombinant mouse interleukin-7 (IL-7, Peprotech, Rocky Hill, NJ). Where indicated, cells were incubated with either 1 μM of GSI X (Calbiochem, Billerica, MA) or

0.1% (v/v) DMSO vehicle control for 48 hours. CellTiter-Blue reagent (Promega, Madison, WI) was used according to manufacturer's instructions to assay viability.

3.3.3 Co-culture of T-LLs on OP9 stromal cell lines

Mouse bone marrow stromal OP9 and OP9-DL1 cell lines were provided by Juan-Carlos Zuniga-Pflucker (Toronto) and were maintained as described previously[157]. Stromal cell lines were passaged in OP9 media: α-MEM, 20% FBS, penicillin and streptomycin (all from Invitrogen). A day prior to experiment, 2 x 10^4 stromal cells were plated in each well of a 24-well plate in 250 μl of OP9 media. Cocultures were established by adding 5 x 10^3 T-LL cells (in 250 μl of T-LL media) into each well containing 5 ng/ml of IL-7. Cells were incubated at 37 ^oC in a humidified atmosphere with 5% CO_2. T-LLs cells were harvested at indicated timepoint to determine live cell number from triplicate wells by Trypan-blue exclusion.

3.3.4 Genomic DNA extraction

High molecular weight genomic DNA was prepared from T-LL single cell suspensions by proteinase K digestion, followed by phenol-chloroform extraction[281]. Briefly, 1x10^7 cells were digested in 800 μl of buffer containing 10mM Tris-Cl (pH 8.0), 25 mM EDTA (pH 8.0), 100 mM NaCl, 0.5% SDS and 0.1 mg/ml proteinase K (Invitrogen) for 12-18 hours at 50 ^oC. DNA was extracted sequentially with an equal volume of phenol (pH 8.0), 25:24:1 (v/v/v) phenol:chloroform:isoamyl alcohol and chloroform. At each extraction step, the top aqueous phase was transferred to a clean tube. After chloroform extraction, DNA was precipitated by increasing the NaCl concentration to 200 mM and by adding 2 volumes of

ice-cold 100% ethanol. DNA was spooled onto an end-sealed 5-3/4 inch glass pipette and washed successively in 70% and 100% ethanol, air dried for 5′, resuspended in Tris buffer (pH 8.0) and stored at 4 °C.

3.3.5 Detection of Notch1 *deletions by genomic PCR*

The DNA fragments with *Notch1* deletions were amplified from T-LL genomic DNA (30-150 ng) by PCR using Phusion® Hot Start II high-fidelity DNA polymerase (Thermo Fisher Scientific). The following primer pairs were used to detect type 1 and 2 deletions as previously described[232]: N1_intron1a_fwd, ATGGTGGAATGCCTACTTTGTA and N1_intron1_rev, CGTTTGGGTAGAAGAGATGCTTTAC; N1_intron1_fwd, TCTACCCATGGTGGAATGCCTAC and N1_exon28_rev, GCCCACAAAGAACAGGAGCACGAA. A final concentration of 300 nM was used for each primer. The cycling conditions for detecting *Notch1* deletions were: 98 ^{o}C for 2'; 35 cycles of 98 ^{o}C for 10", 64 ^{o}C for 30" and 72 ^{o}C for 90"; 72 ^{o}C for 5'. After agarose gel electrophoresis, the PCR products were purified with QIAquick PCR purification kit (QIAGEN, Toronto, ON) and sequenced at the Toronto Centre of Applied Genomics facility (TCAG, Hospital for Sick Children).

3.3.6 Total RNA extraction and poly(A) mRNA enrichment

Total RNA was extracted from T-LL cells and *Rag2*$^{-/-}$ thymocytes using either the guanidinium thiocyanate-phenol-chloroform method[306] or an RNeasy Plus Mini Kit (QIAGEN, Toronto, ON). RNA integrity quality control was performed on the Agilent 2100 Bioanalyzer (Illumina, San Diego, CA) analysis. Poly(A) mRNA was purified from total RNA using the MicroPoly(A)Purist™ Kit (Ambion, Inc.). Briefly, 20-50 μg of total

RNA was mixed with oligo(dT) cellulose to enrich poly(A) mRNA for 60 min at room temperature. The oligo(dT) cellulose was washed twice before elution of poly(A) RNA. The eluted RNA was precipitated with 100% ethanol, washed with 70% ethanol, air dried for 5' and resuspended in RNA storage solution. Total and poly(A) RNA was quantitated with NanoDrop spectrophotometer (Thermo Scientific).

3.3.7 Northern blotting

Total RNA was electrophoresed in 1% agarose containing 1X MOPS and 3%(v/v) formaldehyde for 16 h at 55 V. RNA was transferred to Nylon membranes in 20X SSC after washing with 0.05 N NaOH and neutralizing with 2X SSC. RNA was UV cross-linked to membranes and hybridized with ^{32}P-labelled *Notch1* cDNA fragments (corresponding to exon 34a) obtained from restriction digest of *Notch1* cDNA plasmid with EcoRV and HindIII overnight at 42 ^{o}C. Membranes were washed with 1X SSC/0.1% SDS twice for 10 min followed by 2x5' washes with 0.2X SSC/0.1% SDS at 65 ^{o}C. X-ray film was developed after 2-5 days of exposure at -80 ^{o}C. Membranes were stripped and reprobed with *Hprt* cDNA as loading control.

3.3.8 Rapid amplification of cDNA ends (RACE)

RACE was performed using 50-200 ng poly(A) mRNA and the FirstChoice® RLM-RACE kit (Ambion, Inc.) according to manufacturer's instrunctions. The poly(A) selected RNA was treated with calf intestinal alkaline phosphatase (CIP) to remove free 5'-phosphates from fragmented mRNA, or contaminating genomic DNA, rRNA and tRNA. The CIP reaction was terminated by phenol:chloroform and chloroform extraction steps. The CIP-treated RNA was then treated with tobacco acid pyrophosphatase (TAP) to remove 7-

methylguanosine caps found at the 5' end of intact mRNA. The decapped mRNA with a free 5'-monophosphate was ligated to a 45-base RNA adaptor using T4 RNA ligase. The ligated RNA was reversed transcribed with random primers to give cDNA, which was subjected to 2 different nested PCR amplifications using Expand Long Template PCR system (Roche Applied Science), as well as 5' outer and inner adaptor primers: RACE_adaptor_outer_fwd, GCTGATGGCGATGAATGAACACTG; RACE_adaptor_inner_fwd, GAACACTGCGTTTGCTGGCTTTGATG. Two pairs of *Notch1* specific 3' outer and inner primers were used: 1) N1_e28_RACE_rev (outer), GCCCACAAAGAACAGGAGCACGAA, and N1_e27_RACE_rev (inner), CACACATTGCCGGTTGTCGATCTC; 2) N1_e31_RACE_rev (outer), CAGCAGGTGCATCTTCTTCT, and N1_e30_RACE_rev, (inner) GCTCCTCAAACCGGAACTTCT. The first set of *Notch1* specific RACE primers was described previously by Jon Aster's group[232]. The PCR conditions were the same for outer and inner reactions: 94 ^{o}C for 2'; 35 cycles of 94 ^{o}C for 15", 60 ^{o}C for 30" and 68 ^{o}C for 5'; 68 ^{o}C for 7'. After agarose gel electrophoresis, RACE products were purified, cloned and sequenced at the Toronto Centre of Applied Genomics facility (TCAG, Hospital for Sick Children). Cloning of RACE products was performed using a TOPO® TA Cloning® kit (Invitrogen) according to manufacturer's instructions. The potential open reading frame (ORF) of RACE products was determined using the ATGpr program[307] (Helix Research Institute, http:// atgpr.dbcls.jp/).

3.3.9 Western blotting

T-LL cells and thymocytes were lysed in modified RIPA buffer supplemented with phosphatase inhibitor cocktail and protease inhibitor cocktail (Thermo Scientific, Rockford,

IL), according to Millipore technical publication mcproto402 (www.millipore.com). Protein concentration was determined by Lowry assay (Bio-rad, Missisauga, ON). Whole cell lysates (15-20 μg) were separated by 8% SDS-PAGE, transferred onto PVDF membrane, and these were incubated first with rabbit polyclonal antibody against cleaved Notch1, or rabbit monoclonal antibody against β-actin (Cell Signaling Technology, Danvers, MA), followed by horseradish peroxidase-conjugated secondary goat anti-mouse or anti-rabbit antibodies (Santa Cruz Biotechnology, Santa Cruz, CA). Blots were developed by chemiluminescence using ECL reagents (GE Healthcare).

3.4 RESULTS

3.4.1 Short-term proliferation of ICN1+ Atm$^{-/-}$ T-LL cells does not depend on Notch ligands

As shown in chapter 2, 80% of *Atm*$^{-/-}$ T-LLs (29 of 36 cases) expressed ICN1 (Table 2.1) and here we demonstrated sensitivity of a cohort of 10 ICN1-expressing T-LL samples to Notch inhibition. The viability of all tested samples decreased by 40-90% after 48-72 hours of *in vitro* exposure to γ-secretase inhibitor, GSI (Fig. 3.1A). Furthermore, to confirm that GSI treatment prevented ICN1 production, we measured ICN1 level in 5 T-LL samples by immunoblotting with an antibody that recognizes the valine 1744 epitope created by γ-secretase-mediated cleavage, and found that GSI diminished or abrogated ICN1 as represented by sample 5759 (Fig. 3.1A). These data suggest that expansion of ICN1+ T-LLs was dependent on Notch activation. Since gain-of-function *Notch1* mutations contribute to human and animal models of T-LL[10,214,308], we test for these. Indeed, we found that 70% of *Atm*$^{-/-}$ T-LL cases (16 of 23 cases) contained PEST mutations; whereas only 2 cases (9%) concomitantly harbored ligand-independent activating HD mutations (Table 2.1). It seems likely that both mutations were present on the same *Notch1* allele in these samples, since 18% of human T-LLs contain compound mono-allelic HD+PEST mutations[10]. Both HD mutations are located in the C-terminal portion of HD. The missense mutation found in sample 1756 (p.L1668P) was identified in other murine T-LL models[8,9] and some human T-LLs (p.L1679P)[10], which increased susceptibility to metallopreotease cleavage in a ligand-independent fashion, thereby activating Notch signal[215]. However, the missense mutation (c.5128G>C) found in 6106 that resulted in A1710P amino acid substitution was novel.

Notably, alanine 1710 and valine 1711 normally span the metalloprotease cleavage site (S2), and missense mutation of either might mediate ligand-independent Notch activation as well[80].

The infrequent occurrence of HD mutations suggested that most ICN+ T-LLs required ligand interaction for Notch activation. To determine whether proliferation of these T-LL samples was reliant on ligand-dependent Notch activation, we co-cultured T-LL cells on a bone marrow stroma-derived cell line, OP9, overexpressing Notch ligand Delta-like 1 (OP9-DL1) that induces T-cell differentiation of hematopoietic progenitors *in vitro*[309]. We measured proliferative expansion of ICN1-expressing T-LL cells on control OP9 vs. OP9-DL1 stromal cells over 2 days (between days 3 and 5 of culture). The expansion of T-LLs ranged from 2.8 to 7 folds and 4 to 7.7 folds when cultured on OP9 and OP9-DL1 cells, respectively (Fig. 3.1B) and was not significantly different. Moreover, no statistically significant difference was observed in the number of live T-LL cells recovered on days 3 and 5 between the two co-culturing conditions. In summary, these results demonstrated that although *in vitro* expansion of these ICN1+ T-LL samples was Notch1-dependent, Notch1 activation occurred in a ligand-independent fashion.

3.4.2 Intragenic Notch1 *deletions detected in some T-LLs*

During the course of our investigation, we became aware of studies showing abnormal transcripts resulting from deletions involving the 5' end of *Notch1* that resulted in ligand-independent activation[231,232]. We used the same sets of primers from the study by Ashworth *et al.* to determine if 23 of T-LL samples showed deletions of 5' deletions. We amplified *Notch1* genomic sequences between introns 1a and 2, as well as between introns 1

and 27. PCR products from these reactions were sequenced to look for Type 1 and Type 2 intragenic deletions, respectively. Type 1 deletions, which likely occur via RAG-mediated non-homologous end joining, lack exon 1 and its upstream promoter, hence transcription begins at a cryptic promoter located within exon 25. In contrast, Type 2 deletions involve region from intron 1 to exons 26-28, hence the truncated transcripts contain exon 1. Although Type 1 and Type 2 intragenic *Notch1* deletions are highly prevalent in other murine T-LL models[232], in our cohort of 23 ICN1-expressing $Atm^{-/-}$ T-LLs, Type 1 and Type 2 deletions occurred in only 1 (4%) and 3 (13%) of samples, respectively. Sample 8652 had a deletion from nucleotide 4927 (intron 1a) to nucleotide 16673 (intron 2) that was similar to RAG-mediated Type 1 deletions characterized by Ashworth *et al*., since the deleted region was flanked by putative recombination signal sequences and the junction contained non-templated N- and P-nucleotides (Fig. 3.2A). This large deletion would include the normal transcriptional start site for *Notch1* upstream of exon 1, allowing for abnormal transcription initiation from a cryptic promoter in exon 25, as recently described[232,233,295]. In contrast, samples 2967, 2740 and 6620 had even larger genomic deletion from intron 1 to either intron 26 or 27 (Fig. 3.2B), similar to deletions that result in Type 2 transcripts described by Ashworth *et al.* In summary, Type 1 and Type 2 deletions were found in 17% of ICN1+ T-LLs.

3.4.3 Identification of truncated Notch1 *transcripts in T-LLs*

To determine whether deletions lead to aberrant Notch1 transcripts, we performed Northern blotting to characterize *Notch1* mRNA in 10 ICN1+ T-LLs using a *Notch1* probe corresponding to part of exon 34a. We chose this probe for two reasons: 1) it encodes part

of ICN1; 2) it is likely to capture most of the truncated transcripts resulting from intragenic deletions. Two samples harboring HD and PEST mutations (1756 and 6106) contained only full-length major (9.3 kb) and minor (8 kb) *Notch1* mRNA transcripts (Fig. 3). The difference in length between major and minor transcripts is due to different transcription termination. The former contains exons 1-34b and the latter contains exons 1-34a[231]. Because exon 34b contains only non-coding sequence, the open reading frame is identical between major and minor transcripts. The 9.3 kb *Notch1* mRNA predominated in *Rag2*$^{-/-}$ thymocytes. Notably, the remaining 8 examples lacking HD mutations all contained abnormal truncated transcripts, in addition to the 9.3 and 8.0 kb full-length transcripts. Samples 1910, 2971, 2490, 6925, 6658, and 8652 expressed two truncated *Notch1* transcripts of approximately 3.5 kb and 5 kb. In 2967, the truncated transcripts were smaller in size, about 3 kb and 4.5 kb. Both 1910 and 2971 also contained 2.6 kb transcripts. Sample 6658 also contained a prominent 7.5 kb band and sample 1910 contained an additional faint 6 kb band. Finally, sample 3496 contained faint 9.3 kb and 3.2 kb transcripts. Collectively, T-LL samples lacking HD mutations expressed truncated *Notch1* transcripts that contain the last exon encoding for the C-terminal intracellular domains.

3.4.4 Truncated Notch1 *transcripts start at sites other than exon 1*

In order to characterize the 5'ends of truncated *Notch1* mRNA transcripts, we performed 5' rapid amplification of cDNA ends (RACE) by ligating an adaptor oligonucleotide to the 5' ends of mRNA, which was followed by reverse transcription. The cDNAs were then used as templates for nested PCR amplification with 5' adaptor primer and 3' *Notch1* specific primers corresponding to exons 27/28 or exons 30/31 in order to

capture most of the truncated transcripts. RACE product sequences are shown in Fig. 3.4 and summarized schematically in Fig. 3.5. We were unable to identify the transcription initiation sites of 7.5 kb (in 6658) or 6 kb (in 1910) transcripts by RACE possibly because the long transcript length was not amplified efficiently. Most 5'RACE products began in the middle of exon 25 (1910, 2971, 6925, 8652 and 6658) or exon 26 (3496). T-LL samples with transcripts initiated in exon 25 expressed two truncated *Notch1* transcripts of approximately 3.5 kb and 5 kb detected by Northern blotting (Fig. 3.3). This size difference corresponded to the length of exon 34b (1.3 kb); hence they likely resulted from different transcription termination as observed in other studies[232]. Sample 3496 contained a RACE product that began in exon 26, which likely corresponded to the 3.2 kb mRNA detected by Northern blotting. The RACE product in sample 1910 started in the middle of exon 25; furthermore, due to a splicing error, the splice donor site occurred at the 5th nucleotide of intron 25, rather than at the 5' end, resulting in an extra 4 nucleotides at the splice junction of exons 25 and 26. The truncated transcripts in sample 2967 started 83 nucleotides upstream of exon 1a, followed by exons 1b and 1c, which was spliced to exon 28 and presumably continued to the end of exon 34 (Fig. 3.4B). The transcription start site upstream of exon 1a contained a transcription initiator (Inr) element CTA^{+1}CTCA that matched closely to the consensus sequence, YYA^{+1}NWYY[310]. Interestingly, sample 2967 harbored a genomic deletion downstream of exon 1 (Fig. 3.1B); yet, despite the predicted presence of exon 1, transcription began upstream of exon 1a suggesting that the deleted region likely contained elements important for proper promoter activity at exon 1. Indeed, exon 1a has been identified as an alternative transcription initiation site in thymocytes and radiation-induced T-LLs[231]. The predicted size of abnormal transcripts ending with exon

34a or exon 34 b would be 3.3 kb and 4.5 kb, which approximated the size of truncated transcripts seen in Fig. 3.3. In summary, the 5' RACE studies identified transcriptional starts for truncated transcripts in exons 1a, 25 and 26.

We used the ATGpr program to identify potential ATG (methionine) translation initiation codons followed by an open reading frame (ORF) in each 5' RACE product. The ATGpr prediction criteria include conservation of the Kozak consensus sequence [A/G]xxATGG from analysis of 660 initiation codon-containing DNA sequences[307]. The most likely initiator methionine for each sample is shown in Fig. 3.5 and the predicted polypeptide sequences for each truncated transcript are shown in Fig. 3.6. In sample 1910, the polypeptide was predicted to initiate at an ATG codon with a strong Kozak consensus (GggATGG, Fig. 3.4A) at nucleotide 48266 of the *Notch1* gene. Since the ATG codon was not in frame with the coding sequence of *Notch1*, the initial 55 amino acids did not correspond to the Notch1 protein sequence. However, due to an insertion of 4 intronic nucleotides at the exon 25/26 junction, the protein sequence was put back into frame at the 56th amino acid, which corresponded to amino acid 1529 of Notch1 (Fig. 3.6). The putative initiator methionine was immediately followed by a 12-residue hydrophobic segment that could serve as a signal sequence. However, the absence of a hydrophilic region preceding the hydrophobic segment was atypical[311]. This predicted polypeptide lacked the first 2 LNR repeats that would likely disrupt NRR function to allow ligand-independent Notch1 activation.

The initiator methionine for RACE products found in samples 2971, 6925, 8652, 6658 and 3496 was predicted to correspond to amino acid 1615 of Notch1, which would allow expression of a truncated Notch1 protein lacking all 3 LNR repeats but retaining the

S1, S2 and S3 proteolytic cleavage sites. Following the initiator methionine, a hydrophilic region (positions 1622 to 1633) including positively charged amino acids such as arginine (R) and lysine (K), followed by a hydrophobic segment (position 1636-1648) could serve as signal sequence[311]. Lastly, in sample 2967 the first in-frame ATG codon was located in exon 28 and encoded for methionine at position 1727. The hydrophobic segment immediately following Met^{1727} (positions 1728 to 1747) possibly functioned both as a signal sequence and a transmembrane segment as in a start-stop transfer sequence[311]. Importantly, the predicted translation products of all RACE products would retain the S3 γ-secretase cleavage site.

3.4.5 T-LL cells containing aberrant transcripts express γ-secretase-cleaved ICN1 proteins

Since all truncated transcripts were predicted to encode proteins containing the Notch1 transmembrane domain and S3 site in exon 28, we next determined whether truncated proteins were cleaved by γ-secretase. Lysates from T-LL samples were analyzed by Western blotting with an antibody specific for V1744, the first residue of γ-secretase cleaved Notch1. All samples contained γ-secretase cleaved Notch1 that were ≤ 110 kD (Fig. 3.7 and Fig. 2.1B). Sample 1756 contained a HD mutation that has previously been demonstrated to result in ligand-independent Notch activation[215] and a PEST mutation that truncated 100 amino acids from the carboxyl terminus of ICN1, giving rise to a 75-kD product. Similarly, sample 6106 contained a ~85 kD truncated ICN1 (Fig. 2.1B). It was likely that both types of mutations occurred in the same alleles since only one protein size

was detected. Samples 1910, 2490 (Fig. 3.7) and 2971 (Fig. 2.1B) contained truncated Notch1 proteins with an intact PEST domain, hence 110-kD protein was observed in all three samples. The remaining samples (3496, 6106, 6925, 2967, 6658) contained truncated ICN1 of varying size likely due to different locations of PEST mutations (Table 2.1; Fig. 2.1, 2.2 and 3.7). Truncated ICN1 that likely resulted from PEST mutations detected in samples 6106, 6925, 6658 and 2967 was relatively more abundant than ICN1 containing wildtype PEST domain found in sample 2971 (Fig. 2.1B). This was consistent with the idea that PEST mutations result in removal of the degron sequence that signals for proteosomal degradation, hence increasing ICN1 stability[43]. These results demonstrate that T-LL samples that contain abnormal *Notch1* transcripts express γ-secretase-cleaved ICN1 protein. Collectively, we detected truncated *Notch1* transcripts that started in the middle of exons 25, 26 and upstream of exon 1a. 17% of T-LL samples also contain intragenic *Notch1* deletions that might result in truncated mRNA. All aberrant transcripts lacked part or all of NRR region but retained γ-secretase S3 cleavage site in T-LL samples. Consistent with these findings, most of these transcripts were found in T-LLs that were sensitive to Notch inhibition by GSI and expressed γ-secretase-cleaved ICN1 but proliferated in Notch ligand-independent fashion.

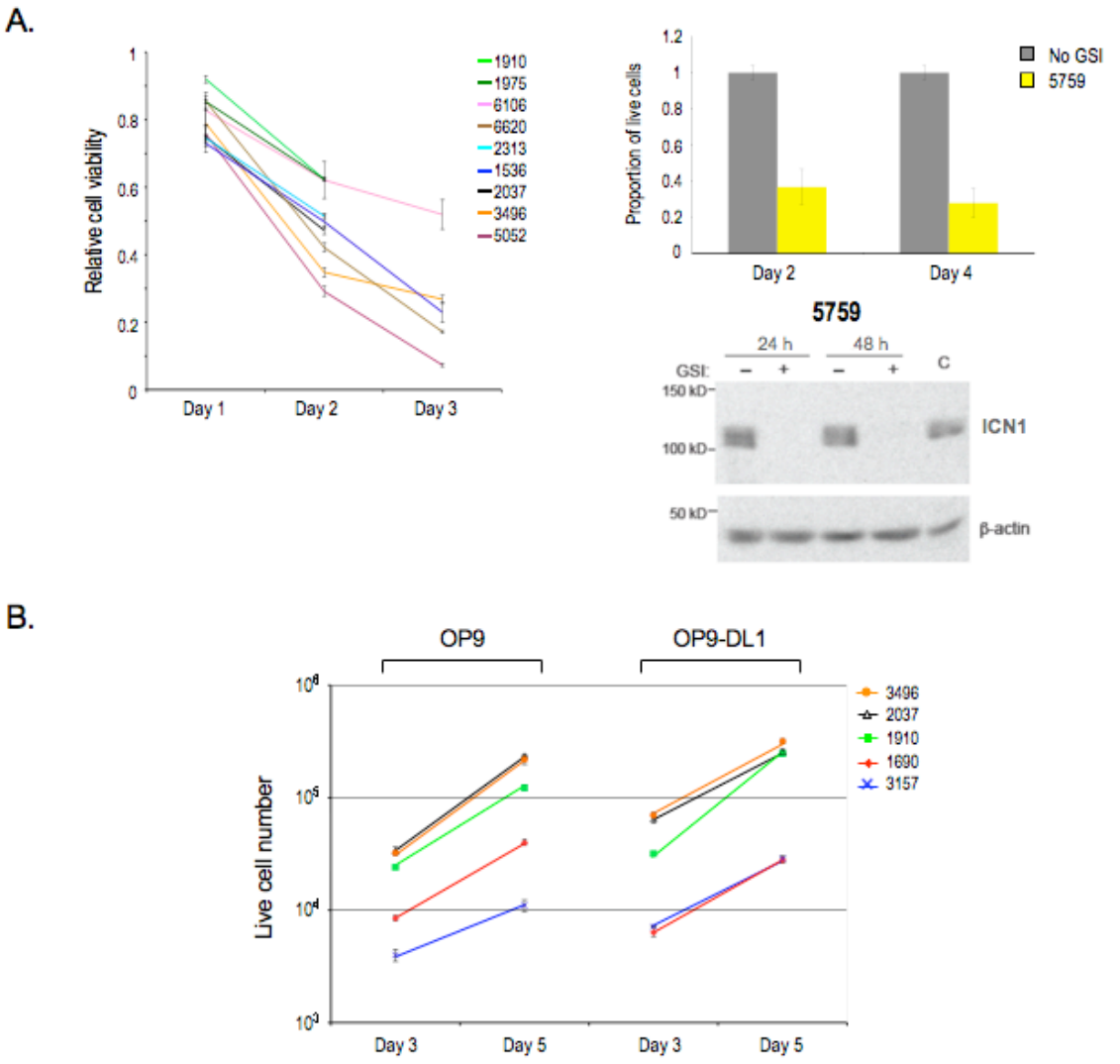

Figure 3.1 Notch ligand-independent proliferation of ICN1-expressing T-LLs. (A) Sensitivity of T-LL cells to Notch inhibitor was determined by CellTiter-Blue viability assay or Trypan-blue exclusion after *in vitro* culture with 1 μM γ-secretase inhibitor X (GSI) or 0.1% (v/v) of DMSO in the presence of 10 ng/ml of IL-7. Relative viability was calculated as the ratio of fluorescence measurements between GSI-treated and DMSO-treated cells. Whole cell lysate (10 μg) prepared from T-LL 5759 cells cultured as above after 24 and 48 hours was immunoblotted for ICN1. (B) Freshly harvested T-LLs cells (5 x 10^3) were cultured in triplicates on OP9 or OP9-DL1 monolayers for 3 or 5 days before determining viable cell counts. Average number of live cells was determined from triplicate wells. (B) Proliferation of T-LLs cells is greatly reduced by GSI and is associated with abrogation of ICN1.

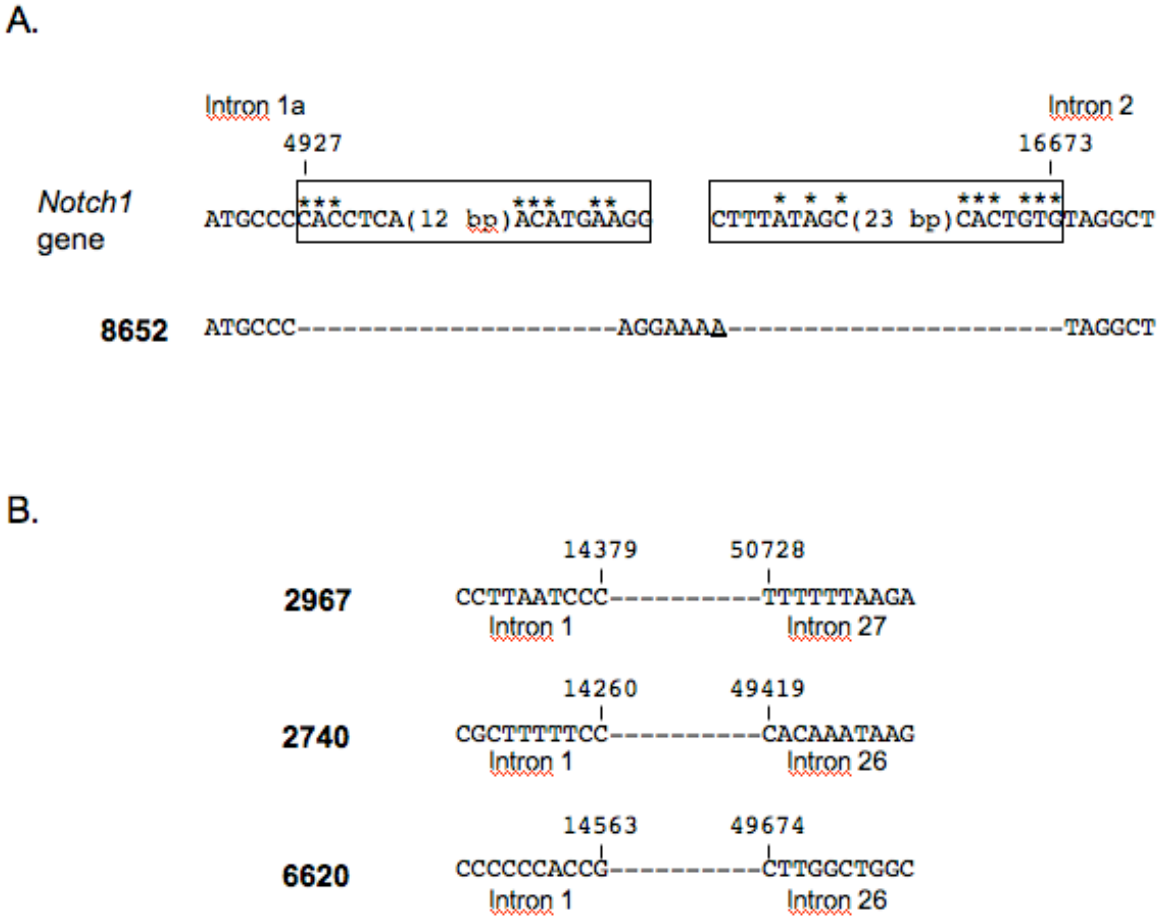

Figure 3.2 ***Notch1*** **gene deletions in T-LL samples**. Total DNA isolated from primary T-LL cells was subjected to amplification with 2 primer pairs: 1) intron 1a and intron 2 primers; and 2) intron 1 and intron 27 primers. The PCR products were gel electrophoresed and then sequenced. Samples 8652, 2967, 2740 and 6620 contain deletions at the *Notch1* gene. The deleted region of 8652 contains recombination signal-like sequences (RSS, indicated by rectangle) at 5' and 3' ends. RSS contains 12- or 23-bp spacer flanked by conserved heptamer and nonamer (* indicates conserved nucleotides). In the middle are N- and P-nucleotides (underlined) that were added at the joining. In 2967, a deletion between nucleotides 14379 (in intron 1) to 50728 (in intron 27) was observed. In 2740 and 6620, deletions were identified between introns 1 and 26 at nucleotides 14260-49419 and nucleotides 14563-49674, respectively. The reference *Notch1* gene sequence used is AB100603.1 from GenBank.

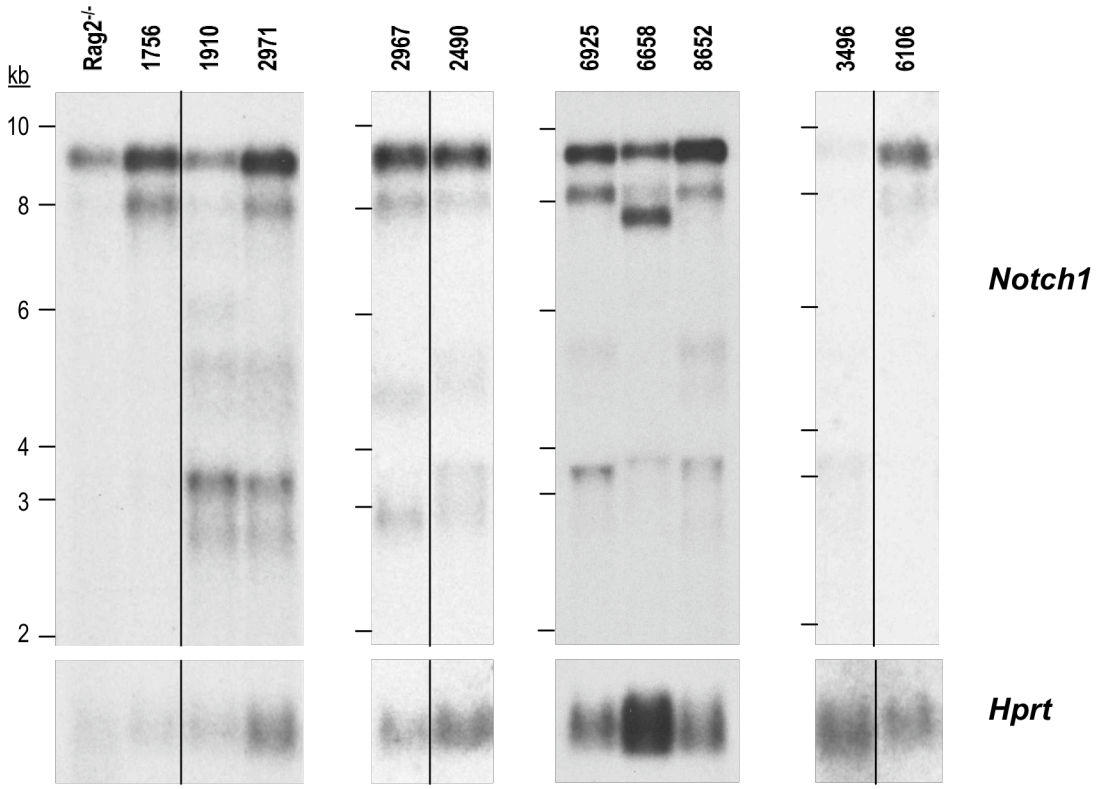

Figure 3.3 Notch1-dependent T-LLs contain truncated *Notch1* mRNA transcripts. Total RNA (9-12 μg) from *Rag2*$^{-/-}$ thymocytes and T-LLs was gel-electrophoresed, transferred to nylon membrane and hybridized with ^{32}P-labeled *Notch1* exon 34a and *Hprt* (as a loading control) cDNA probes sequentially. Full-length wildtype *Notch1* transcripts are 9.3 kb and 8 kb. The size of *Hprt* transcript is 1.4 kb.

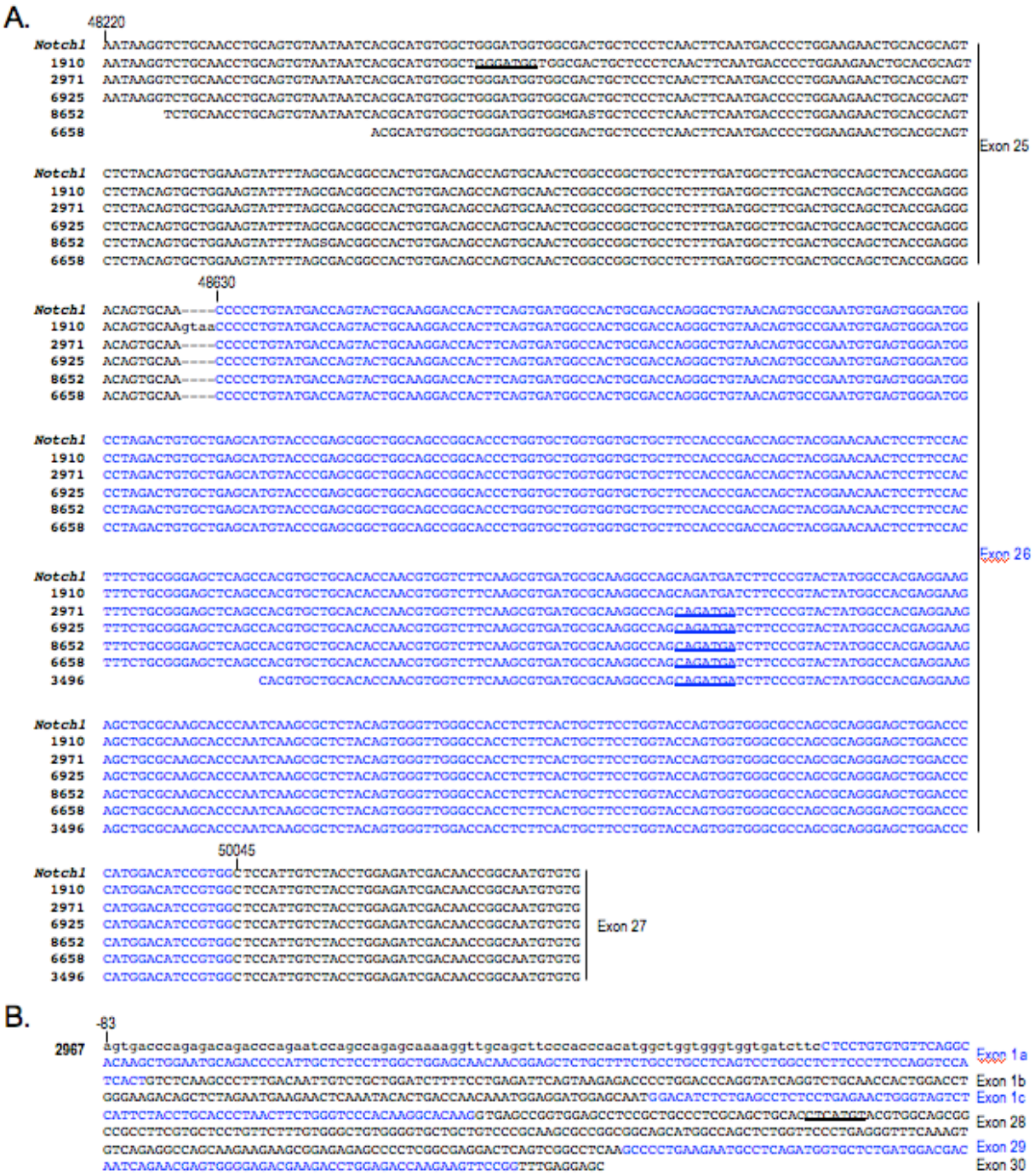

Figure 3.4 Sequences of 5' RACE products. Poly(A) mRNA isolated from T-LL cells was ligated to an adaptor at the 5' end, reversed transcribed and subjected to nested amplification with an adaptor primer and *Notch1* specific exons 27/28 in (A) or 30/31 primers in (B). RACE products were purified by gel electrophoresis, cloned and then sequenced. Nucleotide 48220 is located in the middle of exon 25. The 5' sequences of all RACE products correspond to the inner RACE adaptor sequence. Lowercase represents intronic sequence. Different exons are distinguished by alternating black and blue color. Number on top of the sequence corresponds to position in reference *Notch1* gene (GenBank AB100603.1). Underlined are Kozak sequences that contain possible translation initiation ATG codon. In 1910, gtaa corresponds to the first 4 nucleotides of intron 25.

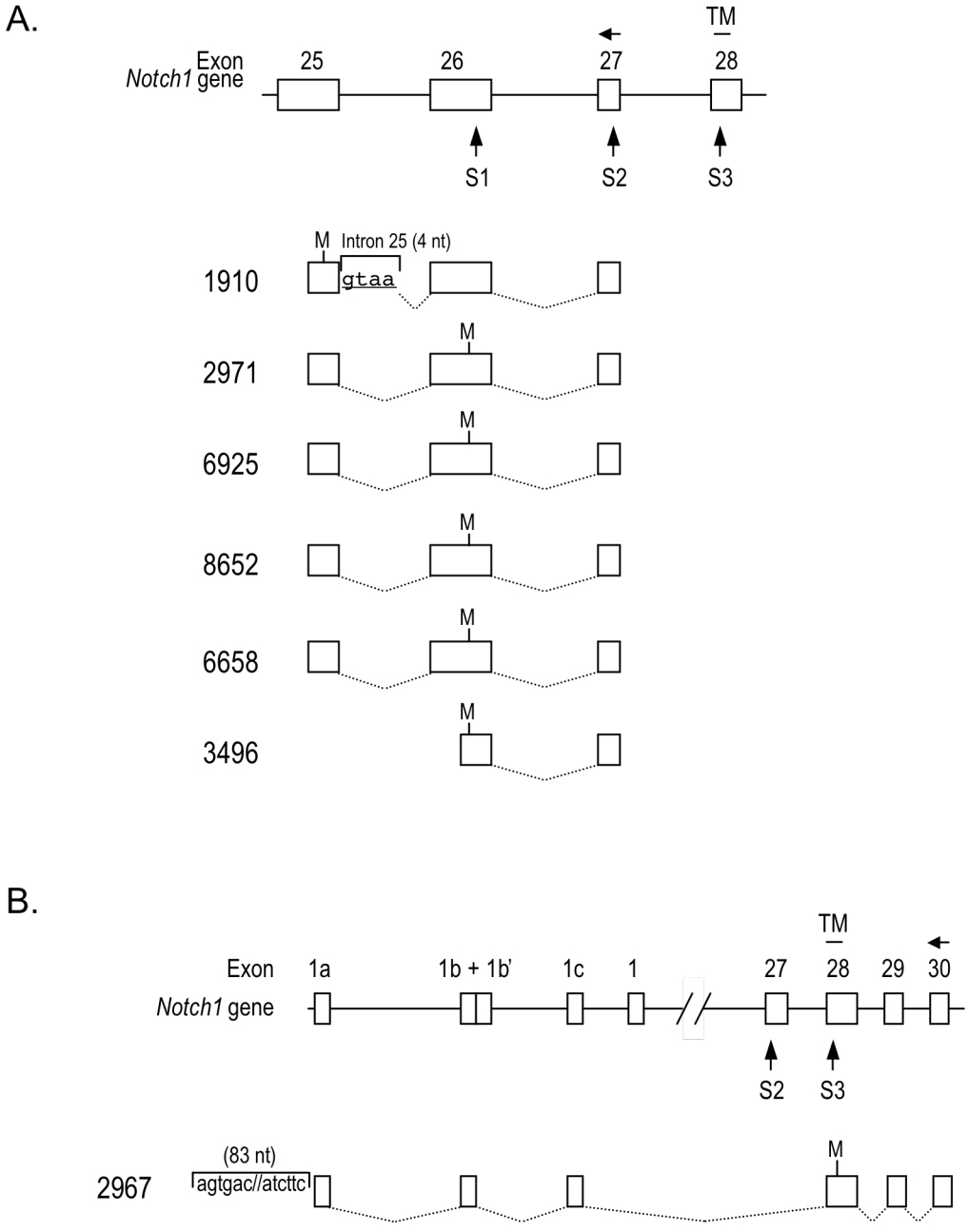

Figure 3.5 Truncated *Notch1* transcripts start at sites other than exon 1. Schematic diagrams showing RACE products as detailed in Fig. 3.4. *Notch1* specific inner primers at exon 27 (A) and exon 30 (B) are represented by horizontal arrow. In sample 2967, transcription initiation site occurred at 83 nucleotides (nt) upstream of first base of exon 1a. TM represents transmembrane domain. S1, S2 and S3 denote proteolytic cleavage sites of furin-convertase, ADAM10 metalloprotease and γ-secretase complex, respectively. M indicates potential translation initiation methionine as predicted by the ATGpr program.

Figure 3.6 Predicted amino acid sequences of 5' RACE products. The amino acid position is shown on top of the Notch1 reference sequence. LNR-C denotes the third Lin12-Notch repeat. S1, S2, S3 indicate proteolytic cleavage sites. TM represents transmembrane domain. Underlined methionines (first amino acid of 1910, at 1615 and 1727) represent putative translation initiation sites predicted by ATGpr program. In 1910, translated sequence began out-of-frame (gray letters), and it was put back into reading frame by a 4-nucleotide insertion (see Fig. 3.4).

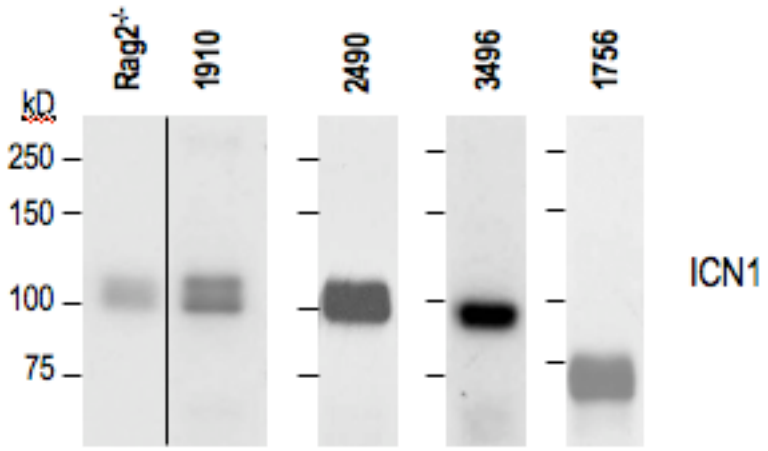

Figure 3.7 Detection of ICN1 in T-LL samples. Western blotting of whole cell lysates from T-LL samples and *Rag2*$^{-/-}$ thymocytes for ICN1 with an antibody that recognize γ-secretase-cleaved Notch1.

3.5 Discussion

The goal of this study is to determine how *Atm*$^{-/-}$ T-LL cells activate Notch signaling since HD mutations that render ligand-independent Notch1 activation occur rarely. Surprisingly, T-LLs cells lacking HD mutations do not depend on ligand binding *in vitro* for their proliferation even though they are Notch-dependent. These results suggest that an alternative ligand-independent mechanism of Notch activation must be operative in these cells. Indeed a recent study has reported spontaneous development of two types of intragenic deletions as mechanisms for aberrantly activating Notch signal in a ligand-independent manner from other genetic models of T-LL[232]. Type 1 deletions occur at breakpoints in intron 1a (upstream of exon 1) and intron 2. These deletions have also been reported in radiation-induced and *Atm*$^{-/-}$ thymic lymphomas[229,230]; however, their functional consequences in the *Atm*$^{-/-}$ model have not been determined. Notably, deleted regions contain RS-sequences on both ends, suggesting that illegitimate V(D)J recombination was responsible. These deletions remove exon 1 and promote intragenic transcription within exon 25 resulting in truncated transcripts lacking extracellular ligand-binding sequences and part of the NRR. These truncated transcripts are also detected when exon 1 and its promoter have been targeted for deletion in Ikaros-deficient thymic lymphomas[233]. In this study we identified truncated transcripts lacking exon 1 in Notch-dependent *Atm*$^{-/-}$ T-LLs. The detection of truncated *Notch1* transcripts in T-LLs arising from diverse genetic background suggest that ligand-independent activation of Notch is highly selected for during T-LL development.

When we looked for RAG-mediated Type 1 deletions by genomic PCR, we found these in 4% of *Atm*$^{-/-}$ T-LL, in contrast to >75% incidence found in other studies[232,233]. Tsuji *et al*. also reported a lower frequency of RSS-flanked *Notch1* deletions in their *Atm*$^{-/-}$ T-LL cohort (24%)[230]. The relative low frequency of RAG-mediated deletion observed in ATM-deficient T-LLs may be related to ATM's function in repair of double-strand DNA break (DSB). Indeed, a loss of γ-H2AX foci has been observed in ATM-deficient cells and is indicative of defective DSB repair[312]. Moreover, in ATM-deficient lymphocytes, a partial block in coding join formation results in accumulation of unrepaired coding ends[271,289,313]. Thus, ATM deficiency compromises the fidelity of non-homologous recombination repair, which may explain the lower incidence of Type 1 deletions observed in *Atm*$^{-/-}$ T-LLs. Tsuji *et al*. identified deletions without RSS in 41% of *Atm*$^{-/-}$ T-LL cases, which were accompanied by microhomology sequences or nucleotide additions at their breakpoints[230]. The deleted regions (nucleotides 5105-25304) in these cases often lied outside of the Type 1 deleted region, hence the primers used here to amplify regions containing Type 1 deletions (nucleotides 4760-17005) would fail to detect such non-RAG-mediated deletions. Most non-RSS-mediated deletions remove exons 1b, 1c, 1 and 2[230]. ATM deficiency also causes an increased frequency of intrachromosomal homologous recombination that can result in intragenic deletions[314], possibly involving repetitive DNA sequences such as Alu repeats or long interspersed elements (LINE). Non-allelic homogolous recombination has been described as a mechanism for genomic deletions of *NF1*[315], causing the tumor-predisposition syndrome neurofibromatosis. Moreover, non-homologous recombination between Alu and LINE-1 repetitive elements can cause deletions in the dystropin gene resulting in muscular dystrophy[316]. Examination of the *Notch1* locus identifies multiple Alu elements in introns

1a and 2, as well as LINE repeats in intron 2. Hence, recombination between repetitive elements could be another potential mechanism for intragenic *Notch1* deletions. Lastly, the frequent Type 1 *Notch1* deletions found by Ashworth *et al*.[232] could result from a strong selection for ligand-independent mutations in murine T-LL cell lines.

Our results reveal a unique case of truncated *Notch1* transcript that begins transcription 83 nucleotides upstream of exon 1a. The presence of an initiator (Inr) element supports this as a transcription start rather than the first nucleotide of exon 1a that lacks Inr and other upstream transcription initiation elements such as TATA or GC-rich boxes. The use of an alternative promoter at exon 1a has been reported in thymocytes, radiation-induced thymic lymphomas and Ikaros-deficient T-LLs[231,233,295]. At the genomic level, the breakpoints for deletion in our case are located in intron 1 and intron 2, similar to those found in Type 2 deletions. It is unclear to us why transcription starts at a 5' alternative promoter in spite of an intact exon 1 with its promoter. We hypothesize that other oncogenic events, for example loss-of-function mutations in Ikaros, may alter the epigenetic profile of *Notch1* such that transcription may begin at non-canonical promoters. In fact, Gomez-del Arco *et al*. has recently shown that loss of *Ikaros*, which normally represses *Notch1* transcription at canonical (exon 1) and non-canonical promoters such as exon 1a and exon 25, increases chromatin accessibility to transcription machinery at these sites[295]. The possibility that loss-of-function mutations in *Ikzf1* may facilitate use of alternative promoters deserves further study in our model.

Deletion-based mechanisms of Notch1 activation and HD mutations are observed in 30% of Notch-dependent $Atm^{-/-}$ T-LLs. There are likely other mechanisms for ligand-independent activation of Notch signaling. For instance, other genomic rearrangements

involving the *Notch1* locus include inversions, duplications and translocations with TCR loci have been reported, but their functional significance has not been determined[230]. Notably, duplications and translocations frequently involve sequence downstream of intron 23 of *Notch1*, which would remove all extracellular EGF repeats and might disrupt NRR. Another possibility is epigenetic remodeling of the *Notch1* locus to permit transcription from alternative promoter, such as that within exon 25, as shown in $Ik^{L/L}$ T-LLs[295].

The truncated *Notch1* transcripts identified in our studies contain 3 methionines (2 locate in exon 26 and one in exon 28) as possible translation initiation sites. Sample 1910 also contains a methionine in exon 25. Ashworth and Gomez-del Arco have examined which methionine in exons 26 and 28 is used as initiator[232,295]. Both groups have mutated all 3 methionines and express in cell lines. Interestingly, only mutation of Met 1727 (exon 28) abrogated expression, suggesting this as the initiator Met. Therefore, we conclude that the exon 28 methionine is likely responsible for initiation of the truncated transcripts found in our study.

Do intragenic deletions of *NOTCH1* occur in human T-LLs? The answer is yes. Ferrando's group has recently identified a T-LL case that harbors a Type 1 deletion[237]. This deletion results in a truncated transcript that begins in exon 26 and codes for a highly active form of NOTCH1 lacking extracellular sequences including NRR; hence, the truncated protein functions in a ligand-independent manner. Intragenic deletions of *NOTCH1* are likely rare events in human T-LLs since analysis of ~200 human T-LL samples fail to detect abnormality although small focal deletions could have been missed[232]. Nevertheless, intragenic deletions add to a growing list of activating *NOTCH1* mutations found in human

T-LLs including HD mutations[10] and t(7;9) that juxtaposes TCRβ locus to exon 25 of *NOTCH1*[21].

3.6 Acknowledgements

The authors thank Dr. Jon Aster for sharing the primer sequences for detecting of Type 1 and Type 2 *Notch1* deletions. This work was supported by the Genome Canada grant to J.S.D. and C.J.G. Salary support for PPCW was provided by the Terry Fox Foundation, Canadian Child Health and Clinician Scientist Program, Christopher Brundage Endowment Fund and the Division of Haematology/Oncology, the Hospital for Sick Children.

CHAPTER 4:

KRÜPPEL-LIKE FACTOR, *KLF9*, PROMOTES PROLIFERATION OF NOTCH-INDEPENDENT T LYMPHOBLASTIC LYMPHOMAS

Peggy P. C. Wong[1,2], Daniele Merico[3], Irina R. Matei[1], Vicki Ling[4], Shaheena Bashir[5], Ildiko Grandal[6], Robin A. Haw[6], Oliver Stueker[3], Gary D. Bader[3], Joseph Beyene[4], Jayne S. Danska[7] and Cynthia J. Guidos[6*]

[1]Department of Medical Biophysics, University of Toronto, Toronto ON M5G 2M9
[2]Division of Haematology/Oncology, Department of Paediatrics, the Hospital for Sick Children, Toronto ON M5G 1X8
[3]Terrence Donnelly Centre for Cellular & Biomolecular Research, University of Toronto, Toronto, ON M5S 3E1
[4]Institute of Health Policy, Management & Evaluation, University of Toronto, Toronto ON M5T 3M6
[5]University Health Network, Toronto, ON M5G 2C4
[6]Program in Developmental and Stem Cell Biology, the Hospital for Sick Children, Toronto ON M5G 1L7
[7]Program in Genetics and Genome Biology, the Hospital for Sick Children, Toronto ON M5G 1L7

Authors' contributions:
All the experiments and data analyzes were performed by P. Wong with the following exceptions: V. Ling, and S. Bashir, performed statistical analyses of gene expression microarray data. D. Merico, O. Stueker, R. Haw and P. Wong performed bioinformatic analyses. I. Matei, I. Grandal and P. Wong prepared RNA from T-LL samples.

4. KRÜPPEL-LIKE FACTOR, *KLF9*, PROMOTES PROLIFERATION OF NOTCH-INDEPENDENT T LYMPHOBLASTIC LYMPHOMAS

4.1 Abstract

Notch1 signaling is required for normal T-cell development, but ectopic Notch1 activity causes T lymphoblastic leukemia/lymphoma (T-LL). Binding to Notch ligands triggers intramembranous Notch1 cleavage, releasing active intracellular Notch1 (ICN1) from the plasma membrane. Gain-of-function *NOTCH1* mutations that promote ligand-independent cleavage or increase ICN1 stability are very frequent in human and mouse T-LLs. However, some studies suggest that wild-type *NOTCH1* portends a worse prognosis for human T-LL. Therefore, we set out to define signals that promote proliferation and survival of ICN1-negative T-LLs that develop spontaneously in mice lacking the *Ataxia-telangiectasia mutated* (*Atm*) tumor suppressor gene. Although $Atm^{-/-}$ T-LLs that were $ICN1^{+}$ displayed Notch-dependent growth, about 20% of $Atm^{-/-}$ T-LLs had undetectable ICN1 (UD-ICN1), expressed low levels of Notch1 targets and exhibited Notch-independent growth. Gene set enrichment analyses of genes differentially expressed between UD-ICN1 and $ICN1^{+}$ T-LLs revealed that UD-ICN1 T-LLs expressed higher levels of Krüppel-like factor 9 (*Klf9*) and other transcription factors associated with the highly proliferative pre-double positive (preDP) stage of normal T-cell development. Klf9 regulates proliferation and survival of non-T-cell malignancies. siRNA knock-down experiments showed that *Klf9* promoted proliferation of UD-ICN1 cells.

4.2 Introduction

T lymphoblastic leukemia and lymphoma result from malignant transformation of T-cell progenitors. Both are regarded as different manifestations of the same disease distinguished by degree of bone marrow infiltration[317]. Childhood survival rates for T-LL are 70-90%[318]; whereas adult survival is worse (50-60%) regardless of disease type[319]. Unfortunately, refractory or relapsed T-LL portends a dismal outcome[4,163,164]. Hence, there is a need to discover more effective therapies. Because gain-of-function *NOTCH1* mutations occur in >50% of human and murine T-LL[10,21]. NOTCH1 signaling has recently emerged as a new therapeutic target in T-LL[320-322].

Notch1 is a heterodimeric transmembrane receptor critical for T-cell-lineage specification, commitment and proliferative expansion of committed T-cell progenitors[323]. Ligand binding to Notch1 extracellular sequences relieves the "auto-inhibited" juxta-membrane negative regulatory region. This exposes the heterodimerization domain (HD) to cell surface ADAM metalloproteases, which cleave between positions 1710 and 1711 of mouse Notch1[24]. The Notch1 transmembrane region is then cleaved by γ-secretase complex to release active ICN1 into the cytoplasm, after which it migrates to the nucleus and binds a transcription factor known as recombination signal binding protein for immunoglobulin kappa J (RBPJ)[106,324]. ICN1 displaces transcriptional co-repressors and recruits co-activators to RBPJ, inducing expression of Notch1 target genes such as *Hes1*, *Dtx1*, *Il2ra* and *Notch3*[106,108]. ICN1 is highly unstable because its C-terminal PEST domain is subjected to Fbw7-mediated ubiquitination and proteosomal degradation[217,218]. Thus during normal T-cell development, Notch1 activation is spatially restricted to Notch ligand-bearing niches

and is of limited duration. However in T-LL, HD mutations allow for ligand-independent Notch1 activation, whereas PEST mutations increase ICN1 stability, leading to ectopic and/or excessive Notch1 activity[10,202,203].

Survival and proliferation of T-LL blasts can be greatly attenuated by treatment with γ-secretase inhibitors (GSI) in cell culture, suggesting that they remain "addicted" to active NOTCH1 signaling[10,325]. This finding, coupled with the high frequency of Notch pathway mutations has made Notch a target for therapeutic intervention[321]. The prognostic significance of *NOTCH1* mutations in human T-LL remains controversial. Some studies conclude that *NOTCH1* status is not predictive of patient outcome[256,259,326]. In contrast, other studies suggest that an absence of NOTCH pathway mutations is associated with less favorable clinical outcomes[251,327]. Thus, it is important to identify mechanisms controlling proliferation of NOTCH-independent T-LLs in order to identify potential therapeutic targets for this subgroup of T-LL.

The phosphatase and tensin homologue (PTEN) tumor suppressor gene is frequently deleted or inactivated in murine and human T-LLs[111,197,246,283]. Loss of PTEN function can sometimes bypass the need for active Notch signaling in established T-LL cell lines with mutant *NOTCH1*[111]. However, a more extensive study of primary murine and human T-LL cells did not support the conclusion that PTEN inactivation endowed T-LLs with Notch1-independent growth capacity[246]. Thus, pathways that promote proliferation and survival of T-LL cells in a Notch-independent fashion are not well defined.

T-LLs arise from a disordered developmental process that leads to accumulation of malignant blasts that show many similarities to normal T-cell progenitors. Most commonly, T-LL blasts resemble early to intermediate stages of normal T-cell development that take

place in the thymic cortex. These stages include CD4/CD8 double negative (DN), CD8 ISP and DP progenitors[5]. T-cell development begins when Notch1 signaling drives T-lineage specification and commitment of thymus-seeding progenitors to progress from DN1 to DN3 in the thymic cortex. Progression through the remaining cortical phases requires successful *Tcrb* gene rearrangement to allow for expression of TCRβ protein, which rescues DN3 thymocytes from cell death by allowing expression of pre-TCR complex. Notch1 and pre-TCR signaling collaborate to promotes self-renewal of TCRβ$^+$ DN cells followed by their differentiation through DN4 and CD8 ISP stages to generate a large number of DP thymocytes in a process known as β-selection[157,328]. DN4 and CD8 ISP progenitors proliferate extensively. These cells are known as "preDP" because they rapidly differentiate into DP cells in the absence of cytokines or stromal cells[329]. Their DP progeny divide less extensively and eventually give rise to quiescent small DP (smDP) cells[13,330]. Proliferation of "β-selected" DN3 and DN4 thymocytes remains highly Notch1-dependent, but proliferation of CD8 ISP and DP cells is Notch1-independent[13,158,331]. Thus, ICN1+ T-LLs arrested at the CD8 ISP or DP stages inappropriately retain Notch-dependence for proliferation.

In this study, we set out to define signals that promote proliferation and survival of murine T-LL cells lacking ICN1 expression. Mice lacking *Atm*, a PI3K-like tumor suppressor protein kinase, develop aggressive T-LLs between 3-6 months of age[264]. Similar to human T-LLs, *Atm*$^{-/-}$ T-LL blasts arrest during cortical stages of thymocyte maturation and harbor translocations involving TCR loci[332]. Thus, *Atm*$^{-/-}$ mice provide a relevant animal model for understanding precursor T-cell malignancy. By characterizing a large cohort of primary T-LLs from *Atm*$^{-/-}$ mice we identified a subset that lacked ICN1,

expressed very low levels of Notch1 target genes and grew in a Notch-independent fashion. Here we provide evidence that *Klf9*, a member of the Krüppel-like factor family of transcriptional regulators implicated in development and differentiation of many cell types[333-335], regulates proliferation of Notch-independent T-LLs, suggesing that *Klf9* may provide a novel therapeutic target for human T-LLs lacking activating *NOTCH1* mutations.

4.3 Materials and Methods

4.3.1 Mice

129S6/SvEvTac-*Atm*^{tm1Awb}/J heterozygotes[264] (Jackson Laboratory, Bar Harbor, ME) were mated to generate *Atm*$^{-/-}$, *Atm*$^{+/-}$ and *Atm*$^{+/+}$ progeny. B6.129S6-*Rag2*^{tm1Fwa} (*Rag2*$^{-/-}$) mice were purchased (Taconic Farms, Germantown, NY). All mice were housed under pathogen-free conditions at the Toronto Centre for Phenogenomics (Toronto, ON). Pre-malignant thymocytes were harvested from *Atm*$^{-/-}$ mice at 4-6 weeks of age. Thymocytes harvested from moribund *Atm*$^{-/-}$ mice with enlarged thymi were the source of primary T-LL samples, and thymocytes from *Atm*$^{+/+}$ littermates were used for comparisons. All procedures met the requirements set forth by the Guidelines and Policies of the Canadian Council on Animal Care.

4.3.2 Cell culture

Atm$^{-/-}$ T-LL cell lines were established by culturing viably frozen T-LL cells in RPMI 1640 media (Wisent, St-Bruno, QC) containing sodium pyruvate, glutamine, non-essential amino acids, HEPES, 2-mercaptoethanol, 10% fetal bovine serum and murine interleukin-7 (IL-7). The cells were maintained by passaging in fresh media containing IL-7 every 2-4 days. Cell lines were established when cells were proliferating and attaining >80% viable cell recovery with each passage. T-LL cell lines were then maintained in the same media in the presence of IL-7. Where indicated, cells were incubated with either 1 μM of GSI X (Calbiochem, Billerica, MA) or 0.1% (v/v) DMSO vehicle control for 48 hours. CellTiter-Blue reagent (Promega, Madison, WI) was used according to manufacturer's instructions to assay

viability. For *in vitro* proliferation assays, BrdU (10 μM) was added one hour prior to cell harvest, and labeled cells were detected using a BrdU flow kit according to the manufacturer's protocol (BD).

4.3.3 Western blotting

T-LL cells and thymocytes were lysed in modified RIPA buffer supplemented with phosphatase inhibitor cocktail and protease inhibitor cocktail (Thermo Scientific, Rockford, IL), according to Millipore technical publication mcproto402 (www.millipore.com). Protein concentration was determined by Lowry assay (Bio-rad, Missisauga, ON). Whole cell lysates (15-20 μg) were separated by 8% SDS-PAGE, transferred onto PVDF membrane, which was incubated first with mouse monoclonal antibody against PTEN (clone 6H2.1; Cascade Bioscience, Winchester, MA), rabbit polyclonal antibody against cleaved Notch1, or rabbit monoclonal antibody against β-actin (Cell Signaling Technology, Danvers, MA), followed by horseradish peroxidase-conjugated secondary goat anti-mouse or anti-rabbit antibodies (Santa Cruz Biotechnology, Santa Cruz, CA). Blots were developed by chemiluminescence using ECL reagents (GE Healthcare).

4.3.4 Flow cytometry

For immunophenotyping, live single-cell suspensions of T-LLs and littermate $Atm^{+/+}$ thymocytes were stained using standard techniques[271] with antibodies purchased from BD Biosciences (San Diego, CA) specific for CD4 (RM4-5), CD8α (53-6.7), CD25 (7D4) and TCRβ (H57-597) conjugated to FITC, PE or APC. After staining, cells were re-suspended in propidium iodide (1 μg/ml). Unstained cells were used for comparison. For detection of BrdU and activated caspase-3, T-LL cells were stained with Fixable Blue (Invitrogen, Grand

Island, NY), fixed and permeabilized prior to staining separately with APC-conjugated anti-BrdU and FITC-conjugated anti-activated caspase-3 (BD), according to manufacturer's protocols. Stained cells were analyzed by LSR II cytometer (BD) and FlowJo software (Tree Star, Ashland, OR).

4.3.5 Notch1 *mutation analysis*

The following primers were used to amplify exons 26, 27 and 34a of mouse *Notch1* from genomic DNA (45 ng) by phenol-chloroform extraction[281]: HD1_fwd, GCTGAGTTTCTTTAGAGTC; HD1_rev, CCTCCCCTGAGGTTACACCT; HD2_fwd, GAGTGTCCCATTGCGGGGCT; HD2_rev, TGCAGAGGTCAGAAAGTGTT; PEST1_fwd, GCTCCCTCATGTACCTCCTG; PEST1_rev, TGCTGGGTCTGCACCAGGTGA; PEST2_fwd, TACCAGGGCCTGCCCAACAC; PEST2_rev, GCCTCTGGAATGTGGGTGAT. PCR cycling conditions were: 94 ^{o}C for 2'; 35 cycles of 94 ^{o}C for 15", 62 ^{o}C for 30" and 72 ^{o}C for 1'; 72 ^{o}C for 10'. PCR products were purified with QIAquick PCR purification kit (QIAGEN, Toronto, ON) and sequenced at the Toronto Centre of Applied Genomics facility (TCAG, Hospital for Sick Children). In some cases, heteroduplex analysis was used to detect PEST mutations[282]. 5'-FAM-conjugated PEST2_fwd & PEST2_rev primers were used to amplify part of exon 34a where PEST mutations frequently clustered. Amplified products were denatured at 95 ^{o}C for 10 min and then gradually cooled to 40 ^{o}C to form mismatch heteroduplexes in mutated samples. These samples were incubated with CEL I (a mismatch-specific endonuclease) at 40 ^{o}C for 1 h followed by analysis of the fragments with ABI Prism Model 3100 capillary electrophoresis machine and GeneMapper software (Applied Biosystems, Carlsbad, CA).

4.3.6 Northern blotting

Total RNA was extracted from T-LL cells and *Rag2*$^{-/-}$ thymocytes using either the guanidinium thiocyanate-phenol-chloroform method[306] or the RNeasy Plus Mini Kit (QIAGEN, Toronto, ON). RNA was quantitated on a NanoDrop spectrophotometer (Thermo Scientific). Total RNA was electrophoresed in 1% agarose containing 1X MOPS and 3%(v/v) formaldehyde for 16 h at 55 V. RNA was transferred to Nylon membranes in 20X SSC after washing with 0.05 N NaOH and neutralizing with 2X SSC. RNA was UV cross-linked to membranes and hybridized with ^{32}P-labelled *Notch1* cDNA fragments (corresponding to exon 34a) obtained from restriction digest of *Notch1* cDNA plasmid with EcoRV and HindIII overnight at 42 ^{o}C. Membranes were washed with 1X SSC/0.1% SDS twice for 10 min followed by 2x5' washes with 0.2X SSC/0.1% SDS at 65 ^{o}C. X-ray film was developed after 2 days of exposure at -80 ^{o}C. Membranes were stripped and reprobed with *Hprt* cDNA as loading control.

4.3.7 Quantitative real-time PCR

Total RNA was reverse transcribed using oligo dT to yield cDNA which was amplified using the following primer pairs: Ptprc_fwd, AAGTCTCTACGCAAAGCACGG; Ptprc_rev, GATAGATGCTGGCGATGATGTC; Dtx1_fwd, CCGCATCGTCTATGACATC; Dtx1_rev, GAGCAATCTCAGCACCTTTC; Hes1_fwd, CACAGACCCGAGCGTGTTG; Hes1_rev, GACAGGAAGCGGGTCACCTC; Notch3_fwd, CAGGCGAAAGCGAGAACAC; Notch3_rev, CACCCTTGGCCATGTTCTTCA. 5'-FAM- and 3'-TAMRA-conjugated Hes1 probe

(CGCGCCGGCTTCAGCGAG) was used along with the primer pair. Primer and probe mixes for *Il2ra* and *Klf9* were purchased from Applied Biosystems Inc. under these conditions: 95 ^{o}C for 10'; 40 cycles of 95 ^{o}C for 15" and 60 ^{o}C for 1'. Standard curves prepared from plasmid DNA (cDNA clones obtained from Open Biosystems) were included for absolute quantification.

4.3.8 **Klf9** *knockdown*

The following Accell siRNA reagents were obtained from Thermo Scientific Dharmacon: SMARTpool - mouse *Klf9* siRNA (*siKlf9*), non-targeting siRNA #1 (*siNT*), and delivery media. Cultured T-LL cells were washed twice with PBS prior to seeding at 250,000 cells/well in 500 μl of serum-free Accell delivery media containing mouse IL-7 (5 ng/ml, Peprotech, Rocky hill, NJ) and 2 μM *siKlf9* or *siNT*. After 48 hours, cells were harvested for RNA extraction, BrdU and activated caspase-3 staining.

4.3.9 Gene expression microarray and data analysis

Twenty primary T-LL samples as well as 4 samples of non-malignant *Atm*$^{-/-}$ thymocytes (Thy) from 4-6 week old mice were subjected to genome-wide expression profiling using Illumina mouse Ref8 v1.1 gene expression microarray chips according to standard protocols (TCAG facility). Raw signals from 24,613 probes were subjected to pre-processing steps including background correction, transformation and normalization using the *lumi* package from Bioconductor[336]. Pre-processed data were then analyzed with Bridge-PLSR[337] (partial least squares regression) a supervised dimension reduction method that represents the underlying variation in the data set by a two-dimension plot. The axes of this plot are referred to latent variables (LV1 and LV2) and they accounted for 27% and 17% of variation

in the data set. The following statistical analyses were also performed on the data set using Limma (linear model for microarray analysis) package[338]: principal component analysis, unsupervised hierarchical clustering, ANOVA F-statistics, and moderated t-statistics. Pre-processed expression values of Notch target genes were used for hierarchical clustering using the complete-linkage method within the R package. Data processing and other statistical analyses were performed with R software.

4.3.10 Gene set enrichment analysis (GSEA)

We selected UD-ICN1 vs. T-ICN1 and UD-ICN1 vs. pre-malignant *Atm*$^{-/-}$ thymocyte comparisons and generated gene lists ranked according to differential expression in each 2-group comparison. Expression data from the 24,613 probe-sets were first collapsed to 17,133 unique genes by selecting probesets with the highest ANOVA F-statistics among those representing the same genes. Unique genes were then ranked for each comparison using moderated t-statistics, a value that reflects the difference in mean expression values for the two groups (magnitude of differential expression) as well as the variance of that gene's expression within each group. Gene sets compared to our ranked lists of differentially expressed genes encompassed diverse biological functions and pathways and were obtained from 5 sources: National Cancer Institute /Nature Pathway Interaction Database (http://pid.nci.nih.gov/PID/index.shtml), Biocarta pathways (http://www.biocarta.com), KEGG Pathway Database (http://www.genome.jp/kegg/pathway.html), the Gene Ontology database (http://www.geneontology/org/), and the Pfam protein families database (http://pfam.sanger.ac.uk/). In addition, a list of transcription regulators differentially expressed between preDP and smDP stages of murine T-cell development was obtained

from Tabrizifard et al.[339] and used to generate 2 gene sets: PreDP > SmDP and PreDP < SmDP.

GSEA was performed as described previously[340]. Briefly, an enrichment score (ES) was calculated according to weighted Kolmogorov-Smirnov-like statistic to reflect the degree of which genes in each set clustered toward either end of the ranked list of differentially expressed genes. Statistical significance for ES (nominal p value) was estimated by permutating genes in the gene set and re-calculating the ES to generate a null distribution. The nominal p value represented the frequency that ES of the permuted data ≥ observed ES. With multiple gene sets, the estimated significance of ES was further adjusted for multiple hypothesis testing to give the false discovery rate (FDR) q value. We included gene sets containing 10-500 genes, and performed 2,000-8,000 gene-set permutations. GSEA results were visualized using Cytoscape and Enrichment Map software[341]. The following filtering criteria were used for displaying gene sets: nominal $p < 0.01$, FDR $q < 0.05$, and the overlap coefficient was set to 0.5.

4.4 Results

4.4.1 Atm$^{-/-}$ *T-LLs exhibit a spectrum of Notch1 activity and CD4/CD8 phenotypes*

As shown in chapter 2, 63% of T-LL expressed high levels of truncated ICN1 due to mutations in the C-terminal PEST domain, whereas 17% expressed non-truncated ICN1 (NT-ICN1) protein with the same apparent molecular weight as wild-type ICN1 (Fig. 2.1B, Table 2.1). A third group of samples (20%) had undetectable ICN1 (UD-ICN1) protein (Fig. 4.1A, Table 2.1) and very low or undetectable, *Notch1* mRNA (Fig. 4.1B). Thus, we identified a distinct subgroup of *Atm*$^{-/-}$ T-LLs that lack expression of *Notch1* mRNA and protein. Since T-LLs are arrested at varying stages of T-cell development, we analyzed the CD4 and CD8 expression to define maturational stage for samples in different *Atm*$^{-/-}$ T-LL subgroups. T-ICN1 samples displayed considerable immunophenotypic heterogeneity, with a majority containing predominantly CD8 SP cells (Table 2.1). All NT-ICN1 and a majority of UD-ICN1 T-LLs examined consisted predominately of DP cells. In all 3 groups, abnormal lymphoblasts expressed low to intermediate levels of surface TCRβ. Therefore, as with the majority of human T-LL cases, *Atm*$^{-/-}$ T-LLs were arrested at CD8 ISP and DP stages of thymocyte differentiation.

4.4.2 ICN1 T-LL subgroups vary in levels of Notch target gene expression

To gain insights into pathways that regulate survival and proliferation of UD-ICN1 T-LLs, we performed genome-wide expression profiling on total RNA from 10 T-ICN1, 4 NT-ICN1 and 6 UD-ICN1 T-LL samples. Pre-malignant *Atm*$^{-/-}$ thymi (n=4) harvested from

4-6 week-old mice and consisting predominantly of normal DP thymocytes were also included. To determine if the 3 distinct ICN1 subgroups had differing levels of Notch1 activity, we performed unsupervised hierarchical clustering of normalized expression values for several direct Notch1 target genes: *Hes1*, *Dtx1*, *Notch3*, *Il2ra*, *Nrarp*, *Ptcra* and *Notch1* (Fig. 4.2A). Strikingly, UD-ICN1 samples and most T-ICN samples formed discrete clusters at opposite ends of the dendrogram, indicating that T-ICN1 and UD-ICN1 protein status was associated with high and low Notch1 activity, respectively. qRT-PCR studies confirmed that T-LL samples expressed significantly higher levels of direct *Notch1* targets such as *Hes1*, *Dtx1*, *Notch3* and *Il2ra* than UD-ICN1 samples (Fig. 4.2B). Furthermore, T-ICN1 samples also expressed significantly higher levels of surface CD25 and had more $CD25^{+}$ cells than the other 2 groups (Fig. 4.2C). Although T-ICN1 T-LLs also expressed significantly higher levels of *Hes1* and *Dtx1* than NT-ICN1 cases, *Il2ra* and *Notch3* levels were highly variable in this group, explaining why this group did not cluster together. Finally, pre-malignant $Atm^{-/-}$ thymocyte samples formed a discrete cluster next to the UD-ICN1 samples, consistent with previous studies demonstrating low Notch activity in DP thymocytes[328,342]. Collectively, these findings demonstrate that UD-ICN1 T-LLs exhibit significantly lower levels of Notch1 activity than T-ICN1 T-LLs, whereas levels of Notch1 activity were more heterogeneous in NT-ICN1 samples.

To test whether Notch1 activity is functionally required for survival and growth of UD-ICN1 T-LL samples, we measured the impact of γ-secretase inhibition on growth of cell-culture adapted primary T-LLs with T-ICN1 or UD-ICN1. As expected, additon of GSI significantly reduced viable cell recoveries from T-ICN1 cell lines, confirming their Notch dependence (Fig. 4.2D). In contrast, viability of UD-ICN1 T-LL cell lines was unaffected

by treatment with GSI, demonstrating that their survival and growth was Notch-independent. Collectively, these data show that although most T-LLs arising have activating *Notch1* mutations and require continued Notch signaling for survival and growth, a significant fraction shows undetectable Notch1 activity and proliferate in a Notch-independent manner.

To determine if PTEN loss could explain the Notch-independence of UD-ICN1 T-LLs, we evaluated PTEN protein expression in T-LL cells belonging to each ICN1 subgroup. This analysis confirmed previous studies showing frequent PTEN loss in human and murine T-LLs[111,283]. However, one UD-ICN1 sample retained PTEN expression, suggesting that PTEN loss was not necessary for Notch-independent growth (Fig. 4.3). Furthermore, growth of all PTEN-negative samples in T-ICN1 (Fig. 4.2D) and NT-ICN1 sub-groups was GSI-sensitive (Fig. 3.1A), demonstrating that PTEN loss is not sufficient to confer Notch-independent growth to Notch-addicted T-LLs that arise spontaneously in *Atm*$^{-/-}$ mice. Thus, in agreement with Meydouf *et al.*[246], we found no correlation between PTEN status and dependence on Notch signaling.

4.4.3 UD-ICN1 T-LL subgroup is enriched with gene sets involved in cell proliferation

To identify proliferation and survival pathways that might sustain Notch-independent UD-ICN1 T-LLs, we carried out more global analysis of our gene expression data set. Specifically we sought to (1) identify genes that distinguished all T-LLs (including the UD-ICN1, NT-ICN1 and T-ICN1 subgroups) from pre-leukemic thymocytes; and (2) identify gene expression profiles associated with ICN1 status. The workflow of our analysis is summarized in Fig. 4.4. In order to determine how much variation in expression across the

24,613 probe-sets can be explained by ICN1 status, we used a supervised dimension-reduction method, called Bridge-partial least squares regression analysis[337]. Using this method, we summarized most of the variation in the data set across all 4 sample groups into two variables, called latent variables (LV1 and LV2), represented by the x- and y-axes (Fig. 4.5A). LV1 and LV2 explained 27% and 17%, respectively, of variation seen in the data set. LV1 clearly distinguished all T-LLs from pre-malignant *Atm*$^{-/-}$ thymocytes, whereas LV2 separated the T-LL subgroups. One sample from NT-ICN1 group clustered with the UD-ICN1 group, suggesting that heterogeneity within this group was not restricted to Notch target expression. Most importantly, however, this analysis revealed consistent differences in global gene expression profiles of T-ICN1 and UD-ICN1 samples.

We used GSEA to assess how differences in gene expression might influence a variety of biological processes, because small changes in many genes, rather than a large change in a few genes, can result in large cumulative effects on cellular processes[340]. This approach compares lists of genes ranked according to differential expression with publicly available gene sets grouped according to involvement in particular pathways or cellular processes. We ranked genes based on differential expression in UD-ICN1 (UD-TLL) vs. T-ICN1 (T-TLL) and UD-ICN1 vs. pre-malignant *Atm*$^{-/-}$ thymocytes comparisons. Rankings were based on moderated t-statistics, a metric that encompasses both magnitude and significance of differentiation expression. In each ranked list, genes expressed at significantly higher levels in group 1 (UD-ICN1 T-LLs in both comparisons) clustered at the top, whereas genes expressed significantly lower levels in group 1 clustered at the bottom. Genes whose expression did not significantly differ between the 2 groups assorted to the middle of the ranked gene lists. We then used GSEA to calculate an ES, a running-sum

statistic that reflects the degree to which genes in a given set were over-represented (or enriched) at either end of the ranked list.

The gene sets evaluated represented diverse biological functions and pathways from public databases, and results were visualized with Cytoscape[341] (Fig. 4.5B). Gene sets (depicted as circular nodes) with high positive ES (red nodes) included genes that were significantly over-represented among those expressed at higher levels in group 1 vs. group 2. In contrast, gene sets with high negative ES (blue nodes) included genes that were over-represented among those expressed at lower levels in group 1 vs. group 2. Nodes with white centers or borders contained genes that were not enriched at either end of the ranked gene list. Some nodes contained white centers and red borders, indicating no enrichment (or differential expression) in the UD-UCN1 vs. T-ICN1 T-LL comparison, but significant positive enrichment (or over-expression) in the UD-ICN1 T-LL vs. *Atm*$^{-/-}$ Thy comparison. This pattern of differential expression highlights biological functions important for the malignant phenotype irrespective of the ICN1 status, and included clusters of nodes involved in proteolysis, amino acid metabolism, RNA polymerase, as well as ribosomal and mitochondrial activity. Importantly however, many nodes had red centers, identifying cellular processes that differentiate UD-ICN1 from T-ICN1 T-LLs. In some cases these nodes had white borders, signifying no enrichment in the UD-ICN1 T-LL vs. *Atm*$^{-/-}$ Thy comparisons. Gene sets in this category were involved in cell cycle control, DNA replication, ubiquitin-mediated proteolysis and chromosome function. Thus, several cellular processes differentiate UD-ICN1 from T-ICN1 T-LLs, but UD-ICN1 T-LLs also shared some biological features of pre-malignant thymocytes.

4.4.4 UD-ICN1 T-LLs exhibit a preDP-like transcription factor gene expression signature

Most UD-ICN1 and T-ICN1 T-LLs were arrested at the preDP or DP stage, during the transition from Notch1-dependent to Notch1-independent proliferation in normal T-cell development. Therefore, we performed GSEA using transcription factor (TF) gene sets defined on the basis of their changing expression across this transition. One gene set included TFs that are more highly expressed in cycling preDP cells compared with quiescent smDP cells (preDP > smDP) whereas the second gene set showed the opposite pattern (preDP < smDP) (Table 4.2)[339]. We used these gene sets to perform GSEA on differentially expressed genes from UD-ICN1 vs. T-ICN1 as well as UD-ICN1 vs. *Atm*$^{-/-}$ Thy comparisons. The preDP > smDP gene set had high positive ES in both comparisons (with FDR q = 0.04 and 0.0003), suggesting that TFs highly expressed in preDP thymocytes (relative to smDP cells) were also more highly expressed in UD-ICN1 relative to T-ICN1 T-LL samples and pre-malignant thymocytes (Fig. 4.6A top plots). Conversely, the preDP < smDP gene set had a high negative ES in the UD-ICN1 T-LL vs. pre-malignant thymocyte comparison, indicating that genes expressed at high levels in smDP cells (relative to preDP cells) were also expressed at high levels in *Atm*$^{-/-}$ thymocytes relative to UD-ICN1 T-LLs (Fig. 4.6A bottom plot; FDR q = 0.0002). This latter finding makes sense because smDP cells are the most abundant subset in pre-malignant *Atm*$^{-/-}$ thymocytes[271]. Collectively, these bioinformatics analyses suggest that UD-ICN1 T-LLs highly express a set of transcription factors that are normally down-regulated as proliferating preDP mature into quiescent smDP cells.

We next carried out a gene-by-gene analysis to identify TFs within the preDP > smDP gene set that contributed to the positive ES for UD-ICN1 vs. T-ICN1 comparison (Fig. 4.6B, blue rectangle). Interestingly, *Hes1* was at the bottom of the list and was already shown to be low in UD-ICN1 relative to T-ICN1 T-LL samples (Fig. 4.6B). Six of the 13 TFs (*Klf9*, *Wdhd1*, *Hmgn5*, *Rfc1*, *Cnot7* and *Mcm4*) that contributed to the positive ES are known to be involved in proliferation or DNA replication in different cell types[334,343-347], suggesting that they might also promote proliferation of preDP cells. Unexpectedly, 2 TFs that are known to suppress cell cycle progression (*Cops2* and *Rbl1*)[348,349] also contributed to the positive ES. At the top of the list was *Krüppel-like factor 9* (*Klf9*), a member of the Krüppel-like TF family, which has been shown to promote proliferation of intestinal crypt cells[334]. However, it's role in T cell development has not been examined. *Klf9* expression was 2.5-fold higher in UD-ICN1 relative to T-ICN1 samples ($p = 0.047$) in the microarray experiment. To validate this difference, we measured *Klf9* mRNA by qRT-PCR and confirmed that although levels varied considerably among individual samples, on average UD-ICN1 T-LLs expressed significantly more *Klf9* mRNA than T-ICN1 T-LLs (7-fold, $p = 0.028$; Fig. 4.6C). The relatively higher *Klf9* expression in UD-ICN1 cells and its known function in regulating proliferation of non-lymphoid cells suggested a similar role for *Klf9* in UD-ICN1 T-LLs.

4.4.5 Klf9 regulates proliferation of UD-ICN1 T-LL cells

Interestingly, *Klf9* represses *NOTCH1* transcription in human glioblastoma cells[350]. Furthermore, *Hes1* was reported to repress expression of a related family member, *Klf4*, in intestinal epithelial precursors[351]. Since *Klf9* expression was highest in T-LLs with low

Notch1 activity, we asked if high *Klf9* expression might be responsible for low *Notch1* expression in UD-ICN1 T-LL cells. However, *Klf9* knockdown did not impact *Notch1* expression in UD-ICN1 cells (data not shown). Furthermore, inhibiting Notch activation with GSI did not increase *Klf9* expression in T-ICN1 T-LLs (data not shown). Therefore, we found no evidence that *Klf9* and *Notch1* regulate each other's expression in $Atm^{-/-}$ T-LLs, suggesting that other mechanisms underlie the almost mutually exclusive expression of *Klf9* and *Notch1* in Notch1-dependent vs. Notch1-independent T-LLs from $Atm^{-/-}$ mice.

Since *Klf9* promotes proliferation in some contexts, we measured the impact of *Klf9* knockdown on cell cycling in 3 UD-ICN1 T-LL cell lines (6625, 6652 and 6924) as well as on the T-ICN1 T-LL cell line with the highest *Klf9* expression among its group (6925). Cells were incubated with *Klf9* siRNA (siKlf9) or non-targeting siRNA (siNT) for 2 days prior to measuring BrdU incorporation. Importantly, *Klf9* knockdown significantly decreased the proportion of $BrdU^+$ cells in all 3 UD-ICN1 cell lines (Fig. 4.7A-B). The mean decrease in proportion of $BrdU^+$ cells was the highest in UD-ICN1 cell line 6652, but ranged from 8% to 19%. The degree of *Klf9* knockdown was also most robust in cell line 6652, and ranged from 20 to 65% (Fig. 4.6C). In contrast, a comparable efficiency of *Klf9* knockdown (60%) did not alter proliferation of T-ICN1 T-LL cell line 6925. Although other *Klf* family members have been reported to regulate apoptosis[352,353], *Klf9* knockdown did not affect survival of UD-ICN1 T-LL cell lines based on proportion of dead cells and activated caspase 3 staining (Fig. 4.8). Collectively, these studies provide evidence that *Klf9* promotes proliferation specifically in Notch-independent UD-ICN1 T-LL samples.

Table 4.1 Characterization of Notch1 protein and *Notch1* mutations in 20 *Atm*$^{-/-}$ T-LLs

Mouse ID	ICN1 MW[1] (kD)	*Notch1* Mutation	
		PEST	HD
T-ICN1 (n=10)			
1756	70	c.7300C>T	c.5003T>C
1975	100	MUT[2]	WT[3]
2037	80	MUT	WT
2967	100	MUT	WT
3496	100	c.7076G>C; c.7078_7079insG	WT
5173	100	MUT	WT
6106	75	MUT	c.5128G>C
6620	65	c.7352_7364delTGACCACTACCCA	WT
6658	65	MUT	WT
6925	90	c.7076G>A; c.7076_7077insAAAA	WT
NT-ICN1 (n=4)			
1910	110	WT	WT
2490	110	WT	WT
2971	110	WT	WT
2103	110	--[4]	--
UD-ICN1 (n=6)			
1755	UD	WT	WT
1898	UD	--	--
4299	UD	WT	WT
6625	UD	WT	WT
6652	UD	WT	WT
6924	UD	WT	WT

NM_008714.3 is used as the *Notch1* coding DNA reference sequence and nucleotide 1 refers to the first base of ATG-translation initiation codon.

Footnotes:

(1) MW, molecular weight.

(2) MUT, *Notch1* PEST mutations detected by heteroduplex assay.

(3) WT, wildtype.

(4) --, not determined.

Table 4.2 Differentially expressed transcription factors at PreDP and SmDP stages of thymocyte development

PreDP > SmDP		PreDP < SmDP	
Ahr	*Mcm6*	*1110051M20Rik*	*Mef2b*
Ankrd49	*Mcm7*	*1700113A16Rik*	*Meis3*
Aurkaip1	*Mybl2*	*Aes*	*Mll1*
Bard1	*Myc*	*Aff1*	*Mtf1*
Bola2	*Nfix*	*Arid3b*	*Mxd4*
Carm1	*Nr1h4*	*Arnt*	*Mxi1*
Cebpb	*Nucks1*	*Arntl*	*Myb*
Clpb	*Polr3d*	*Asb3*	*Nab2*
Cnbp	*Pou2af1*	*Ash1l*	*Ncoa3*
Cnot7	*Pou2f3*	*Atm*	*Nfatc3*
Cops2	*Ptrf*	*Bcl6*	*Nfil3*
E2f1	*Rbbp7*	*Ciita*	*Nfkbiz*
Foxm1	*Rbl1*	*Cited2*	*Npas1*
Hand1	*Rbpjl*	*Clock*	*Nr1d1*
Hdac6	*Rfc1*	*Cnot8*	*Nr21*
Hes1	*Rnf141*	*Creb1*	*Nr3c1*
Hmgb3	*Rpf2*	*Csrp1*	*Nrip1*
Hmgcs1	*Ruvbl2*	*Ddit3*	*Pbx2*
Hmgn5	*Sox13*	*Dedd*	*Per1*
Hoxb8	*Sox3*	*Dusp16*	*Phf1*
Hoxd3	*Ssrp1*	*E2f3*	*Pou6f1*
Htr5a	*Tacc3*	*E2f5*	*Prep*
Irf8	*Tcerg1*	*E4f1*	*Rara*
Irx3	*Tfdp1*	*Egr1*	*Rbl2*
Kat2a	*Thra*	*Egr2*	*Rest*
Kdm1b	*Tmpo*	*Elf1*	*Rfx2*
Klf9	*Tmpo*	*Elf4*	*Rfxank*
Mcm2	*Uhrf1*	*Elk3*	*Rnf14*
Mcm3	*Wdhd1*	*Esrra*	*Rnf14*
Mcm4	*Zfp239*	*Ets2*	*Rnf4*
Mcm5		*Ezh1*	*Rora*
		Gata6	*Rorc*
		Gcfc1	*Smarca2*
		Gfi1	*Sox4*
		Gtf2h4	*Sp4*
		Hdac5	*Sqstm1*
		Hdac7	*Ssbp2*
		Hhex	*Tbx6*
		Hivep1	*Tle1*
		Hnf1a	*Tob1*
		Hoxb8	*Trpv2*
		Ikbkg	*Tsc22d4*
		Ing4	*Xbp1*
		Irf3	*Zbtb17*
		Irf6	*Zbtb20*
		Junb	*Zfp110*
		Kat2b	*Zfp276*
		Kcnh2	*Zfp29*
		Kdm3a	*Zfp358*
		Kdm3b	*Zfp36*
		Klf13	*Zfp385a*
		Klf3	*Zfp46*
		Klf6	*Zfp61*
		Klf7	*Zfp653*
		Ldb1	*Zfp821*
		Mdm2	*Zkscan14*
		Mecp2	*Zkscan6*
		Med1	

Gene lists were obtained from Tabrizifard *et al*.[339]

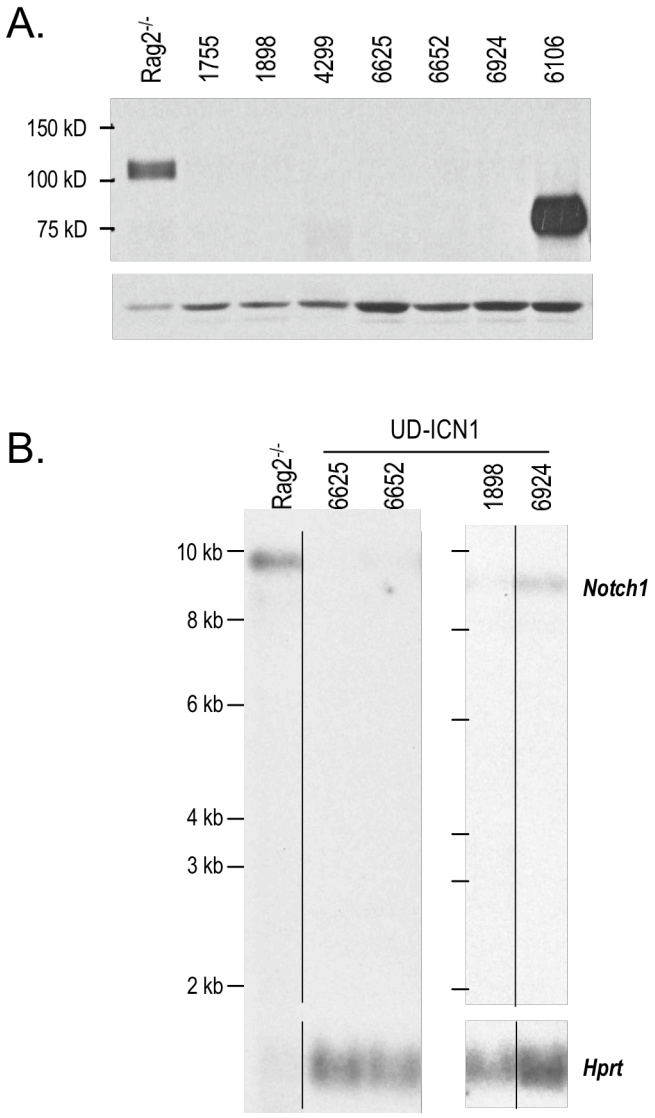

Figure 4.1 Characterization of ICN1 and *Notch1* mRNA expression in *Atm*$^{-/-}$ T-LLs
(A) Immunoblot analysis of ICN1 expression in *Atm*$^{-/-}$ T-LLs. Protein whole cell lysates from primary *ex vivo* T-LL samples were immunoblotted for ICN1 using an antibody recognizing Val1744, and with an antibody to β-actin as a loading control. A representative blot showing 7 primary *Atm*$^{-/-}$ T-LLs along with *Rag*2$^{-/-}$ thymocytes as control for wildtype ICN1 (~110 kD) are shown on the left. (B) Northern blots of *Notch1* mRNA in T-LLs. Total RNA (9-12 μg) from *Rag2*$^{-/-}$ thymocytes and UD-ICN1 T-LLs were gel-electrophoresed, transferred to nylon membrane and hybridized with ^{32}P-labeled *Notch1* and *Hprt* (as a loading control) cDNA probes. *Notch1* transcripts are 9.3 kb and 8 kb and *Hprt* is 1.4 kb.

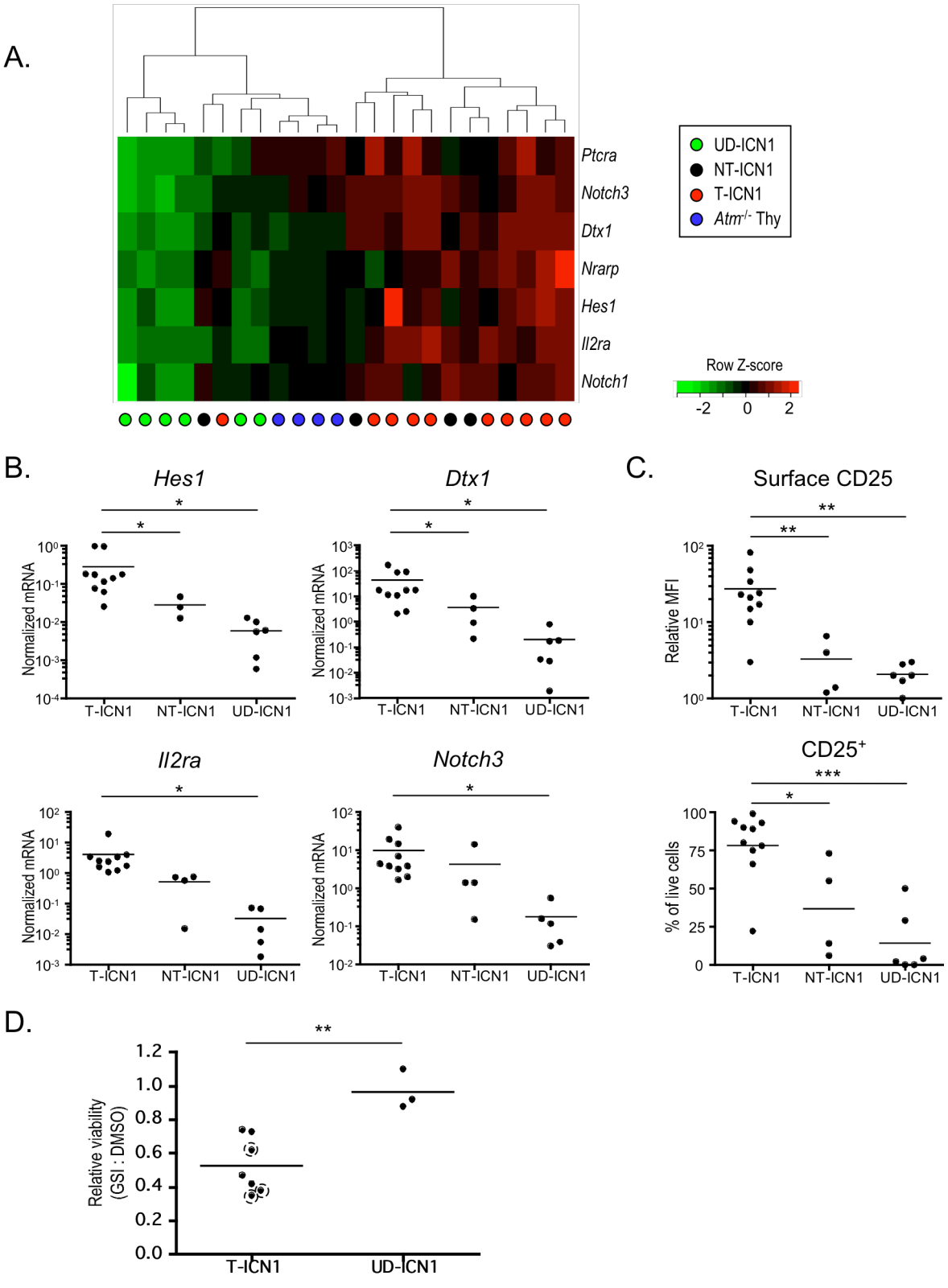
A.
Ptcra
Notch3
Dtx1
Nrarp
Hes1
Il2ra
Notch1
UD-ICN1
NT-ICN1
T-ICN1
Atm-/- Thy
Row Z-score
-2
0
2
B.
Hes1
Dtx1
Il2ra
Notch3
Normalized mRNA
T-ICN1
NT-ICN1
UD-ICN1
C.
Surface CD25
Relative MFI
CD25+
% of live cells
D.
Relative viability
(GSI : DMSO)

Figure 4.2 T-LL subgroups differ in Notch activity and dependence
(A) Hierarchical clustering of T-LLs and pre-malignant *Atm*$^{-/-}$ thymocytes based on Notch target gene expression. Total RNA from 20 T-LLs and 4 samples of pre-malignant *Atm*$^{-/-}$ thymocytes were hybridized to Illumina Ref-8 microarray chips and gene expression signals of 24,613 probes were quantified and then pre-processed. Ubsupervized hierarchical clustering was performed using expression values for 7 Notch1 targets from 10 T-ICN1 (●), 4 NT-ICN1 (●), and 6 UD-ICN1 (●) T-LLs, along with 4 pre-malignant *Atm*$^{-/-}$ thymocyte samples (●). Each row is scaled by the Z-score (number of standard deviations above (red) or below (green) the mean expression among all samples for each gene). (B) Validation of Notch1 target expression among T-LL subgroups. qRT-PCR experiments were performed to measure *Hes1*, *Dtx1*, *Il2ra*, *Notch3* and *Ptprc* mRNA levels among 3 T-LL subgroups as indicated in (A). Scatter plots show mean mRNA levels (relative to *Ptprc*) for each gene in the 3 ICN1 sub-groups. *,$p < 0.05$. (C) Cell surface expression of CD25 in 3 T-LL subgroups. Single cell suspensions from primary *ex vivo* T-LLs were stained with fluorchrome-labeled antibodies specific for CD4, CD8 and CD25 and analyzed by flow cytomtery. *Top graph*: ratio of median CD25 cell surface immunostaining fluorescence intensity of live T-LL cells normalized to that littermate *Atm*$^{+/+}$ DP thymocytes analyzed in the same experiment. *Bottom graph*: Percentage of live cells that were CD25^{+}. ***, $p < 0.0005$; **, $p < 0.005$; *, $p < 0.05$. (D) Dependence of T-LLs on active Notch signaling. T-ICN1 and UD-ICN1 T-LL cell lines were cultured with DMSO vehicle (0.1%v/v) or 1 μM GSI-X for 48 hours in the presence of 10 ng/ml of IL-7. Cell viability was quantified using the CellTitre Blue fluorescence assay, and relative viability was calculated as the ratio of fluorescence between GSI-treated divided by DMSO-treated conditions for each sample at each time-point. Statistical significance was determined by two-tailed Student's t-test (**$p = 0.0034$). Dashed-line circled dots indicate samples that lacked PTEN expression (see Fig. 4.3).

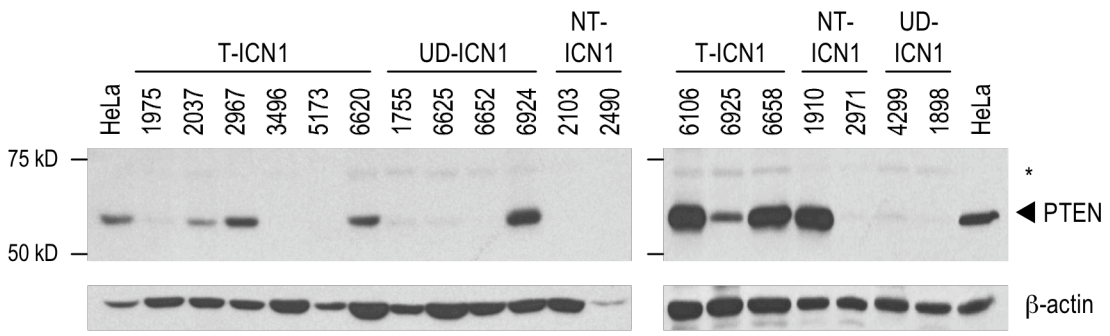

Figure 4.3 Characterization of PTEN protein expression in T-LL subgroups
Immunoblot analysis of PTEN expression in *Atm*$^{-/-}$ T-LLs. Whole cell lysates of primary *ex vivo* T-LL cells were immunoblotted for PTEN and β-actin as a loading control. Two representative blots showing 9 T-ICN1, 4 NT-ICN1 and 6 UD-ICN1 T-LL samples along with HeLa cells as positive control for PTEN (◀, 60 kD). * represents non-specific band.

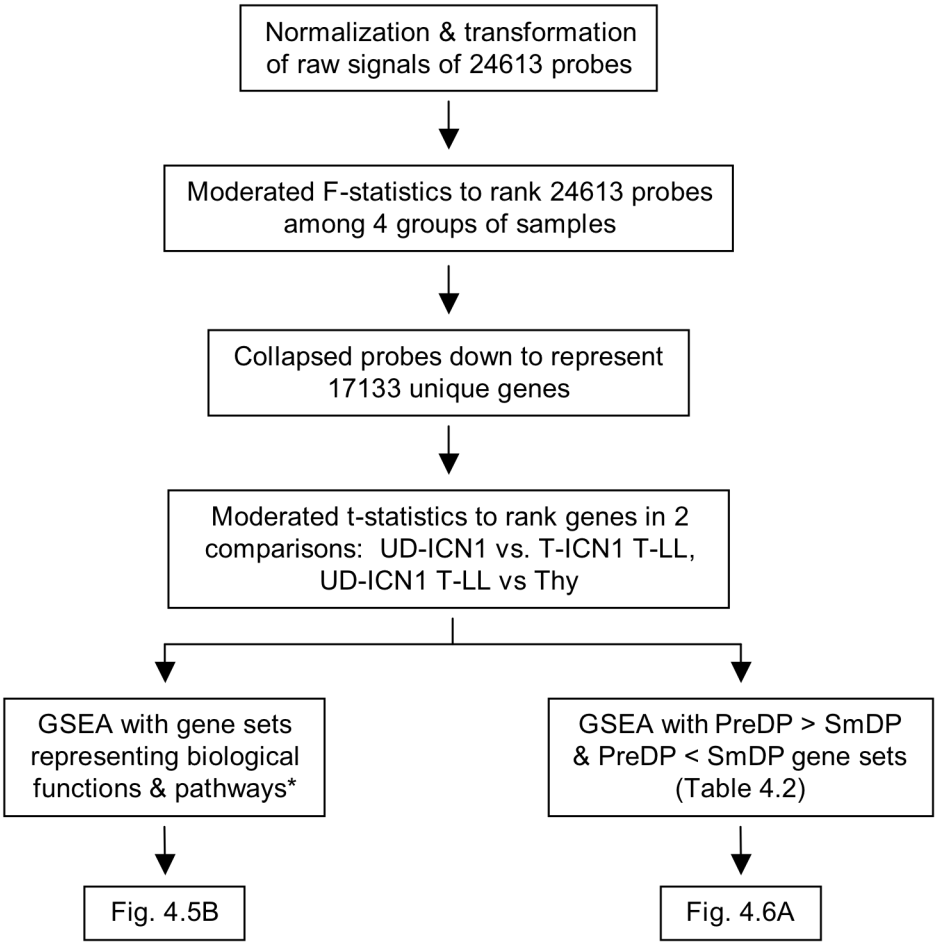

Figure 4.4 Workflow of GSEA on gene expression data
*Gene sets encompassing diverse biological functions and pathways were obtained from 5 sources: NCI/nature Pathway Interaction Database, Biocarta pathways, KEGG pathways, the Gene Ontology database, and the Pfam protein families database.

A.

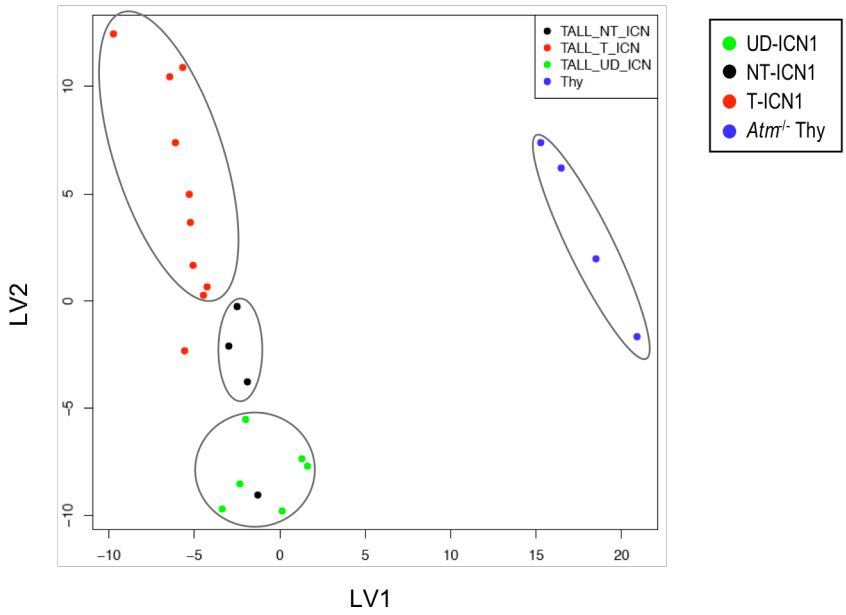
TALL_NT_ICN
TALL_T_ICN
TALL_UD_ICN
Thy
UD-ICN1
NT-ICN1
T-ICN1
Atm-/- Thy
LV2
LV1
10
5
0
−5
−10
−10
−5
0
5
10
15
20

B.

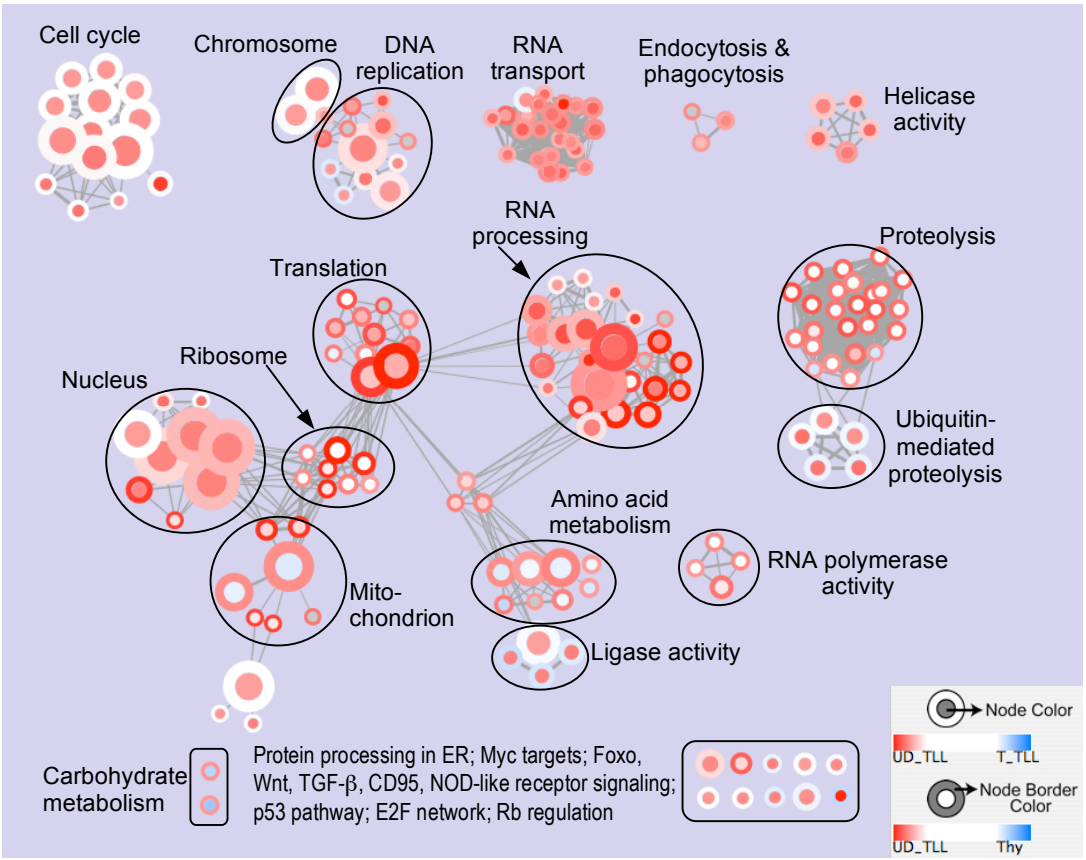
Cell cycle
Chromosome
DNA replication
RNA transport
Endocytosis & phagocytosis
Helicase activity
RNA processing
Proteolysis
Translation
Ribosome
Nucleus
Ubiquitin-mediated proteolysis
Amino acid metabolism
RNA polymerase activity
Mito-chondrion
Ligase activity
Carbohydrate metabolism
Protein processing in ER; Myc targets; Foxo, Wnt, TGF-β, CD95, NOD-like receptor signaling; p53 pathway; E2F network; Rb regulation
Node Color
UD_TLL
T_TLL
Node Border Color
UD_TLL
Thy

Figure 4.5 Gene expression data separate T-LL subgroups and reveal distinct gene set enrichment profiles

(A) Supervised Bridge-PLSR plot of gene expression data. Pre-processed gene expression data for 24,613 probe-sets from 20 T-LLs and 4 pre-malignant thymocyte samples were subjected to Bridge-PLSR to summarize data variation across samples in a two-dimensional plot. The x- and y-axes (LV1 and LV2) represent 27% and 17% of variation in the data set. Each dot indicates a sample.. (B) Cytoscape enrichment map of GSEA outputs from UD-ICN1 vs. T-ICN1 and UD-ICN1 vs. *Atm*$^{-/-}$ thymocytes comparisons. The GSEA workflow is summarized in Fig. 4.4. Gene sets displayed had significant ES (nominal $p < 0.01$ and FDR $q < 0.05$). Circular nodes symbolize gene sets and node size is proportional to the number of genes in the set. Red nodes have significant high positive ES, whereas blue nodes have high negative ES. Node centers represents ES significance for the UD-ICN1 vs. T-ICN1 T-LL comparison, whereas node borders depict ES significance for the UD-ICN1 T-LL vs. Thy comparisons. Node color intensity is proportional to ES significance. Lines connecting two gene sets indicate common genes and the thickness signifies degree of overlap between the gene sets. Gene sets with similar biological features were grouped and labeled under single names for ease of viewing.

A.

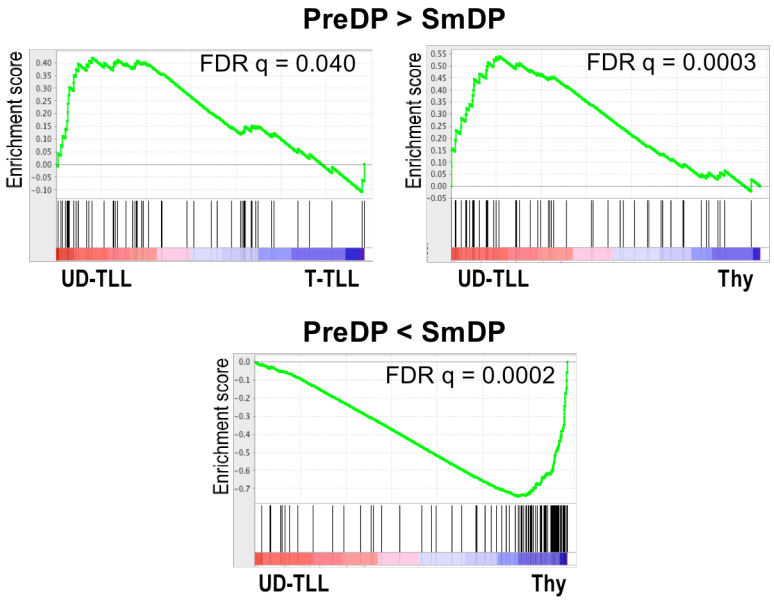
PreDP > SmDP
Enrichment score
FDR q = 0.040
UD-TLL
T-TLL
Enrichment score
FDR q = 0.0003
UD-TLL
Thy
PreDP < SmDP
Enrichment score
FDR q = 0.0002
UD-TLL
Thy

B.


Thy
UD-ICN1 T-LL
T-ICN1 T-LL
Klf9
Klf9
Wdhd1
Hmgn5
Cops2
Rfc1
Ankrd49
Hmgcs1
Cnot7
Mcm4
Rbl1
Tmpo
Nfix
Hand1
Zfp239
Ahr
Rbpjl
Cnbp
Nr1h4
Hoxd3
Ptrf
Rpf2
Hmgb3
Polr3d
Irx3
Hoxb8
Tcerg1
Htr5a
Kdm1b
Rnf141
Nucks1
Pou2f3
Clpb
Aurkaip1
Tacc3
Mcm7
Mcm5
Mcm2
Rbbp7
Tfdp1
Bard1
Uhrf1
Mybl2
Foxm1
Bola2
Ruvbl2
Kat2a
Thra
E2f1
Mcm6
Myc
Irf8
Sox13
Cebpb
Pou2af1
Hes1
Fold expression
(log2)
-1.32
0
1.32

C.

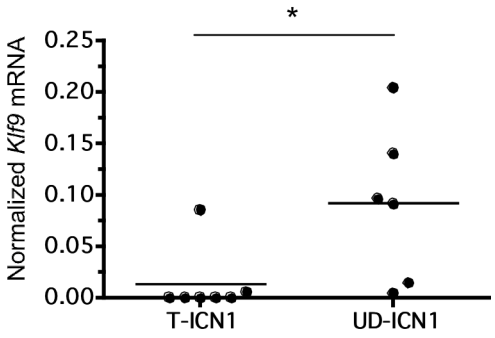
*
Normalized Klf9 mRNA
0.25
0.20
0.15
0.10
0.05
0.00
T-ICN1
UD-ICN1

Figure 4.6 UD-ICN1 T-LL samples exhibit a "preDP-like" gene expression signature
(A) GSEA enrichment plots of UD-ICN1 T-LL vs. T-ICN1 T-LL and UD-ICN1 T-LL vs. *Atm*$^{-/-}$ thymocyte comparisons. GSEA was performed on the same comparisons as Fig. 4B using the PreDP > SmDP and PreDP < SmDP gene-sets (refer to Table 4.2). *Top plots:* Enrichment plots for PreDP > SmDP gene set. Each plot depicts the location of genes in the gene set in the ranked list for each comparison (x-axis) versus the ES (y-axis). The ranked list for each plot is ordered (left to right) to show: significantly over-expressed genes in the first group (red zone), non-significant genes (white zone) and significantly under-expressed genes in the second group of each comparison (blue zone). Vertical black lines depict genes in the ranked list found in the gene set. The green line represents the running sum of the ES, which increases when ranked genes are found in the gene set and decreases when ranked genes are not found in the gene set. The peak ES was used to determined statistical significance. False discovery rate (FDR) is the estimated probability that the peak ES is a false positive. *Bottom plot*: Enrichment plot for PreDP < SmDP gene set using UD-ICN1 T-LL vs. *Atm*$^{-/-}$ thymocytes ranked list. (B) Heatmap showing differential expression of transcription factors in PreDP > SmDP gene set. Fold expression of 55 transcription factors (rows) computed as ratio of gene expression of each sample (columns) to mean expression of T-ICN1 group. The top 13 genes (in blue rectangle) are genes that contribute to the peak enrichment score in top left plot in (A). (C) qRT-PCR analysis of *Klf9* expression in UD-ICN1 (n=6) relative to T-ICN1 (n=7) T-LL. Relative *Klf9* mRNA levels were computed by normalizing to *Ptprc* mRNA levels measured in each sample. Relative *Klf9* mRNA means were 0.013 ± 0.012 for T-ICN1 and 0.092 ± 0.031 for UD-ICN1 groups (*p = 0.028).

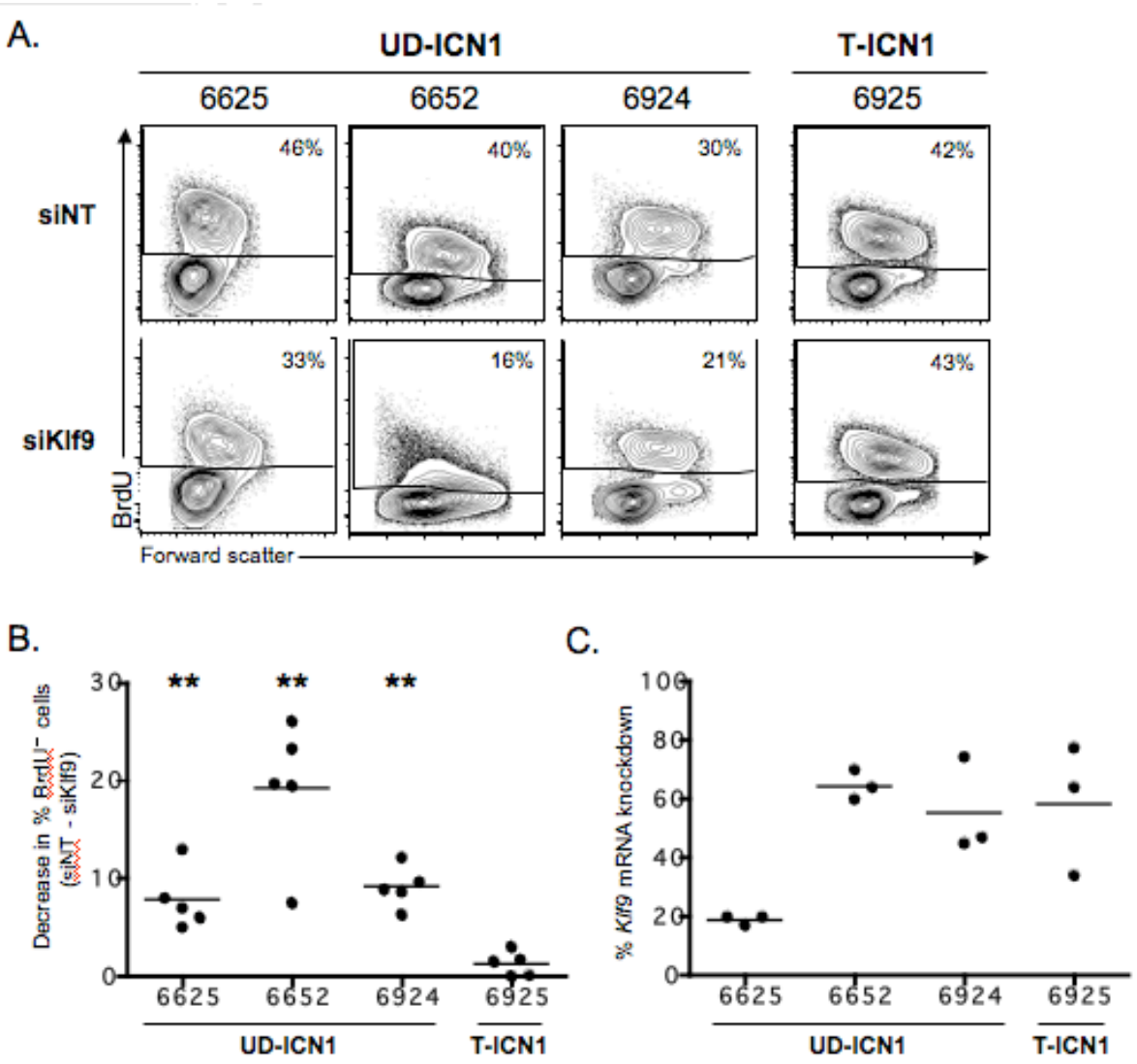

Figure 4.7 *Klf9* promotes proliferation of UD-ICN1 T-LL cell lines
(A) *Klf9* siRNA knockdown reduces proliferation of UD-ICN1 T-LL cell lines. The indicated T-LL cell lines were cultured in the presence of *Klf9*-targeting siRNA (siKlf9) or non-targeting siRNA (siNT) for 2 days, and BrdU was added 1 h prior to harvesting. Cells were then stained with anti-BrdU and analyzed by flow cytometry. Representative anti-BrdU vs. forward scatter profiles (5% probability, including outliers) pre-gated on live singlets are shown. BrdU gates were set using unstained control samples, and the % $BrdU^+$ cells within the live subset is indicated. Data from 4 independent experiments for 6625 and 3 independent experiments for 6652, 6924 and 6925 are summarized in (B). Statistically significant differences in % $BrdU^+$ cells between siNT and siKlf9 are determined using paired two-tailed Student's t-tests are indicated (**, $p < 0.005$). (C) Efficiency of *Klf9* knockdown. *Klf9* mRNA abundance was measured by qRT-PCR and normalized to *Ptprc* mRNA. Proportion (%) of *Klf9* mRNA knockdown represents (siNT-siKlf9)/siNT for 3 independent experiments with each cell line.

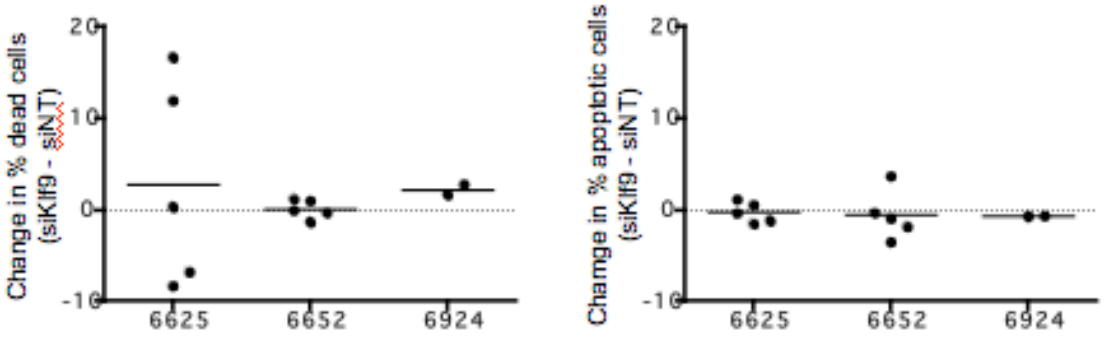

Figure 4.8 *Klf9* did not affect survival of UD-ICN1 T-LLs
Klf9 siRNA knockdown did not affect survival of UD-ICN1 T-LLs. The indicated T-LL cell lines were cultured in the presence of *Klf9*-targeting siRNA (siKlf9) or non-targeting siRNA (siNT) for 2 days. Cells were then stained with Fixable Blue (for dead cell identification), fixed, permeabilized and stained with anti-activated caspase-3 antibody prior to analysis by flow cytometry. Fixable Blue (FB) and activated caspase-3 (AC3) gates were set using unstained control samples, and the % FB^+ cells (dead cells) and $AC3^+$ cells (apoptotic cells) were determined. Dotted line at 0% represents no difference between siKlf9 and siNT conditions. Paired two-tailed t-test did not reveal statistically significant difference in % dead or apoptotic cells between siKlf9 and siNT from 2-4 independent experiments.

4.5 Discussion

In this study, we showed that 20% of our *Atm*$^{-/-}$ T-LL cohort had undetectable ICN1 protein, expressed very low levels of direct ICN1 target genes, and their growth was insensitive to Notch inhibition. Although a previous study suggested that PTEN loss can confer Notch-independent growth to T-LL cell lines with mutant *NOTCH1*, we did not observe a difference in Notch dependence between PTEN^{+} and PTEN^{-} samples in the T-ICN1 group, suggesting that PTEN loss does not confer Notch independence to *Atm*$^{-/-}$ T-LLs. We compared global gene expression profiles from T-ICN1 and UD-ICN1 T-LL samples to identify genes that regulate cell proliferation and survival of T-LL cells lacking activated Notch1. These experiments suggested that ICN1 status profoundly influences gene expression patterns among *Atm*$^{-/-}$ T-LLs. Using GSEA, we identified several cellular processes that appeared to be differentially active in UD-ICN1 vs. T-ICN1 T-LLs. For example, sets of genes implicated in cell cycle control and ubiquitin-mediated proteolysis were highly enriched in the UD-ICN1 group relative to the T-ICN1 group, suggesting that these processes are regulated differently in T-LLs with high versus low Notch activity. Genes regulating other processes, such as amino acid metabolism, general proteolysis, ribosome function and translation, were not enriched in either T-LL group, suggesting that they are not highly regulated by Notch signaling. However most of these gene sets were enriched in the UD-ICN1 vs. thymocytes comparison, suggesting that they are features of the malignant phenotype.

Most T-LLs are developmentally arrested during the process of β-selection, so we also evaluated expression of groups of TFs that are highly regulated during this transition.

Interestingly, the UD-ICN1 subset expressed higher levels of a group of TFs whose expression normally declines during the preDP to smDP transition of normal T-cell development. The leading edge of this group contains 6 TFs (Klf9[334], Wdhd1[347], Hmgn5[345], Rfc1[346], Cnot7[343] and Mcm4[344]) that either facilitate DNA replication at S phase or more generally promote proliferation in various cell types. Notably, mutations in *Mcm4* (minichromosome maintenance-deficient 4), which encodes a subunit of the DNA replication licensing factor MCM2-7 complex, are oncogenic[344,354]. Specifically, the heterozygous missense mutation, $Mcm4^{D573H}$, cause T-LL in mice[344]. The importance of the remaining five TFs in T-cell development or leukemogenesis has not been examined.

The most significantly over-expressed member of this group was *Klf9* – a transcription factor that regulates differentiation, proliferation and cell survival in different tissues[333-335,355,356]. Interestingly, *Klf9* expression was required for maximal proliferation of UD-ICN1 T-LLs but not for proliferation of T-ICN1 cells. The dissimilar *Klf9* mRNA levels among UD-ICN1 T-LL samples likely contributed to the different degree of *Klf9* knockdown between T-LL cell lines, which in turn resulted in varying effects on proliferation. Klf9 is a zinc-finger-containing transcription factor that binds to GC-rich sites in gene promoters or enhancers[357]. A proliferative role of Klf9 has been reported in non-lymphoid tissues including mouse intestinal crypt cells[334] and endometrial cells[335]. However, Klf9's role is context-dependent since Klf9 has also been shown to reduce endometrial sensitivity to the mitogenic action of estrogen[334]. Whether Klf9 functions as a transcription activator or repressor also seems to be context-dependent. In myogenesis, Klf9 activates *fgfr1* (fibroblast growth factor receptor 1) transcription to induce myoblast proliferation; whereas it suppresses *fgfr1* transcription in differentiated myotubes possibly

by recruiting co-repressor via its Sin3A-binding domain[333]. In human glioblastoma cells, KLF9 has been shown to repress NOTCH1 transcription thereby inducing differentiation[350]. We hypothesized that a similar mechanism could explain low level expression of *Notch1* in UD-ICN1 T-LLs. However *Klf9* knockdown did not augment *Notch1* level in these cells (data not shown) suggesting that other mechanisms underly low *Notch1* expression in this context. Lastly, higher *Klf9* expression is observed in high-risk *BCR-ABL*+ B-ALL relative to standard risk B-ALL, suggesting its association with poor prognosis[358]. Collectively, these observations suggest that further studies of Klf9 function in B- and T-cell malignancies may provide new avenues for therapeutic intervention.

4.6 Acknowledgements

The authors thank G. Casallo (TCAG, the Hospital for Sick Children) for technical assistance with microarray experiments. This work was supported by a Genome Canada grant to J.S.D. and C.J.G. Salary support for PPCW was provided by the Terry Fox Foundation, Canadian Child Health and Clinician Scientist Program, Christopher Brundage Endowment Fund and the Division of Haematology/Oncology, the Hospital for Sick Children.

CHAPTER 5:

SUMMARY OF RESULTS AND GENERAL DISCUSSION

5. SUMMARY OF RESULTS AND GENERAL DISCUSSION

5.1 Summary of Results

This thesis examined the molecular pathogenesis of Notch-dependent and Notch-independent T-LL that developed spontaneously in mice lacking Atm. In chapter 2, I first characterized the immunophenotypes and Notch1 expression and mutational status in a cohort of 41 *Atm*$^{-/-}$ T-LL cases. Most T-LL samples were arrested at CD8 ISP and/or CD4/8 DP stages of early T-cell differentiation. Assessment of the *Notch1* sequence revealed PEST mutations encoding truncated ICN1 protein in 70% of T-LL; however, activating HD mutations were only detected in 9% of cases. Previous gene expression profiling of *Atm*$^{-/-}$ T-LL indicated aberrant upregulation of *Il7r* and *Sdc1* relative to non-malignant *Atm*$^{-/-}$ thymocytes[280]. Indeed, normal CD8 ISP and DP thymocytes lack IL-7Rα expression[138], yet their malignant counterparts expressed IL-7Rα[280]. Sdc1 is a cell surface proteoglycan that was expressed by malignant but not normal thymocytes, making it a useful marker of malignant transformation. Furthermore, we detected Sdc1 expression by thymocytes harvested from healthy mice displaying features of the earliest discernible stage of T-LL progression: a lack of thymic enlargement, normal thymocyte numbers (<100 x 10^6) and CD4/8 profiles, but increased cell size (>15% of blasts). Therefore, Sdc1 served as a useful marker for early stages of T-LL progression. Both Notch1 and IL-7R pathways are critical for sustaining T-LL[10,277,325,359], however, it was unclear whether aberrant Notch1 and IL-7Rα expression represented early events in *Atm*$^{-/-}$ T-LL transformation. We found both truncated ICN1 and IL-7Rα expressed by thymocytes at the earliest discernible stage of T-LL, suggesting possible roles in cancer initiation in addition to T-LL maintenance.

The rare occurrence of *Notch1* HD mutations in $Atm^{-/-}$ T-LL prompted us to investigate for possible mechanisms of Notch1 activation. In chapter 3, I showed that Notch inhibition by GSI suppressed the viability of ICN1-expressing T-LL cells, demonstrating their Notch-dependence. Surprisingly, T-LL cells that expressed Notch1 proteins with wildtype HD domain proliferated equally well in the presence or absence of Notch ligand, DL-1, suggesting that ligand-independent Notch1 activation contributed to T-LL viability. At the time of our investigations, Ashworth *et al*. reported 2 types of intragenic deletions that resulted in short *Notch1* transcripts encoding for Notch1 proteins that initiated within the transmembrane domain in various T-LL-prone mouse models[232]. The truncated Notch1 protein is activated independently of ligand, but requires γ-secretase proteolysis. Therefore, we determined whether the 2 types of deletions might be mechanisms for ligand-independent Notch1 activation seen in some ICN1-expressing $Atm^{-/-}$ T-LL and found them in 17% of cases. To determine whether T-LL cells expressed truncated *Notch1* transcripts, we analyzed RNAs isolated from 10 ICN1+ T-LL. Expectedly, the 2 samples that harbored HD mutations (1756 and 6106) expressed only full-length *Notch1* transcripts. The remaining 8 T-LL samples, including two that contained intragenic deletions (8652 and 2967), all expressed short transcripts ranging from 3-5 kb. PCR amplification followed by sequencing of the 5' ends of the transcripts revealed alternate transcription initiation within exons 25/26 or upstream of exon 1a. Using the ATGpr program[307], the aberrant *Notch1* transcripts were predicted to encode truncated Notch1 proteins that lacked functional NRR but retained S3 site hence permitting ligand-independent but γ-secretase-reliant Notch1 activation.

In chapter 4, I demonstrated that 20% of *Atm*$^{-/-}$ T-LL lacked ICN1 expression (UD-ICN1), which was accompanied by undetectable to low levels of *Notch1* mRNA, significantly lower levels of Notch1 transcriptional targets, and a resistance to Notch inhibition by GSI. These findings identified a subgroup of Notch-independent T-LLs; thus, our objective was to gain insights into pathways that regulate their survival and proliferation. Since PTEN loss has been suggested to bypass Notch requirement in human T-LL cell lines[111], we determined whether loss of PTEN protein was associated with Notch-independence. We found that almost all UD-ICN1 T-LL samples (5 out of 6) lost PTEN expression, consistent with the idea that PTEN loss relieves T-LL cells from dependence on Notch signal. However, PTEN loss did not confer resistance to Notch inhibition in ICN1-positive T-LL, similar to the findings in primary human T-LL samples[246]. To identify proliferative and survival signals that sustained Notch-independent UD-ICN1 T-LLs, we performed gene-set enrichment analysis of the genome-wide expression profiling of UD-ICN1 T-LLs. We found that *Klf9*, a member of the Kruppel-like transcription factor family that regulates cellular differentiation, survival and proliferation[360,361], was expressed at significantly higher levels in UD-ICN1 than ICN1-positive T-LLs. Notably, *Klf9* positively regulated proliferation of Notch-independent UD-ICN1 T-LLs, suggesting that *Klf9* might be a potential therapeutic target for human T-LLs with absent or low Notch activity.

5.2 General Discussion

The clonal evolution in cancer follows the basic tenets of Darwinian natural selection[362,363]. According to the Darwinian model, a cell divides and its descendent

population forms subclones that are genetically diverse and they are subjected to selection (e.g. constraints of the micro-environment, competition between subclones, exposure to carcinogens, and chemotherapeutic drugs). This process is reiterative such that subclones become more fit and gain dominance by accruing advantageous traits such as self-renewal capacity, extensive proliferation, evading apoptosis, angiogenesis and migration[364,365]. Genetic studies of identical twins concordant for ALL demonstrated that overt leukemic clones evolved from common ancestral cancer cells[366,367]. Genome-wide DNA copy number analyses of paired diagnostic and relapsed pediatric B- and T-ALL samples revealed that a majority of relapsed cases evolved from ancestral subclones[368,369]. Moreover, backtracking studies of specific lesions demonstrated that in most cases, the relapse clone could be detected as a minor subclone in the diagnostic sample before therapy. In order for the earlier subclones to persist and evolve to a dominant clone at relapse, they likely had acquired the self-renewal capacity[370,371]. Hence, targeting these cancer-propagating cells will likely be the most effective therapeutic strategy[363].

It is impossible to study the evolution of T-LL prospectively in humans since for the most part it is clinically silent until when the patient presents with overt leukemia; however, at this point, the evolutionary course is already history. By contrast, genetically-engineered mice, with a high disease penetrance and a predictable onset, allow prospective examination of early events of cancer development. Therefore, we used *Atm*-deficient mice that spontaneously developed T-LL beginning at 12 weeks of age as a tool to identify genetic changes at earlier stages of T-LL progression. In chapter 2, we examined a large cohort of $Atm^{-/-}$ T-LLs and identified PEST mutations resulting in truncated ICN1 protein in a majority of cases (70%), suggesting truncating *Notch1* PEST mutations as a frequent genetic

event, as found in other murine T-LL models[7-9,223,224]. Previous gene expression profiles of *Atm*$^{-/-}$ T-LLs performed in our laboratory have identified two additional abnormalities, namely the aberrant expression of cell surface proteoglycan, *Sdc1*, and *Il7r*[280], which we validated their protein expression in our T-LL cohort. We detected SDC1, IL-7Rα, and truncated ICN1 on thymocytes at the earliest discernible stage of lymphomatous progression suggested by an increased frequency of blasts in clinically healthy *Atm*$^{-/-}$ mice. Therefore, *Notch1* PEST mutations along with aberrant IL-7Rα and SDC1 expression represent early events in *Atm*$^{-/-}$ T-lymphomagenesis.

Since cancer-propagating (or initiating) cells are able to self-renew and evolve with additional 'driver' mutations to reappear after therapy[368,370-372], targeting these cells or their self-renewal machinery is a rational approach to eradicate disease. Notch and IL-7 signaling pathways have been implicated in self-renewal of normal T-cell progenitors. Our laboratory has demonstrated that Notch ligand DL-induced Notch signaling promotes self-renewal of β-selected DN3b and DN4 thymocytes in an IL-7-dependent manner[331]. Notch and IL-7 signaling also sustains the self-renewal potential of DN1 and DN2 progenitors[135] and a drop in IL-7 level induces an upregulation of transcription factor Bcl11b, which aborts precursor expansion and promotes T-cell commitment and differentiation to DN3[132,133,208]. Interestingly, hemizygous deletions of *Bcl11b* are frequently detected in mouse *Atm*$^{-/-}$ T-LLs[284] and Bcl11b suppresses T-LL development induced by γ-radiation[209], and p53 haploinsufficiency[210]. Recurrent loss-of-function *BCL11B* mutations and deletions are observed in various molecular subtypes of human T-LLs[200,201]. These data suggest that Notch and IL-7 signaling promotes self-renewal of thymocyte progenitors. Furthermore,

down-regulation of Bcl11b is critical for sustaining self-renewal functionality in normal progenitors and likely in murine and human T-LL as well.

Aberrant Notch signaling has been demonstrated to be an early transforming event and promote T-cell leukemia-propagating activity in murine and human T-LL models. TAL1/SCL and LMO (LMO1 or LMO2) are over-expressed in 50-60% of human T-LLs[176]. Expectedly, *SCL*^{tg}*LMO1*^{tg} mice[8,293] and a related model, *Tal1/Lmo2* mice[294] both develop T-LL, which frequently harbor *Notch1* mutations. Both models show an accumulation of DN3 and DN4 progenitors in the pre-leukemic phase and *Notch1* PEST mutations are detected in these progenitors associated with Notch activation. Serial transplantation experiments identified self-renewal capacity enriched mainly in DN3 and/or DN4 populations of T-LLs. Furthermore, Notch inhibition decreased leukemia-initiating cell frequency and delayed disease onset[294]. On the other hand, enforced expression of constitutively active ICN1 beginning at the DN2 stage in *Notch1*^{tg}*SCL*^{tg}*LMO1*^{tg} mice accelerated the onset of leukemia and confers leukemogenic potential to DN1-4 progenitors from pre-leukemic mice[293]. These findings suggest that aberrant Notch1 activation occurs early and drives leukemogenesis in some murine T-LL models. Leukemia-propagating potential has also been revealed in human T-ALL, although the identity of cellular fractions possessing the self-renewal capacity remains a contentious subject[373,374]. This is not surprising in light of recent evidence demonstrating that cancer progression is a dynamic process and cancer cells (including cancer-propagating cells) change their genotype/phenotype to adapt to new selective pressures[368,370-372]. However, the defining feature of a cancer-propagating cell, namely its self-renewal capability remains constant. Xenotransplantation studies of human T-ALL reveal Notch dependence in T-LL propagation in sequential transplants[373,375].

Furthermore, Giambra *et al.* recently showed that Notch1 signaling repressed PKC-θ expression, which limited reactive oxygen species production and enhanced T-LL self-renewal capacity[375]. In summary, Notch activation can promote T-LL propagation in both human and mice.

In contrast, a role for IL-7 signaling in regulating T-LL-propagating activity has not been demonstrated. However, crosstalk between Notch and IL-7 signaling exists at different levels. Notch1 signaling activates *IL7R* transcription in human T-cell progenitors and their malignant counterparts[239]. Moreover, it has been reported in human T-LL cell lines that Notch1 activation potentiates PI-3K signaling, a downstream effector of IL-7R, by repressing the expression of PI-3K antagonist, *PTEN*[111]. Future experiments should investigate whether Notch1 and IL-7R signaling cooperate to propagate T-LL in $Atm^{-/-}$ mice (see section 5.3). Our discovery of SDC1 expression on thymocytes at an early stage of transformation (chapter 2) will allow us to isolate these early transformed cells and examine their self-renewal capacity prospectively.

SDC1 is a cell surface heparan sulfate proteoglycan that modulates disease processes such as cancer cell proliferation, apoptosis, invasion and angiogenesis[376]. Dysregulation of SDC1 expression has been observed in many cancers including carcinomas of the breast[377], prostate[378], and colon[379]. For example, $Sdc1^{-/-}$ mice avoid Wnt-induced mammary tumorigenesis and the heparan sulfate-containing ectodomain of SDC1 positively modulates Wnt signaling[380]. B-cell progenitors, plasma cells and their malignant counterparts in multiple myeloma also express SDC1, also known as CD138[304]. SDC1 binds via its heparan sulfate chains at the ectodomain to hepatocyte growth factor, which promotes Met signaling, and leads to growth and survival of myeloma cells[290,381]. Therefore, the heparan sulfate

chains in SDC1 may serve as a scaffold that brings ligand and receptor into close proximity[376], limit the diffusion of growth factors and act as a reservoir for HS-binding growth factors[304]. Indeed, SDC1-expressing pro-B cells that lack heparan sulfate dramatically reduce binding and responsiveness to IL-7, which is critical for early B-cell development[305]. Therefore expression of SDC1 by T-LL may positively regulate IL-7R-driven signal by capturing IL-7. Further studies are required to examine whether changes in SDC1 expression alter IL-7 dose responsiveness in T-LL cells (section 5.3). Recent gene expression profiles of human T-LL lacking *TLX1* and *TLX3* indicate a subgroup that upregulates SDC1, suggesting a potential role for SDC1 in some human T-LL cases[200].

Our finding of frequent PEST mutations without concomitant activating HD mutations in *Atm*$^{-/-}$ T-LL cases seems puzzling because previous studies have demonstrated that PEST mutations alone are not oncogenic[221]. As shown in chapter 3, viability of most *Atm*$^{-/-}$ T-LL cases requires γ-secretase-mediated Notch activation, but it does not require ligand interaction. Just when we started to investigate for alternative mechanisms of aberrant Notch activation, two studies reported novel activating *Notch1* mutations in other murine T-LLs[232,233]. Ashworth and colleagues identifed 2 types of intragenic *Notch1* deletions that result in abnormal transcripts lacking the extracellular ligand-binding domain in different mouse T-LL cell lines. Both types of transcripts encode for truncated Notch1 proteins that undergo ligand-independent but γ-secretase-dependent activation. Type 1 deletions span exon 1 and its promoter, are flanked by RSS-like sequences suggestive of illegitimate VDJ recombination, and initiate transcription in the middle of exon 25. In contrast, type 2 deletions involve a region downstream of exon 1 such that the mRNA begins at exon 1, which is spliced into exons 27/28. In another mouse model where

homozygous hypomorphic *Ikzf1* mutation induces T-LL, deletion of *Notch1* exon 1 and promoter region accelerates the oncogenic process associated with truncated Notch1 mRNA accumulation[233] (similar to type 1 transcripts).

We looked for Type 1 and Type 2 deletions and found them in only 4% and 13% of *Atm*$^{-/-}$ T-LL cases, respectively. Eight ICN1+ T-LL samples contain truncated *Notch1* mRNA and their sequences initiate either in the middle of exons 25/26 or exon 1a, an exon upstream of exon 1, including two cases containing Types 1 and 2 deletions. Hence, we observed a very low frequency of RAG-mediated (Type 1) deletions in our *Atm*$^{-/-}$ T-LL mouse model. Tsuji *et al*. also reported a lower frequency of RSS-flanked *Notch1* deletions in their *Atm*$^{-/-}$ T-LL cohort (24%)[230]. The relative low frequency of RAG-mediated deletion observed in ATM-deficient T-LLs may be related to ATM's function in repair of double-strand DNA breaks (DSB)[312]. Moreover, in ATM-deficient lymphocytes, a partial block in the coding join formation results in an accumulation of unrepaired coding ends[271,289,313]. Tsuji *et al*. identified deletions without RSS in 41% of *Atm*$^{-/-}$ T-LL cases, which were accompanied by microhomology sequences or nucleotide additions at their breakpoints[230]. Others reported that ATM deficiency causes an increased frequency of intrachromosomal homologous recombination that can result in intragenic deletions[314], possibly involving repetitive DNA sequences such as Alu repeats or long interspersed elements (LINE). Non-allelic homogolous recombination has been described as a mechanism for genomic deletions of *NF1* gene[315], causing tumor-predisposition syndrome neurofibromatosis. Moreover, non-homologous recombination between Alu and LINE-1 repetitive elements can cause deletions in the dystropin gene resulting in muscular dystrophies[316]. Examination of the *Notch1* locus identifies multiple Alu elements in introns 1a and 2, as well as LINE repeats in intron 2.

Hence, recombination between repetitive elements could be another potential mechanism for intragenic *Notch1* deletions.

The truncated *Notch1* transcripts identified in *Atm*$^{-/-}$ T-LLs use alternative promoters at exon 1a and exons 25/26. We have not demonstrated mechanistically how this is achieved, but a loss of Ikaros function may facilitate this process[233,295]. Ikaros is a zinc-finger transcription factor that antagonizes the action of Notch in its target gene transcription in developing thymocytes[382]. A loss of Ikaros, which represses *Notch1* transcription at canonical (exon 1) and alternative promoters, increases chromatin accessibility to active transcription machinery at these sites[233,295]. Therefore, loss-of-function mutations in *Ikzf1* may facilitate use of alternative promoters and this possibility deserves future examination in the *Atm*$^{-/-}$ T-LL model.

In chapter 4, I focused the attention on a subgroup of *Atm*$^{-/-}$ T-LLs that was Notch-independent and determined the signals that were important for their cell survival and proliferation. We identified Kruppel-like factor 9 (*Klf9*) that promoted proliferation of Notch-independent *Atm*$^{-/-}$ T-LL cells. Klf9 is a zinc-finger transcription factor that controls proliferation, differentiation and cell fate decision of several tissue types. Female *Klf9*$^{-/-}$ mice exhibited subfertility due to an impaired proliferative response to progesterone by luminal epithelium that increases risk of unsuccessful implantation of embryos[335]. However, Klf9's role is context-dependent since Klf9 has also been shown to reduce endometrial sensitivity to the mitogenic action of estrogen[334]. Furthermore, ablation of *Klf9* suppresses intestinal crypt cell proliferation and favors Paneth cell lineage choice over goblet cell fate[334]. By contrast, naïve B cell activation results in downregulation of several transcription factors including Klf9 in memory B cells, which is critical for rapid proliferation of memory

B cells during secondary antibody responses[383]. Whether Klf9 functions as a transcription activator or repressor also seems to be context-dependent. In myogenesis, Klf9 activates *fgfr1* (fibroblast growth factor receptor 1) transcription to induce chicken myoblast proliferation; whereas it suppresses *fgfr1* transcription in differentiated myotubes possibly by recruiting a co-repressor via its Sin3A-binding domain[333]. Lastly, KLF9 promotes differentiation of glioblastoma-initiating cells via repression of *NOTCH1* transcription[350]. We hypothesized that a similar mechanism could explain the low levels of *Notch1* in UD-ICN1 T-LLs. However *Klf9* knockdown did not augment *Notch1* level in these cells suggesting that low *Notch1* level occurred through Klf9-independent mechanisms. A higher *KLF9* expression has recently been reported in high-risk *BCR-ABL*+ B-ALL relative to standard risk disease, suggesting its association with poor prognosis[358]. Hence, an understanding of Klf9 function in B- and T-LL may have therapeutic implications.

Two mouse models provide additional insights into the development of Notch-independent T-LL. First, conditional deletion of Pten in mouse fetal liver hematopoietic stem cells results in development of myeloproliferative disorder that evolves into T-ALL blast crisis[384]. Both leukemia-propagating population (c-kit^{mid}CD3^{+}Lin^{-}) and its descendent bulk leukemic blasts (c-kit^{-}CD3^{+}Lin^{-}) express high levels of the activated unphosphorylated form of β-catenin. Conditional deletion of one allele of *Ctnnb1* (β-catenin) in Pten-null mice decreases and delays onset of T-LL, suggesting β-catenin is critical in leukemogenesis. A frequent secondary event found only in leukemic blasts is t(14;15) translocation that results in upregulation of c-Myc expression driven by the Tcrα/δ promoter. Interestingly, T-LL cases are associated with wildtype *Notch1* sequence in the HD and PEST domains and low level of Notch target *Hes1* (similar levels to wildtype thymocytes consists mainly of DP

cells that lack Notch signal). In the second mouse model, conditional deletion of exon 3 of *Ctnnb1* renders the protein constitutively active since it cannot be phosphorylated and degraded[385]. Deletion from DN2 and DN4 stages of T-cell development leads to T-LLs with the same predominantly CD4/8 DP phenotype. Again, c-Myc overexpression coincides with the evolution to overt disease and homozygous deletion of *Myc* abrogates T-LL development. Similarly, T-LL oncogenesis occurs independently of Notch signal. However, the Pten status of these T-LL cases was not determined. Collectively, these 2 T-LL models suggest that Pten inactivation and constitutively active β-catenin can propagate T-LL in a Notch-independent fashion. Furthermore, c-Myc overexpression is a common secondary event. In Notch-independent $Atm^{-/-}$ T-LL cases, we found a majority (5/6) lacked detectable PTEN protein. Further investigation on β-catenin signaling in Notch-independent subgroup of $Atm^{-/-}$ T-LL is warranted. More importantly, human T-LL cases that lack gain-of-function *NOTCH1* mutations and exhibit low Notch target gene expression should be investigated for dysregulated β-catenin/Wnt signaling as this may lead to a novel therapeutic target for the disease.

5.3 Limitations of the present study and future directions

1. In chapter 2, we identified aberrant SDC1, Notch1 and IL-7Rα expression as early events in T-LL development, however their functions in disease propagation have not been addressed. Transplantation studies using pre-malignant $SDC1^{+}$ thymocytes to determine the role of Notch1 and IL-7R signals in T-LL propagation are warranted. Briefly, thymocytes will be harvested from healthy-looking 8-12 week-old $Atm^{-/-}$ mice and assessed by cell counting and immuophenotyping to select for

thymi at the earliest stage of T-LL development: normal cellularity (<100 x10^6), normal CD4/8 profile and upregulation of SDC1. Both IL-7Rα and ICN1 expression will be determined. Fluorescence-activated cell sorting will be used to isolate $SDC1^+$ thymocytes, which are subjected to lentiviral transfection with dominant-negative MAML (dn-MAML; GFP^+) to knockdown Notch signal. 10^3-10^6 GFP^+ or non-transfected cells will be injected into the bone marrow of *Rag2*$^{-/-}$; *Il7*$^{+/+}$ or *Rag2*$^{-/-}$;*Il7*$^{-/-}$ recipient mice, which will be monitored by signs of T-LL development. Notch targets including *Hes1* and *Dtx1* will be used to assess efficiency of Notch inhibition by dn-MAML. To assess the effect of Notch and IL-7R signal on T-LL self-renewal capacity, sequential transplantations will be performed.

2. To determine the function of SDC1, knockdown of its expression by lentiviral-mediated transfer of Sdc1 shRNA in IL-7 sensitive $SDC1^+$ T-LL cell lines will be performed. Non-targeting shRNA will be used as a control. Effectiveness of knockdown will be determined by flow cytometry. These cells will be cultured in the presence of 0-10 ng/ml of recombinant murine IL-7 and live cell number will be determined after 3 days of culture. The IL-7 dose-response curves for each cell lines with and without Sdc1 knockdown will be compared. A shift of the curve to the right would suggest a higher dose of IL-7 is needed to compensate for a loss in SDC1 expression in order to achieve the same level of proliferative expansion.
3. To determine whether human T-LLs express SDC1, 40 samples of pediatric and adult T-LL will be screened for SDC1 expression by flow cytometry. Expression of IL-7Rα in each T-LL will be analyzed and their *in vitro* sensitivity to IL-7 stimulation will be evaluated. If a subset of T-LLs that express SDC1 and IL-7Rα

can be identified, and they are responsive to IL-7, knockdown of SDC1 expression will be performed and its impact on IL-7 responsiveness will be measured. The identification of a subgroup of human T-LLs that express SDC1 would have clinical implications since Phase1/2 trials using anti-SDC1 antibody conjugated to a chemotherapeutic agent (BT062) suggest some efficacy and tolerable side-effect profiles in myeloma patients[386].

4. In chapter 3, we were not able to characterize genomic deletions for 6 cases of T-LL that expressed truncated *Notch1* transcripts using primers specifically designed to amplify regions containing Types 1 and 2 deletions[232]. Tsuji *et al*. reported deleted regions (nucleotides 5105-25304) in *Atm*$^{-/-}$ T-LLs[230] that lay outside of the Type 1 deleted region (nucleotides 4760-17005); we will design new primers that span nucleotides 5105-25304 of the *Notch1* gene to test for this.
5. We have not characterized the structure or activity of the protein encoded by truncated *Notch1* transcripts. RACE products will be cloned into pcDNA3 expression vector, which will be co-transfected with Notch-sensitive reporter plasmid pGL2 4xCSL-luciferase, and a *Renilla* luciferase internal control plasmid into U2OS cells[232]. Dual luciferase assays will be performed on lysates prepared from U2OS cells. Transfected U2OS cells will be treated with 1 μM GSI-X (Calbiochem) or carrier for 24 hours before harvesting for protein analysis by immunoblotting anti-Notch1 antibodies that recognize γ-secretase-cleaved Notch1 (Val1744; Cell Signaling) and intracellular portion of Notch1 (5B5; Cell Signaling) to determine sensitivity to γ-secretase and metalloprotease proteolysis.

6. Studies suggest a loss-of-function mutation in Ikaros increases chromatin accessibility at alternative Notch1 promoters, hence permitting transcription at these sites[233,295]. Furthermore, Ikzf1 inactivation occurs frequently in murine T-LL models[387] and falls into 4 categories: (1) null expression; (2) expression of smaller dominant-negative isoforms; (3) missense mutations at the DNA-binding domain; and (4) nonsense mutations leading to truncated protein[388]. We will perform RT-PCR to amplify *Ikzf1* cDNA between exons 2-7 to assess expression and to sequence transcripts for missense and nonsense mutations in $Atm^{-/-}$ T-LLs. We will analyze Ikaros protein expression by immunoblotting.
7. Since increased β-catenin signaling is critical for propagation of Notch-independent T-LLs[384,385], we will determine the level of unphosphorylated activated β-catenin by flow cytometry in our cohort of Notch-independent $Atm^{-/-}$ T-LL. Levels will be compared to levels in non-malignant $Atm^{-/-}$ thymocytes (~80% DP cells with low β-catenin level) and Notch-dependent $Atm^{-/-}$ T-LLs.
8. In the same panel of 40 human T-LLs mentioned in (3), unphosphorylated β-catenin expression will be assessed by flow cytometry. NOTCH1 status in these samples will also be characterized: HD and PEST mutations, ICN1 expression, target gene levels and GSI sensitivity. Correlation between β-catenin expression and NOTCH1 expression and activity will be determined. From mouse T-LL studies[384,385], we would expect high β-catenin level in T-LLs to correlate with low NOTCH1 activity.

5.4 Conclusions

This thesis provides insights into the molecular pathogenesis of *Atm*$^{-/-}$ T-LLs. In chapter 2, I identified 3 groups of T-LL based on activated Notch1 protein expression: T-ICN1 due to PEST mutations (63%); NT-ICN1 with wildtype HD and PEST domains (17%); and UD-ICN1 (20%). Activating HD mutations were rarely identified (9%) and co-existed with PEST mutations. I found truncated ICN1 expression, aberrant IL-7R and SDC1 expression in thymocytes at the earliest discernible stage of T-LL transformation, suggesting possible collaboration among these pathways to propagate T-LL. In chapter 3, I identified a group of Notch-dependent T-LLs without HD mutation, yet could expand *in vitro* without ligand interaction. Some of these samples were found to express truncated *Notch1* transcripts that initiated at alternative *Notch1* promoters: upstream of exon 1a and middle of exons 25/26. Most of these transcripts initiated at sites similar to those recently reported, which encoded for Notch1 protein that lacked an extracellular domain and underwent ligand-independent activation[232]. In chapter 4, I demonstrated that UD-ICN1 sample proliferated in a Notch-independent fashion and expressed low levels of Notch target genes. Most of the samples (5/6) lost PTEN expression, suggesting that PTEN loss may substitute partially for low Notch activity. Gene set enrichment analysis of differentially expressed genes between UD-ICN1 and ICN1^{+} T-LLs revealed upregulation of *Klf9* along with other transcription factors highly expressed in proliferating pre-DP thymocytes. siRNA knockdown studies demonstrated that *Klf9* promoted proliferation of Notch-independent T-LLs. Collectively, these data suggest that *Klf9* may provide a novel therapeutic target for human T-LLs lacking *NOTCH1* mutations.

6. REFERENCES

1. Hoelzer D, Gokbuget N. T-cell lymphoblastic lymphoma and T-cell acute lymphoblastic leukemia: a separate entity? Clin Lymphoma Myeloma. 2009;9 Suppl 3:S214-221.

2. Pui CH, Campana D, Evans WE. Childhood acute lymphoblastic leukaemia--current status and future perspectives. Lancet Oncol. 2001;2:597-607.

3. Sallan SE. Myths and lessons from the adult/pediatric interface in acute lymphoblastic leukemia. Hematology Am Soc Hematol Educ Program. 2006:128-132.

4. Nguyen K, Devidas M, Cheng SC, et al. Factors influencing survival after relapse from acute lymphoblastic leukemia: a Children's Oncology Group study. Leukemia. 2008;22:2142-2150.

5. Rothenberg EV, Moore JE, Yui MA. Launching the T-cell-lineage developmental programme. Nat Rev Immunol. 2008;8:9-21.

6. Karlsson A, Ungerback J, Rasmussen A, French JE, Soderkvist P. Notch1 is a frequent mutational target in chemically induced lymphoma in mouse. Int J Cancer. 2008;123:2720-2724.

7. Kindler T, Cornejo MG, Scholl C, et al. K-RasG12D-induced T-cell lymphoblastic lymphoma/leukemias harbor Notch1 mutations and are sensitive to gamma-secretase inhibitors. Blood. 2008;112:3373-3382.

8. Lin YW, Nichols RA, Letterio JJ, Aplan PD. Notch1 mutations are important for leukemic transformation in murine models of precursor-T leukemia/lymphoma. Blood. 2006;107:2540-2543.

9. O'Neil J, Calvo J, McKenna K, et al. Activating Notch1 mutations in mouse models of T-ALL. Blood. 2006;107:781-785.

10. Weng AP, Ferrando AA, Lee W, et al. Activating mutations of NOTCH1 in human T cell acute lymphoblastic leukemia. Science. 2004;306:269-271.

11. Fehling HJ, Krotkova A, Saint-Ruf C, von Boehmer H. Crucial role of the pre-T-cell receptor alpha gene in development of alpha beta but not gamma delta T cells. Nature. 1995;375:795-798.

12. Guidos CJ. Synergy between the pre-T cell receptor and Notch: cementing the alphabeta lineage choice. J Exp Med. 2006;203:2233-2237.

13. Egerton M, Shortman K, Scollay R. The kinetics of immature murine thymocyte development in vivo. Int Immunol. 1990;2:501-507.

14. Surh CD, Sprent J. T-cell apoptosis detected in situ during positive and negative selection in the thymus. Nature. 1994;372:100-103.

15. Maillard I, Fang T, Pear WS. Regulation of lymphoid development, differentiation, and function by the Notch pathway. Annu Rev Immunol. 2005;23:945-974.

16. Morgan TH. The theory of the gene. The American Naturalist. 1917;51:513-544.

17. Kidd S, Kelley MR, Young MW. Sequence of the notch locus of Drosophila melanogaster: relationship of the encoded protein to mammalian clotting and growth factors. Mol Cell Biol. 1986;6:3094-3108.

18. Wharton KA, Johansen KM, Xu T, Artavanis-Tsakonas S. Nucleotide sequence from the neurogenic locus notch implies a gene product that shares homology with proteins containing EGF-like repeats. Cell. 1985;43:567-581.

19. Reynolds TC, Smith SD, Sklar J. Analysis of DNA surrounding the breakpoints of chromosomal translocations involving the beta T cell receptor gene in human lymphoblastic neoplasms. Cell. 1987;50:107-117.

20. del Amo FF, Gendron-Maguire M, Swiatek PJ, Jenkins NA, Copeland NG, Gridley T. Cloning, analysis, and chromosomal localization of Notch-1, a mouse homolog of Drosophila Notch. Genomics. 1993;15:259-264.

21. Ellisen LW, Bird J, West DC, et al. TAN-1, the human homolog of the Drosophila notch gene, is broken by chromosomal translocations in T lymphoblastic neoplasms. Cell. 1991;66:649-661.

22. Blaumueller CM, Qi H, Zagouras P, Artavanis-Tsakonas S. Intracellular cleavage of Notch leads to a heterodimeric receptor on the plasma membrane. Cell. 1997;90:281-291.

23. Logeat F, Bessia C, Brou C, et al. The Notch1 receptor is cleaved constitutively by a furin-like convertase. Proc Natl Acad Sci U S A. 1998;95:8108-8112.

24. Kopan R, Ilagan MX. The canonical Notch signaling pathway: unfolding the activation mechanism. Cell. 2009;137:216-233.

25. Lardelli M, Dahlstrand J, Lendahl U. The novel Notch homologue mouse Notch 3 lacks specific epidermal growth factor-repeats and is expressed in proliferating neuroepithelium. Mech Dev. 1994;46:123-136.

26. Lardelli M, Lendahl U. Motch A and motch B--two mouse Notch homologues coexpressed in a wide variety of tissues. Exp Cell Res. 1993;204:364-372.

27. Stifani S, Blaumueller CM, Redhead NJ, Hill RE, Artavanis-Tsakonas S. Human homologs of a Drosophila Enhancer of split gene product define a novel family of nuclear proteins. Nat Genet. 1992;2:119-127.

28. Uyttendaele H, Marazzi G, Wu G, Yan Q, Sassoon D, Kitajewski J. Notch4/int-3, a mammary proto-oncogene, is an endothelial cell-specific mammalian Notch gene. Development. 1996;122:2251-2259.

29. Fehon RG, Kooh PJ, Rebay I, et al. Molecular interactions between the protein products of the neurogenic loci Notch and Delta, two EGF-homologous genes in Drosophila. Cell. 1990;61:523-534.

30. Rebay I, Fleming RJ, Fehon RG, Cherbas L, Cherbas P, Artavanis-Tsakonas S. Specific EGF repeats of Notch mediate interactions with Delta and Serrate: implications for Notch as a multifunctional receptor. Cell. 1991;67:687-699.

31. de Celis JF, Bray S. Feed-back mechanisms affecting Notch activation at the dorsoventral boundary in the Drosophila wing. Development. 1997;124:3241-3251.

32. Cordle J, Redfieldz C, Stacey M, et al. Localization of the delta-like-1-binding site in human Notch-1 and its modulation by calcium affinity. J Biol Chem. 2008;283:11785-11793.

33. Aster JC, Simms WB, Zavala-Ruiz Z, Patriub V, North CL, Blacklow SC. The folding and structural integrity of the first LIN-12 module of human Notch1 are calcium-dependent. Biochemistry. 1999;38:4736-4742.

34. Vardar D, North CL, Sanchez-Irizarry C, Aster JC, Blacklow SC. Nuclear magnetic resonance structure of a prototype Lin12-Notch repeat module from human Notch1. Biochemistry. 2003;42:7061-7067.

35. Greenwald I, Seydoux G. Analysis of gain-of-function mutations of the lin-12 gene of Caenorhabditis elegans. Nature. 1990;346:197-199.

36. Rand MD, Grimm LM, Artavanis-Tsakonas S, et al. Calcium depletion dissociates and activates heterodimeric notch receptors. Mol Cell Biol. 2000;20:1825-1835.

37. Sanchez-Irizarry C, Carpenter AC, Weng AP, Pear WS, Aster JC, Blacklow SC. Notch subunit heterodimerization and prevention of ligand-independent proteolytic activation depend, respectively, on a novel domain and the LNR repeats. Mol Cell Biol. 2004;24:9265-9273.

38. Brou C, Logeat F, Gupta N, et al. A novel proteolytic cleavage involved in Notch signaling: the role of the disintegrin-metalloprotease TACE. Mol Cell. 2000;5:207-216.

39. Mumm JS, Schroeter EH, Saxena MT, et al. A ligand-induced extracellular cleavage regulates gamma-secretase-like proteolytic activation of Notch1. Mol Cell. 2000;5:197-206.

40. De Strooper B, Annaert W, Cupers P, et al. A presenilin-1-dependent gamma-secretase-like protease mediates release of Notch intracellular domain. Nature. 1999;398:518-522.

41. Nam Y, Weng AP, Aster JC, Blacklow SC. Structural requirements for assembly of the CSL.intracellular Notch1.Mastermind-like 1 transcriptional activation complex. J Biol Chem. 2003;278:21232-21239.

42. Tamura K, Taniguchi Y, Minoguchi S, et al. Physical interaction between a novel domain of the receptor Notch and the transcription factor RBP-J kappa/Su(H). Curr Biol. 1995;5:1416-1423.

43. Fryer CJ, White JB, Jones KA. Mastermind recruits CycC:CDK8 to phosphorylate the Notch ICD and coordinate activation with turnover. Mol Cell. 2004;16:509-520.

44. Rechsteiner M, Rogers SW. PEST sequences and regulation by proteolysis. Trends Biochem Sci. 1996;21:267-271.

45. Fleming RJ. Structural conservation of Notch receptors and ligands. Semin Cell Dev Biol. 1998;9:599-607.

46. Henderson ST, Gao D, Lambie EJ, Kimble J. lag-2 may encode a signaling ligand for the GLP-1 and LIN-12 receptors of C. elegans. Development. 1994;120:2913-2924.

47. Tax FE, Yeargers JJ, Thomas JH. Sequence of C. elegans lag-2 reveals a cell-signalling domain shared with Delta and Serrate of Drosophila. Nature. 1994;368:150-154.

48. Parks AL, Stout JR, Shepard SB, et al. Structure-function analysis of delta trafficking, receptor binding and signaling in Drosophila. Genetics. 2006;174:1947-1961.

49. Komatsu H, Chao MY, Larkins-Ford J, et al. OSM-11 facilitates LIN-12 Notch signaling during Caenorhabditis elegans vulval development. PLoS Biol. 2008;6:e196.

50. Pintar A, De Biasio A, Popovic M, Ivanova N, Pongor S. The intracellular region of Notch ligands: does the tail make the difference? Biol Direct. 2007;2:19.

51. Deblandre GA, Lai EC, Kintner C. Xenopus neuralized is a ubiquitin ligase that interacts with XDelta1 and regulates Notch signaling. Dev Cell. 2001;1:795-806.

52. Itoh M, Kim CH, Palardy G, et al. Mind bomb is a ubiquitin ligase that is essential for efficient activation of Notch signaling by Delta. Dev Cell. 2003;4:67-82.

53. Koo BK, Lim HS, Song R, et al. Mind bomb 1 is essential for generating functional Notch ligands to activate Notch. Development. 2005;132:3459-3470.

54. Koo BK, Yoon KJ, Yoo KW, et al. Mind bomb-2 is an E3 ligase for Notch ligand. J Biol Chem. 2005;280:22335-22342.

55. Lai EC, Deblandre GA, Kintner C, Rubin GM. Drosophila neuralized is a ubiquitin ligase that promotes the internalization and degradation of delta. Dev Cell. 2001;1:783-794.

56. Yeh E, Dermer M, Commisso C, Zhou L, McGlade CJ, Boulianne GL. Neuralized functions as an E3 ubiquitin ligase during Drosophila development. Curr Biol. 2001;11:1675-1679.

57. Barsi JC, Rajendra R, Wu JI, Artzt K. Mind bomb1 is a ubiquitin ligase essential for mouse embryonic development and Notch signaling. Mech Dev. 2005;122:1106-1117.

58. Koo BK, Yoon MJ, Yoon KJ, et al. An obligatory role of mind bomb-1 in notch signaling of mammalian development. PLoS One. 2007;2:e1221.

59. Kovall RA, Hendrickson WA. Crystal structure of the nuclear effector of Notch signaling, CSL, bound to DNA. Embo J. 2004;23:3441-3451.

60. Tun T, Hamaguchi Y, Matsunami N, Furukawa T, Honjo T, Kawaichi M. Recognition sequence of a highly conserved DNA binding protein RBP-J kappa. Nucleic Acids Res. 1994;22:965-971.

61. Friedmann DR, Kovall RA. Thermodynamic and structural insights into CSL-DNA complexes. Protein Sci. 2010;19:34-46.

62. Wilson JJ, Kovall RA. Crystal structure of the CSL-Notch-Mastermind ternary complex bound to DNA. Cell. 2006;124:985-996.

63. Okajima T, Irvine KD. Regulation of notch signaling by o-linked fucose. Cell. 2002;111:893-904.

64. Shi S, Stanley P. Protein O-fucosyltransferase 1 is an essential component of Notch signaling pathways. Proc Natl Acad Sci U S A. 2003;100:5234-5239.

65. Harris RJ, Spellman MW. O-linked fucose and other post-translational modifications unique to EGF modules. Glycobiology. 1993;3:219-224.

66. Shao L, Moloney DJ, Haltiwanger R. Fringe modifies O-fucose on mouse Notch1 at epidermal growth factor-like repeats within the ligand-binding site and the Abruptex region. J Biol Chem. 2003;278:7775-7782.

67. Ge C, Stanley P. The O-fucose glycan in the ligand-binding domain of Notch1 regulates embryogenesis and T cell development. Proc Natl Acad Sci U S A. 2008;105:1539-1544.

68. Bruckner K, Perez L, Clausen H, Cohen S. Glycosyltransferase activity of Fringe modulates Notch-Delta interactions. Nature. 2000;406:411-415.

69. Moloney DJ, Panin VM, Johnston SH, et al. Fringe is a glycosyltransferase that modifies Notch. Nature. 2000;406:369-375.

70. Panin VM, Papayannopoulos V, Wilson R, Irvine KD. Fringe modulates Notch-ligand interactions. Nature. 1997;387:908-912.

71. Xu A, Haines N, Dlugosz M, et al. In vitro reconstitution of the modulation of Drosophila Notch-ligand binding by Fringe. J Biol Chem. 2007;282:35153-35162.

72. Visan I, Yuan JS, Tan JB, Cretegny K, Guidos CJ. Regulation of intrathymic T-cell development by Lunatic Fringe- Notch1 interactions. Immunol Rev. 2006;209:76-94.

73. Hicks C, Johnston SH, diSibio G, Collazo A, Vogt TF, Weinmaster G. Fringe differentially modulates Jagged1 and Delta1 signalling through Notch1 and Notch2. Nat Cell Biol. 2000;2:515-520.

74. Kopan R, Schroeter EH, Weintraub H, Nye JS. Signal transduction by activated mNotch: importance of proteolytic processing and its regulation by the extracellular domain. Proc Natl Acad Sci U S A. 1996;93:1683-1688.

75. Gordon WR, Roy M, Vardar-Ulu D, et al. Structure of the Notch1-negative regulatory region: implications for normal activation and pathogenic signaling in T-ALL. Blood. 2009;113:4381-4390.

76. Gordon WR, Vardar-Ulu D, Histen G, Sanchez-Irizarry C, Aster JC, Blacklow SC. Structural basis for autoinhibition of Notch. Nat Struct Mol Biol. 2007;14:295-300.

77. Nichols JT, Miyamoto A, Olsen SL, D'Souza B, Yao C, Weinmaster G. DSL ligand endocytosis physically dissociates Notch1 heterodimers before activating proteolysis can occur. J Cell Biol. 2007;176:445-458.

78. Kidd S, Lieber T. Furin cleavage is not a requirement for Drosophila Notch function. Mech Dev. 2002;115:41-51.

79. Bozkulak EC, Weinmaster G. Selective use of ADAM10 and ADAM17 in activation of Notch1 signaling. Mol Cell Biol. 2009;29:5679-5695.

80. van Tetering G, van Diest P, Verlaan I, van der Wall E, Kopan R, Vooijs M. Metalloprotease ADAM10 is required for Notch1 site 2 cleavage. J Biol Chem. 2009;284:31018-31027.

81. Hartmann D, de Strooper B, Serneels L, et al. The disintegrin/metalloprotease ADAM 10 is essential for Notch signalling but not for alpha-secretase activity in fibroblasts. Hum Mol Genet. 2002;11:2615-2624.

82. Shah S, Lee SF, Tabuchi K, et al. Nicastrin functions as a gamma-secretase-substrate receptor. Cell. 2005;122:435-447.

83. Struhl G, Adachi A. Requirements for presenilin-dependent cleavage of notch and other transmembrane proteins. Mol Cell. 2000;6:625-636.

84. Fraering PC, Ye W, Strub JM, et al. Purification and characterization of the human gamma-secretase complex. Biochemistry. 2004;43:9774-9789.

85. Struhl G, Greenwald I. Presenilin is required for activity and nuclear access of Notch in Drosophila. Nature. 1999;398:522-525.

86. Wolfe MS, Xia W, Ostaszewski BL, Diehl TS, Kimberly WT, Selkoe DJ. Two transmembrane aspartates in presenilin-1 required for presenilin endoproteolysis and gamma-secretase activity. Nature. 1999;398:513-517.

87. Chandu D, Huppert SS, Kopan R. Analysis of transmembrane domain mutants is consistent with sequential cleavage of Notch by gamma-secretase. J Neurochem. 2006;96:228-235.

88. Okochi M, Steiner H, Fukumori A, et al. Presenilins mediate a dual intramembranous gamma-secretase cleavage of Notch-1. Embo J. 2002;21:5408-5416.

89. Kovall RA. Structures of CSL, Notch and Mastermind proteins: piecing together an active transcription complex. Curr Opin Struct Biol. 2007;17:117-127.

90. Kovall RA, Blacklow SC. Mechanistic insights into Notch receptor signaling from structural and biochemical studies. Curr Top Dev Biol. 2010;92:31-71.

91. Dou S, Zeng X, Cortes P, et al. The recombination signal sequence-binding protein RBP-2N functions as a transcriptional repressor. Mol Cell Biol. 1994;14:3310-3319.

92. Hsieh JJ, Hayward SD. Masking of the CBF1/RBPJ kappa transcriptional repression domain by Epstein-Barr virus EBNA2. Science. 1995;268:560-563.

93. Hsieh JJ, Henkel T, Salmon P, Robey E, Peterson MG, Hayward SD. Truncated mammalian Notch1 activates CBF1/RBPJk-repressed genes by a mechanism resembling that of Epstein-Barr virus EBNA2. Mol Cell Biol. 1996;16:952-959.

94. Brou C, Logeat F, Lecourtois M, et al. Inhibition of the DNA-binding activity of Drosophila suppressor of hairless and of its human homolog, KBF2/RBP-J kappa, by direct protein-protein interaction with Drosophila hairless. Genes Dev. 1994;8:2491-2503.

95. Kuroda K, Han H, Tani S, et al. Regulation of marginal zone B cell development by MINT, a suppressor of Notch/RBP-J signaling pathway. Immunity. 2003;18:301-312.

96. Schweisguth F, Posakony JW. Antagonistic activities of Suppressor of Hairless and Hairless control alternative cell fates in the Drosophila adult epidermis. Development. 1994;120:1433-1441.

97. Barolo S, Stone T, Bang AG, Posakony JW. Default repression and Notch signaling: Hairless acts as an adaptor to recruit the corepressors Groucho and dCtBP to Suppressor of Hairless. Genes Dev. 2002;16:1964-1976.

98. Tsuji M, Shinkura R, Kuroda K, Yabe D, Honjo T. Msx2-interacting nuclear target protein (Mint) deficiency reveals negative regulation of early thymocyte differentiation by Notch/RBP-J signaling. Proc Natl Acad Sci U S A. 2007;104:1610-1615.

99. Del Bianco C, Aster JC, Blacklow SC. Mutational and energetic studies of Notch 1 transcription complexes. J Mol Biol. 2008;376:131-140.

100. Friedmann DR, Wilson JJ, Kovall RA. RAM-induced allostery facilitates assembly of a notch pathway active transcription complex. J Biol Chem. 2008;283:14781-14791.

101. Petcherski AG, Kimble J. LAG-3 is a putative transcriptional activator in the C. elegans Notch pathway. Nature. 2000;405:364-368.

102. Wu L, Aster JC, Blacklow SC, Lake R, Artavanis-Tsakonas S, Griffin JD. MAML1, a human homologue of Drosophila mastermind, is a transcriptional co-activator for NOTCH receptors. Nat Genet. 2000;26:484-489.

103. Nam Y, Sliz P, Song L, Aster JC, Blacklow SC. Structural basis for cooperativity in recruitment of MAML coactivators to Notch transcription complexes. Cell. 2006;124:973-983.

104. Amsen D, Antov A, Jankovic D, et al. Direct regulation of Gata3 expression determines the T helper differentiation potential of Notch. Immunity. 2007;27:89-99.

105. Fang TC, Yashiro-Ohtani Y, Del Bianco C, Knoblock DM, Blacklow SC, Pear WS. Notch directly regulates Gata3 expression during T helper 2 cell differentiation. Immunity. 2007;27:100-110.

106. Jarriault S, Brou C, Logeat F, Schroeter EH, Kopan R, Israel A. Signalling downstream of activated mammalian Notch. Nature. 1995;377:355-358.

107. Krebs LT, Deftos ML, Bevan MJ, Gridley T. The Nrarp gene encodes an ankyrin-repeat protein that is transcriptionally regulated by the notch signaling pathway. Dev Biol. 2001;238:110-119.

108. Palomero T, Lim WK, Odom DT, et al. NOTCH1 directly regulates c-MYC and activates a feed-forward-loop transcriptional network promoting leukemic cell growth. Proc Natl Acad Sci U S A. 2006;103:18261-18266.

109. Sharma VM, Calvo JA, Draheim KM, et al. Notch1 contributes to mouse T-cell leukemia by directly inducing the expression of c-myc. Mol Cell Biol. 2006;26:8022-8031.

110. Weng AP, Millholland JM, Yashiro-Ohtani Y, et al. c-Myc is an important direct target of Notch1 in T-cell acute lymphoblastic leukemia/lymphoma. Genes Dev. 2006;20:2096-2109.

111. Palomero T, Sulis ML, Cortina M, et al. Mutational loss of PTEN induces resistance to NOTCH1 inhibition in T-cell leukemia. Nat Med. 2007;13:1203-1210.

112. Whelan JT, Forbes SL, Bertrand FE. CBF-1 (RBP-J kappa) binds to the PTEN promoter and regulates PTEN gene expression. Cell Cycle. 2007;6:80-84.

113. Chiang MY, Xu ML, Histen G, et al. Identification of a conserved negative regulatory sequence that influences the leukemogenic activity of NOTCH1. Mol Cell Biol. 2006;26:6261-6271.

114. Rothenberg EV. T cell lineage commitment: identity and renunciation. J Immunol. 2011;186:6649-6655.

115. Radtke F, Wilson A, Stark G, et al. Deficient T cell fate specification in mice with an induced inactivation of Notch1. Immunity. 1999;10:547-558.

116. Han H, Tanigaki K, Yamamoto N, et al. Inducible gene knockout of transcription factor recombination signal binding protein-J reveals its essential role in T versus B lineage decision. Int Immunol. 2002;14:637-645.

117. Heinzel K, Benz C, Martins VC, Haidl ID, Bleul CC. Bone marrow-derived hemopoietic precursors commit to the T cell lineage only after arrival in the thymic microenvironment. J Immunol. 2007;178:858-868.

118. Masuda K, Kakugawa K, Nakayama T, Minato N, Katsura Y, Kawamoto H. T cell lineage determination precedes the initiation of TCR beta gene rearrangement. J Immunol. 2007;179:3699-3706.

119. Yui MA, Feng N, Rothenberg EV. Fine-scale staging of T cell lineage commitment in adult mouse thymus. J Immunol. 2010;185:284-293.

120. Mandel EM, Grosschedl R. Transcription control of early B cell differentiation. Curr Opin Immunol. 2010;22:161-167.

121. Taghon TN, David ES, Zuniga-Pflucker JC, Rothenberg EV. Delayed, asynchronous, and reversible T-lineage specification induced by Notch/Delta signaling. Genes Dev. 2005;19:965-978.

122. Weber BN, Chi AW, Chavez A, et al. A critical role for TCF-1 in T-lineage specification and differentiation. Nature. 2011;476:63-68.

123. Hozumi K, Negishi N, Tsuchiya I, et al. Notch signaling is necessary for GATA3 function in the initiation of T cell development. Eur J Immunol. 2008;38:977-985.

124. Rosenbauer F, Owens BM, Yu L, et al. Lymphoid cell growth and transformation are suppressed by a key regulatory element of the gene encoding PU.1. Nat Genet. 2006;38:27-37.

125. Taghon T, Yui MA, Rothenberg EV. Mast cell lineage diversion of T lineage precursors by the essential T cell transcription factor GATA-3. Nat Immunol. 2007;8:845-855.

126. Carotta S, Dakic A, D'Amico A, et al. The transcription factor PU.1 controls dendritic cell development and Flt3 cytokine receptor expression in a dose-dependent manner. Immunity. 2010;32:628-641.

127. Laiosa CV, Stadtfeld M, Graf T. Determinants of lymphoid-myeloid lineage diversification. Annu Rev Immunol. 2006;24:705-738.

128. Huang G, Zhang P, Hirai H, et al. PU.1 is a major downstream target of AML1 (RUNX1) in adult mouse hematopoiesis. Nat Genet. 2008;40:51-60.

129. Spooner CJ, Cheng JX, Pujadas E, Laslo P, Singh H. A recurrent network involving the transcription factors PU.1 and Gfi1 orchestrates innate and adaptive immune cell fates. Immunity. 2009;31:576-586.

130. Georgescu C, Longabaugh WJ, Scripture-Adams DD, et al. A gene regulatory network armature for T lymphocyte specification. Proc Natl Acad Sci U S A. 2008;105:20100-20105.

131. Sakata-Yanagimoto M, Nakagami-Yamaguchi E, Saito T, et al. Coordinated regulation of transcription factors through Notch2 is an important mediator of mast cell fate. Proc Natl Acad Sci U S A. 2008;105:7839-7844.

132. Ikawa T, Hirose S, Masuda K, et al. An essential developmental checkpoint for production of the T cell lineage. Science. 2010;329:93-96.

133. Li L, Leid M, Rothenberg EV. An early T cell lineage commitment checkpoint dependent on the transcription factor Bcl11b. Science. 2010;329:89-93.

134. Li P, Burke S, Wang J, et al. Reprogramming of T cells to natural killer-like cells upon Bcl11b deletion. Science. 2010;329:85-89.

135. Balciunaite G, Ceredig R, Fehling HJ, Zuniga-Pflucker JC, Rolink AG. The role of Notch and IL-7 signaling in early thymocyte proliferation and differentiation. Eur J Immunol. 2005;35:1292-1300.

136. Maraskovsky E, O'Reilly LA, Teepe M, Corcoran LM, Peschon JJ, Strasser A. Bcl-2 can rescue T lymphocyte development in interleukin-7 receptor-deficient mice but not in mutant rag-1-/- mice. Cell. 1997;89:1011-1019.

137. Munitic I, Williams JA, Yang Y, et al. Dynamic regulation of IL-7 receptor expression is required for normal thymopoiesis. Blood. 2004;104:4165-4172.

138. Sudo T, Nishikawa S, Ohno N, et al. Expression and function of the interleukin 7 receptor in murine lymphocytes. Proc Natl Acad Sci U S A. 1993;90:9125-9129.

139. Van De Wiele CJ, Marino JH, Murray BW, Vo SS, Whetsell ME, Teague TK. Thymocytes between the beta-selection and positive selection checkpoints are nonresponsive to IL-7 as assessed by STAT-5 phosphorylation. J Immunol. 2004;172:4235-4244.

140. Yu Q, Park JH, Doan LL, Erman B, Feigenbaum L, Singer A. Cytokine signal transduction is suppressed in preselection double-positive thymocytes and restored by positive selection. J Exp Med. 2006;203:165-175.

141. Miyazaki T, Kawahara A, Fujii H, et al. Functional activation of Jak1 and Jak3 by selective association with IL-2 receptor subunits. Science. 1994;266:1045-1047.

142. Russell SM, Johnston JA, Noguchi M, et al. Interaction of IL-2R beta and gamma c chains with Jak1 and Jak3: implications for XSCID and XCID. Science. 1994;266:1042-1045.

143. Foxwell BM, Beadling C, Guschin D, Kerr I, Cantrell D. Interleukin-7 can induce the activation of Jak 1, Jak 3 and STAT 5 proteins in murine T cells. Eur J Immunol. 1995;25:3041-3046.

144. Lin JX, Migone TS, Tsang M, et al. The role of shared receptor motifs and common Stat proteins in the generation of cytokine pleiotropy and redundancy by IL-2, IL-4, IL-7, IL-13, and IL-15. Immunity. 1995;2:331-339.

145. Venkitaraman AR, Cowling RJ. Interleukin-7 induces the association of phosphatidylinositol 3-kinase with the alpha chain of the interleukin-7 receptor. Eur J Immunol. 1994;24:2168-2174.

146. Sharfe N, Dadi HK, Roifman CM. JAK3 protein tyrosine kinase mediates interleukin-7-induced activation of phosphatidylinositol-3' kinase. Blood. 1995;86:2077-2085.

147. Leonard WJ. Cytokines and immunodeficiency diseases. Nat Rev Immunol. 2001;1:200-208.

148. Akashi K, Kondo M, von Freeden-Jeffry U, Murray R, Weissman IL. Bcl-2 rescues T lymphopoiesis in interleukin-7 receptor-deficient mice. Cell. 1997;89:1033-1041.

149. Peschon JJ, Morrissey PJ, Grabstein KH, et al. Early lymphocyte expansion is severely impaired in interleukin 7 receptor-deficient mice. J Exp Med. 1994;180:1955-1960.

150. Shortman K, Egerton M, Spangrude GJ, Scollay R. The generation and fate of thymocytes. Semin Immunol. 1990;2:3-12.

151. Capone M, Hockett RD, Jr., Zlotnik A. Kinetics of T cell receptor beta, gamma, and delta rearrangements during adult thymic development: T cell receptor rearrangements are present in CD44(+)CD25(+) Pro-T thymocytes. Proc Natl Acad Sci U S A. 1998;95:12522-12527.

152. Livak F, Tourigny M, Schatz DG, Petrie HT. Characterization of TCR gene rearrangements during adult murine T cell development. J Immunol. 1999;162:2575-2580.

153. Saint-Ruf C, Ungewiss K, Groettrup M, Bruno L, Fehling HJ, von Boehmer H. Analysis and expression of a cloned pre-T cell receptor gene. Science. 1994;266:1208-1212.

154. von Boehmer H, Fehling HJ. Structure and function of the pre-T cell receptor. Annu Rev Immunol. 1997;15:433-452.

155. Wolfer A, Bakker T, Wilson A, et al. Inactivation of Notch 1 in immature thymocytes does not perturb CD4 or CD8T cell development. Nat Immunol. 2001;2:235-241.

156. Tanigaki K, Tsuji M, Yamamoto N, et al. Regulation of alphabeta/gammadelta T cell lineage commitment and peripheral T cell responses by Notch/RBP-J signaling. Immunity. 2004;20:611-622.

157. Ciofani M, Schmitt TM, Ciofani A, et al. Obligatory role for cooperative signaling by pre-TCR and Notch during thymocyte differentiation. J Immunol. 2004;172:5230-5239.

158. Maillard I, Tu L, Sambandam A, et al. The requirement for Notch signaling at the beta-selection checkpoint in vivo is absolute and independent of the pre-T cell receptor. J Exp Med. 2006;203:2239-2245.

159. Ciofani M, Zuniga-Pflucker JC. Notch promotes survival of pre-T cells at the beta-selection checkpoint by regulating cellular metabolism. Nat Immunol. 2005;6:881-888.

160. Swerdlow SH, Campo E, Harris NL, et al. WHO Classification of Tumours of Haematopoietic and Lymphoid Tissues: IARC; 2008.

161. Kraszewska MD, Dawidowska M, Szczepanski T, Witt M. T-cell acute lymphoblastic leukaemia: recent molecular biology findings. Br J Haematol. 2012;156:303-315.

162. Schrappe M, Valsecchi MG, Bartram CR, et al. Late MRD response determines relapse risk overall and in subsets of childhood T-cell ALL: results of the AIEOP-BFM-ALL 2000 study. Blood. 2011;118:2077-2084.

163. Burkhardt B, Reiter A, Landmann E, et al. Poor outcome for children and adolescents with progressive disease or relapse of lymphoblastic lymphoma: a report from the berlin-frankfurt-muenster group. J Clin Oncol. 2009;27:3363-3369.

164. Fielding AK, Richards SM, Chopra R, et al. Outcome of 609 adults after relapse of acute lymphoblastic leukemia (ALL); an MRC UKALL12/ECOG 2993 study. Blood. 2007;109:944-950.

165. Zohren F, Souroullas GP, Luo M, et al. The transcription factor Lyl-1 regulates lymphoid specification and the maintenance of early T lineage progenitors. Nat Immunol. 2012;13:761-769.

166. Palii CG, Perez-Iratxeta C, Yao Z, et al. Differential genomic targeting of the transcription factor TAL1 in alternate haematopoietic lineages. Embo J. 2011;30:494-509.

167. Taghon T, Thys K, De Smedt M, et al. Homeobox gene expression profile in human hematopoietic multipotent stem cells and T-cell progenitors: implications for human T-cell development. Leukemia. 2003;17:1157-1163.

168. Chervinsky DS, Zhao XF, Lam DH, Ellsworth M, Gross KW, Aplan PD. Disordered T-cell development and T-cell malignancies in SCL LMO1 double-transgenic mice: parallels with E2A-deficient mice. Mol Cell Biol. 1999;19:5025-5035.

169. Herblot S, Steff AM, Hugo P, Aplan PD, Hoang T. SCL and LMO1 alter thymocyte differentiation: inhibition of E2A-HEB function and pre-T alpha chain expression. Nat Immunol. 2000;1:138-144.

170. O'Neil J, Shank J, Cusson N, Murre C, Kelliher M. TAL1/SCL induces leukemia by inhibiting the transcriptional activity of E47/HEB. Cancer Cell. 2004;5:587-596.

171. Braunstein M, Anderson MK. HEB in the spotlight: Transcriptional regulation of T-cell specification, commitment, and developmental plasticity. Clin Dev Immunol. 2012;2012:678705.

172. Su XY, Della-Valle V, Andre-Schmutz I, et al. HOX11L2/TLX3 is transcriptionally activated through T-cell regulatory elements downstream of BCL11B as a result of the t(5;14)(q35;q32). Blood. 2006;108:4198-4201.

173. Soulier J, Clappier E, Cayuela JM, et al. HOXA genes are included in genetic and biologic networks defining human acute T-cell leukemia (T-ALL). Blood. 2005;106:274-286.

174. Caudell D, Zhang Z, Chung YJ, Aplan PD. Expression of a CALM-AF10 fusion gene leads to Hoxa cluster overexpression and acute leukemia in transgenic mice. Cancer Res. 2007;67:8022-8031.

175. Graux C, Cools J, Melotte C, et al. Fusion of NUP214 to ABL1 on amplified episomes in T-cell acute lymphoblastic leukemia. Nat Genet. 2004;36:1084-1089.

176. Ferrando AA, Neuberg DS, Staunton J, et al. Gene expression signatures define novel oncogenic pathways in T cell acute lymphoblastic leukemia. Cancer Cell. 2002;1:75-87.

177. Van Vlierberghe P, van Grotel M, Tchinda J, et al. The recurrent SET-NUP214 fusion as a new HOXA activation mechanism in pediatric T-cell acute lymphoblastic leukemia. Blood. 2008;111:4668-4680.

178. Cave H, Suciu S, Preudhomme C, et al. Clinical significance of HOX11L2 expression linked to t(5;14)(q35;q32), of HOX11 expression, and of SIL-TAL fusion in childhood T-cell malignancies: results of EORTC studies 58881 and 58951. Blood. 2004;103:442-450.

179. Ferrando AA, Neuberg DS, Dodge RK, et al. Prognostic importance of TLX1 (HOX11) oncogene expression in adults with T-cell acute lymphoblastic leukaemia. Lancet. 2004;363:535-536.

180. Kees UR, Heerema NA, Kumar R, et al. Expression of HOX11 in childhood T-lineage acute lymphoblastic leukaemia can occur in the absence of cytogenetic aberration at 10q24: a study from the Children's Cancer Group (CCG). Leukemia. 2003;17:887-893.

181. Schneider NR, Carroll AJ, Shuster JJ, et al. New recurring cytogenetic abnormalities and association of blast cell karyotypes with prognosis in childhood T-cell acute

lymphoblastic leukemia: a pediatric oncology group report of 343 cases. Blood. 2000;96:2543-2549.

182. van Grotel M, Meijerink JP, Beverloo HB, et al. The outcome of molecular-cytogenetic subgroups in pediatric T-cell acute lymphoblastic leukemia: a retrospective study of patients treated according to DCOG or COALL protocols. Haematologica. 2006;91:1212-1221.

183. Ferrando AA, Armstrong SA, Neuberg DS, et al. Gene expression signatures in MLL-rearranged T-lineage and B-precursor acute leukemias: dominance of HOX dysregulation. Blood. 2003;102:262-268.

184. Okada Y, Feng Q, Lin Y, et al. hDOT1L links histone methylation to leukemogenesis. Cell. 2005;121:167-178.

185. Okada Y, Jiang Q, Lemieux M, Jeannotte L, Su L, Zhang Y. Leukaemic transformation by CALM-AF10 involves upregulation of Hoxa5 by hDOT1L. Nat Cell Biol. 2006;8:1017-1024.

186. Daigle SR, Olhava EJ, Therkelsen CA, et al. Selective killing of mixed lineage leukemia cells by a potent small-molecule DOT1L inhibitor. Cancer Cell. 2011;20:53-65.

187. Coustan-Smith E, Mullighan CG, Onciu M, et al. Early T-cell precursor leukaemia: a subtype of very high-risk acute lymphoblastic leukaemia. Lancet Oncol. 2009;10:147-156.

188. Inukai T, Kiyokawa N, Campana D, et al. Clinical significance of early T-cell precursor acute lymphoblastic leukaemia: results of the Tokyo Children's Cancer Study Group Study L99-15. Br J Haematol. 2012;156:358-365.

189. Ma M, Wang X, Tang J, et al. Early T-cell precursor leukemia: a subtype of high risk childhood acute lymphoblastic leukemia. Front Med. 2012;6:416-420.

190. Neumann M, Heesch S, Gokbuget N, et al. Clinical and molecular characterization of early T-cell precursor leukemia: a high-risk subgroup in adult T-ALL with a high frequency of FLT3 mutations. Blood Cancer J. 2012;2:e55.

191. Zhang J, Ding L, Holmfeldt L, et al. The genetic basis of early T-cell precursor acute lymphoblastic leukaemia. Nature. 2012;481:157-163.

192. Bertin R, Acquaviva C, Mirebeau D, Guidal-Giroux C, Vilmer E, Cave H. CDKN2A, CDKN2B, and MTAP gene dosage permits precise characterization of mono- and bi-allelic 9p21 deletions in childhood acute lymphoblastic leukemia. Genes Chromosomes Cancer. 2003;37:44-57.

193. Hebert J, Cayuela JM, Berkeley J, Sigaux F. Candidate tumor-suppressor genes MTS1 (p16INK4A) and MTS2 (p15INK4B) display frequent homozygous deletions in

primary cells from T- but not from B-cell lineage acute lymphoblastic leukemias. Blood. 1994;84:4038-4044.

194. Herman JG, Jen J, Merlo A, Baylin SB. Hypermethylation-associated inactivation indicates a tumor suppressor role for p15INK4B. Cancer Res. 1996;56:722-727.

195. Merlo A, Herman JG, Mao L, et al. 5' CpG island methylation is associated with transcriptional silencing of the tumour suppressor p16/CDKN2/MTS1 in human cancers. Nat Med. 1995;1:686-692.

196. Flex E, Petrangeli V, Stella L, et al. Somatically acquired JAK1 mutations in adult acute lymphoblastic leukemia. J Exp Med. 2008;205:751-758.

197. Gutierrez A, Sanda T, Grebliunaite R, et al. High frequency of PTEN, PI3K, and AKT abnormalities in T-cell acute lymphoblastic leukemia. Blood. 2009;114:647-650.

198. Shochat C, Tal N, Bandapalli OR, et al. Gain-of-function mutations in interleukin-7 receptor-alpha (IL7R) in childhood acute lymphoblastic leukemias. J Exp Med. 2011;208:901-908.

199. Zenatti PP, Ribeiro D, Li W, et al. Oncogenic IL7R gain-of-function mutations in childhood T-cell acute lymphoblastic leukemia. Nat Genet. 2011;43:932-939.

200. De Keersmaecker K, Real PJ, Gatta GD, et al. The TLX1 oncogene drives aneuploidy in T cell transformation. Nat Med. 2010;16:1321-1327.

201. Gutierrez A, Kentsis A, Sanda T, et al. The BCL11B tumor suppressor is mutated across the major molecular subtypes of T-cell acute lymphoblastic leukemia. Blood. 2011;118:4169-4173.

202. O'Neil J, Grim J, Strack P, et al. FBW7 mutations in leukemic cells mediate NOTCH pathway activation and resistance to gamma-secretase inhibitors. J Exp Med. 2007;204:1813-1824.

203. Thompson BJ, Buonamici S, Sulis ML, et al. The SCFFBW7 ubiquitin ligase complex as a tumor suppressor in T cell leukemia. J Exp Med. 2007;204:1825-1835.

204. De Keersmaecker K, Marynen P, Cools J. Genetic insights in the pathogenesis of T-cell acute lymphoblastic leukemia. Haematologica. 2005;90:1116-1127.

205. Sherr CJ. The INK4a/ARF network in tumour suppression. Nat Rev Mol Cell Biol. 2001;2:731-737.

206. Okamoto A, Demetrick DJ, Spillare EA, et al. Mutations and altered expression of p16INK4 in human cancer. Proc Natl Acad Sci U S A. 1994;91:11045-11049.

207. Fasseu M, Aplan PD, Chopin M, et al. p16INK4A tumor suppressor gene expression and CD3epsilon deficiency but not pre-TCR deficiency inhibit TAL1-linked T-lineage leukemogenesis. Blood. 2007;110:2610-2619.

208. Wakabayashi Y, Watanabe H, Inoue J, et al. Bcl11b is required for differentiation and survival of alphabeta T lymphocytes. Nat Immunol. 2003;4:533-539.

209. Wakabayashi Y, Inoue J, Takahashi Y, et al. Homozygous deletions and point mutations of the Rit1/Bcl11b gene in gamma-ray induced mouse thymic lymphomas. Biochem Biophys Res Commun. 2003;301:598-603.

210. Kamimura K, Ohi H, Kubota T, et al. Haploinsufficiency of Bcl11b for suppression of lymphomagenesis and thymocyte development. Biochem Biophys Res Commun. 2007;355:538-542.

211. Barata JT, Silva A, Brandao JG, Nadler LM, Cardoso AA, Boussiotis VA. Activation of PI3K is indispensable for interleukin 7-mediated viability, proliferation, glucose use, and growth of T cell acute lymphoblastic leukemia cells. J Exp Med. 2004;200:659-669.

212. Silva A, Laranjeira AB, Martins LR, et al. IL-7 contributes to the progression of human T-cell acute lymphoblastic leukemias. Cancer Res. 2011;71:4780-4789.

213. Bains T, Heinrich MC, Loriaux MM, et al. Newly described activating JAK3 mutations in T-cell acute lymphoblastic leukemia. Leukemia. 2012;26:2144-2146.

214. Pear WS, Aster JC, Scott ML, et al. Exclusive development of T cell neoplasms in mice transplanted with bone marrow expressing activated Notch alleles. J Exp Med. 1996;183:2283-2291.

215. Malecki MJ, Sanchez-Irizarry C, Mitchell JL, et al. Leukemia-associated mutations within the NOTCH1 heterodimerization domain fall into at least two distinct mechanistic classes. Mol Cell Biol. 2006;26:4642-4651.

216. Sulis ML, Williams O, Palomero T, et al. NOTCH1 extracellular juxtamembrane expansion mutations in T-ALL. Blood. 2008;112:733-740.

217. Gupta-Rossi N, Le Bail O, Gonen H, et al. Functional interaction between SEL-10, an F-box protein, and the nuclear form of activated Notch1 receptor. J Biol Chem. 2001;276:34371-34378.

218. Oberg C, Li J, Pauley A, Wolf E, Gurney M, Lendahl U. The Notch intracellular domain is ubiquitinated and negatively regulated by the mammalian Sel-10 homolog. J Biol Chem. 2001;276:35847-35853.

219. Wu G, Lyapina S, Das I, et al. SEL-10 is an inhibitor of notch signaling that targets notch for ubiquitin-mediated protein degradation. Mol Cell Biol. 2001;21:7403-7415.

220. Onoyama I, Tsunematsu R, Matsumoto A, et al. Conditional inactivation of Fbxw7 impairs cell-cycle exit during T cell differentiation and results in lymphomatogenesis. J Exp Med. 2007;204:2875-2888.

221. Chiang MY, Xu L, Shestova O, et al. Leukemia-associated NOTCH1 alleles are weak tumor initiators but accelerate K-ras-initiated leukemia. J Clin Invest. 2008;118:3181-3194.

222. Meijerink JP. Genetic rearrangements in relation to immunophenotype and outcome in T-cell acute lymphoblastic leukaemia. Best Pract Res Clin Haematol. 2010;23:307-318.

223. Reschly EJ, Spaulding C, Vilimas T, et al. Notch1 promotes survival of E2A-deficient T cell lymphomas through pre-T cell receptor-dependent and -independent mechanisms. Blood. 2006;107:4115-4121.

224. Dumortier A, Jeannet R, Kirstetter P, et al. Notch activation is an early and critical event during T-Cell leukemogenesis in Ikaros-deficient mice. Mol Cell Biol. 2006;26:209-220.

225. Girard L, Hanna Z, Beaulieu N, et al. Frequent provirus insertional mutagenesis of Notch1 in thymomas of MMTVD/myc transgenic mice suggests a collaboration of c-myc and Notch1 for oncogenesis. Genes Dev. 1996;10:1930-1944.

226. Girard L, Jolicoeur P. A full-length Notch1 allele is dispensable for transformation associated with a provirally activated truncated Notch1 allele in Moloney MuLV-infected MMTV(D)/myc transgenic mice. Oncogene. 1998;16:517-522.

227. Hoemann CD, Beaulieu N, Girard L, Rebai N, Jolicoeur P. Two distinct Notch1 mutant alleles are involved in the induction of T-cell leukemia in c-myc transgenic mice. Mol Cell Biol. 2000;20:3831-3842.

228. Shen H, Suzuki T, Munroe DJ, et al. Common sites of retroviral integration in mouse hematopoietic tumors identified by high-throughput, single nucleotide polymorphism-based mapping and bacterial artificial chromosome hybridization. J Virol. 2003;77:1584-1588.

229. Tsuji H, Ishii-Ohba H, Katsube T, et al. Involvement of illegitimate V(D)J recombination or microhomology-mediated nonhomologous end-joining in the formation of intragenic deletions of the Notch1 gene in mouse thymic lymphomas. Cancer Res. 2004;64:8882-8890.

230. Tsuji H, Ishii-Ohba H, Noda Y, Kubo E, Furuse T, Tatsumi K. Rag-dependent and Rag-independent mechanisms of Notch1 rearrangement in thymic lymphomas of Atm(-/-) and scid mice. Mutat Res. 2009;660:22-32.

231. Tsuji H, Ishii-Ohba H, Ukai H, Katsube T, Ogiu T. Radiation-induced deletions in the 5' end region of Notch1 lead to the formation of truncated proteins and are involved in the development of mouse thymic lymphomas. Carcinogenesis. 2003;24:1257-1268.

232. Ashworth TD, Pear WS, Chiang MY, et al. Deletion-based mechanisms of Notch1 activation in T-ALL: key roles for RAG recombinase and a conserved internal translational start site in Notch1. Blood. 2010;116:5455-5464.

233. Jeannet R, Mastio J, Macias-Garcia A, et al. Oncogenic activation of the Notch1 gene by deletion of its promoter in Ikaros-deficient T-ALL. Blood. 2010;116:5443-5454.

234. Georgopoulos K, Bigby M, Wang JH, et al. The Ikaros gene is required for the development of all lymphoid lineages. Cell. 1994;79:143-156.

235. Kim J, Sif S, Jones B, et al. Ikaros DNA-binding proteins direct formation of chromatin remodeling complexes in lymphocytes. Immunity. 1999;10:345-355.

236. Sridharan R, Smale ST. Predominant interaction of both Ikaros and Helios with the NuRD complex in immature thymocytes. J Biol Chem. 2007;282:30227-30238.

237. Haydu JE, De Keersmaecker K, Duff MK, et al. An activating intragenic deletion in NOTCH1 in human T-ALL. Blood. 2012;119:5211-5214.

238. Bray S, Bernard F. Notch targets and their regulation. Curr Top Dev Biol. 2010;92:253-275.

239. Gonzalez-Garcia S, Garcia-Peydro M, Martin-Gayo E, et al. CSL-MAML-dependent Notch1 signaling controls T lineage-specific IL-7R{alpha} gene expression in early human thymopoiesis and leukemia. J Exp Med. 2009;206:779-791.

240. Pear WS. Hooked on Hes: a T-ALL of addiction. Immunity. 2010;33:645-647.

241. Fischer A, Gessler M. Delta-Notch--and then? Protein interactions and proposed modes of repression by Hes and Hey bHLH factors. Nucleic Acids Res. 2007;35:4583-4596.

242. Felli MP, Maroder M, Mitsiadis TA, et al. Expression pattern of notch1, 2 and 3 and Jagged1 and 2 in lymphoid and stromal thymus components: distinct ligand-receptor interactions in intrathymic T cell development. Int Immunol. 1999;11:1017-1025.

243. Maillard I, Koch U, Dumortier A, et al. Canonical notch signaling is dispensable for the maintenance of adult hematopoietic stem cells. Cell Stem Cell. 2008;2:356-366.

244. Kawamata S, Du C, Li K, Lavau C. Overexpression of the Notch target genes Hes in vivo induces lymphoid and myeloid alterations. Oncogene. 2002;21:3855-3863.

245. Wendorff AA, Koch U, Wunderlich FT, et al. Hes1 is a critical but context-dependent mediator of canonical Notch signaling in lymphocyte development and transformation. Immunity. 2010;33:671-684.

246. Medyouf H, Gao X, Armstrong F, et al. Acute T-cell leukemias remain dependent on Notch signaling despite PTEN and INK4A/ARF loss. Blood. 2010;115:1175-1184.

247. Pallard C, Stegmann AP, van Kleffens T, Smart F, Venkitaraman A, Spits H. Distinct roles of the phosphatidylinositol 3-kinase and STAT5 pathways in IL-7-mediated development of human thymocyte precursors. Immunity. 1999;10:525-535.

248. Reya T, Morrison SJ, Clarke MF, Weissman IL. Stem cells, cancer, and cancer stem cells. Nature. 2001;414:105-111.

249. Pelengaris S, Khan M, Evan G. c-MYC: more than just a matter of life and death. Nat Rev Cancer. 2002;2:764-776.

250. Douglas NC, Jacobs H, Bothwell AL, Hayday AC. Defining the specific physiological requirements for c-Myc in T cell development. Nat Immunol. 2001;2:307-315.

251. Kox C, Zimmermann M, Stanulla M, et al. The favorable effect of activating NOTCH1 receptor mutations on long-term outcome in T-ALL patients treated on the ALL-BFM 2000 protocol can be separated from FBXW7 loss of function. Leukemia. 2010;24:2005-2013.

252. Asnafi V, Buzyn A, Le Noir S, et al. NOTCH1/FBXW7 mutation identifies a large subgroup with favorable outcome in adult T-cell acute lymphoblastic leukemia (T-ALL): a Group for Research on Adult Acute Lymphoblastic Leukemia (GRAALL) study. Blood. 2009;113:3918-3924.

253. Malyukova A, Dohda T, von der Lehr N, et al. The tumor suppressor gene hCDC4 is frequently mutated in human T-cell acute lymphoblastic leukemia with functional consequences for Notch signaling. Cancer Res. 2007;67:5611-5616.

254. Park MJ, Taki T, Oda M, et al. FBXW7 and NOTCH1 mutations in childhood T cell acute lymphoblastic leukaemia and T cell non-Hodgkin lymphoma. Br J Haematol. 2009;145:198-206.

255. Clappier E, Collette S, Grardel N, et al. NOTCH1 and FBXW7 mutations have a favorable impact on early response to treatment, but not on outcome, in children with T-cell acute lymphoblastic leukemia (T-ALL) treated on EORTC trials 58881 and 58951. Leukemia. 2010;24:2023-2031.

256. Larson Gedman A, Chen Q, Kugel Desmoulin S, et al. The impact of NOTCH1, FBW7 and PTEN mutations on prognosis and downstream signaling in pediatric T-cell

acute lymphoblastic leukemia: a report from the Children's Oncology Group. Leukemia. 2009;23:1417-1425.

257. Mansour MR, Sulis ML, Duke V, et al. Prognostic implications of NOTCH1 and FBXW7 mutations in adults with T-cell acute lymphoblastic leukemia treated on the MRC UKALLXII/ECOG E2993 protocol. J Clin Oncol. 2009;27:4352-4356.

258. Zhu YM, Zhao WL, Fu JF, et al. NOTCH1 mutations in T-cell acute lymphoblastic leukemia: prognostic significance and implication in multifactorial leukemogenesis. Clin Cancer Res. 2006;12:3043-3049.

259. Zuurbier L, Homminga I, Calvert V, et al. NOTCH1 and/or FBXW7 mutations predict for initial good prednisone response but not for improved outcome in pediatric T-cell acute lymphoblastic leukemia patients treated on DCOG or COALL protocols. Leukemia. 2010;24:2014-2022.

260. Buonamici S, Trimarchi T, Ruocco MG, et al. CCR7 signalling as an essential regulator of CNS infiltration in T-cell leukaemia. Nature. 2009;459:1000-1004.

261. Deangelo DJ, Stone RM, Silverman LB, et al. A phase I clinical trial of the notch inhibitor MK-0752 in patients with T-cell acute lymphoblastic leukemia/lymphoma (T-ALL) and other leukemias. ASCO Annual Meeting; 2006.

262. Fouladi M, Stewart CF, Olson J, et al. Phase I trial of MK-0752 in children with refractory CNS malignancies: a pediatric brain tumor consortium study. J Clin Oncol. 2011;29:3529-3534.

263. Krop I, Demuth T, Guthrie T, et al. Phase I pharmacologic and pharmacodynamic study of the gamma secretase (Notch) inhibitor MK-0752 in adult patients with advanced solid tumors. J Clin Oncol. 2012;30:2307-2313.

264. Barlow C, Hirotsune S, Paylor R, et al. Atm-deficient mice: a paradigm of ataxia telangiectasia. Cell. 1996;86:159-171.

265. Elson A, Wang Y, Daugherty CJ, et al. Pleiotropic defects in ataxia-telangiectasia protein-deficient mice. Proc Natl Acad Sci U S A. 1996;93:13084-13089.

266. Xu Y, Ashley T, Brainerd EE, Bronson RT, Meyn MS, Baltimore D. Targeted disruption of ATM leads to growth retardation, chromosomal fragmentation during meiosis, immune defects, and thymic lymphoma. Genes Dev. 1996;10:2411-2422.

267. Shiloh Y. ATM and related protein kinases: safeguarding genome integrity. Nat Rev Cancer. 2003;3:155-168.

268. Shiloh Y. Ataxia-telangiectasia, ATM and genomic stability: maintaining a delicate balance. Two international workshops on ataxia-telangiectasia, related disorders and the ATM protein. Biochim Biophys Acta. 1998;1378:R11-18.

269. Meyn MS. Ataxia-telangiectasia, cancer and the pathobiology of the ATM gene. Clin Genet. 1999;55:289-304.

270. Morrell D, Cromartie E, Swift M. Mortality and cancer incidence in 263 patients with ataxia-telangiectasia. J Natl Cancer Inst. 1986;77:89-92.

271. Matei IR, Gladdy RA, Nutter LM, Canty A, Guidos CJ, Danska JS. ATM deficiency disrupts Tcra locus integrity and the maturation of CD4+CD8+ thymocytes. Blood. 2007;109:1887-1896.

272. Allman D, Karnell FG, Punt JA, et al. Separation of Notch1 promoted lineage commitment and expansion/transformation in developing T cells. J Exp Med. 2001;194:99-106.

273. Tan JB, Visan I, Yuan JS, Guidos CJ. Requirement for Notch1 signals at sequential early stages of intrathymic T cell development. Nat Immunol. 2005;6:671-679.

274. Michie AM, Chan AC, Ciofani M, et al. Constitutive Notch signalling promotes CD4 CD8 thymocyte differentiation in the absence of the pre-TCR complex, by mimicking pre-TCR signals. Int Immunol. 2007;19:1421-1430.

275. Ziegler SE, Morella KK, Anderson D, et al. Reconstitution of a functional interleukin (IL)-7 receptor demonstrates that the IL-2 receptor gamma chain is required for IL-7 signal transduction. Eur J Immunol. 1995;25:399-404.

276. Laouar Y, Crispe IN, Flavell RA. Overexpression of IL-7R alpha provides a competitive advantage during early T-cell development. Blood. 2004;103:1985-1994.

277. Barata JT, Cardoso AA, Nadler LM, Boussiotis VA. Interleukin-7 promotes survival and cell cycle progression of T-cell acute lymphoblastic leukemia cells by down-regulating the cyclin-dependent kinase inhibitor p27(kip1). Blood. 2001;98:1524-1531.

278. Dibirdik I, Langlie MC, Ledbetter JA, et al. Engagement of interleukin-7 receptor stimulates tyrosine phosphorylation, phosphoinositide turnover, and clonal proliferation of human T-lineage acute lymphoblastic leukemia cells. Blood. 1991;78:564-570.

279. Touw I, Pouwels K, van Agthoven T, et al. Interleukin-7 is a growth factor of precursor B and T acute lymphoblastic leukemia. Blood. 1990;75:2097-2101.

280. Matei IR, Wong PPC, Montpellier B, et al. Critical role for Notch1-dependent interleukin-7 signaling during T-cell development and leukemogenesis. Toronto: The Hospital for Sick Children; 2012.

281. Strauss WM. Preparation of genomic DNA from mammalian tissue. Curr Protoc Mol Biol. 2001;Chapter 2:Unit2 2.

282. Kulinski J, Besack D, Oleykowski CA, Godwin AK, Yeung AT. CEL I enzymatic mutation detection assay. Biotechniques. 2000;29:44-46, 48.

283. Maser RS, Choudhury B, Campbell PJ, et al. Chromosomally unstable mouse tumours have genomic alterations similar to diverse human cancers. Nature. 2007;447:966-971.

284. Zha S, Bassing CH, Sanda T, et al. ATM-deficient thymic lymphoma is associated with aberrant tcrd rearrangement and gene amplification. J Exp Med. 2010;207:1369-1380.

285. De Keersmaecker K, Lahortiga I, Mentens N, et al. In vitro validation of gamma-secretase inhibitors alone or in combination with other anti-cancer drugs for the treatment of T-cell acute lymphoblastic leukemia. Haematologica. 2008;93:533-542.

286. Szczepanski T, van der Velden VH, van Dongen JJ. Flow-cytometric immunophenotyping of normal and malignant lymphocytes. Clin Chem Lab Med. 2006;44:775-796.

287. Taylor AM, Metcalfe JA, Thick J, Mak YF. Leukemia and lymphoma in ataxia telangiectasia. Blood. 1996;87:423-438.

288. Matei IR, Guidos CJ, Danska JS. ATM-dependent DNA damage surveillance in T-cell development and leukemogenesis: the DSB connection. Immunol Rev. 2006;209:142-158.

289. Vacchio MS, Olaru A, Livak F, Hodes RJ. ATM deficiency impairs thymocyte maturation because of defective resolution of T cell receptor alpha locus coding end breaks. Proc Natl Acad Sci U S A. 2007;104:6323-6328.

290. Derksen PW, Keehnen RM, Evers LM, van Oers MH, Spaargaren M, Pals ST. Cell surface proteoglycan syndecan-1 mediates hepatocyte growth factor binding and promotes Met signaling in multiple myeloma. Blood. 2002;99:1405-1410.

291. Stanley MJ, Liebersbach BF, Liu W, Anhalt DJ, Sanderson RD. Heparan sulfate-mediated cell aggregation. Syndecans-1 and -4 mediate intercellular adhesion following their transfection into human B lymphoid cells. J Biol Chem. 1995;270:5077-5083.

292. Borghesani PR, Alt FW, Bottaro A, et al. Abnormal development of Purkinje cells and lymphocytes in Atm mutant mice. Proc Natl Acad Sci U S A. 2000;97:3336-3341.

293. Tremblay M, Tremblay CS, Herblot S, et al. Modeling T-cell acute lymphoblastic leukemia induced by the SCL and LMO1 oncogenes. Genes Dev. 2010;24:1093-1105.

294. Tatarek J, Cullion K, Ashworth T, Gerstein R, Aster JC, Kelliher MA. Notch1 inhibition targets the leukemia-initiating cells in a Tal1/Lmo2 mouse model of T-ALL. Blood. 2011;118:1579-1590.

295. Gomez-del Arco P, Kashiwagi M, Jackson AF, et al. Alternative promoter usage at the Notch1 locus supports ligand-independent signaling in T cell development and leukemogenesis. Immunity. 2010;33:685-698.

296. Fearon ER, Vogelstein B. A genetic model for colorectal tumorigenesis. Cell. 1990;61:759-767.

297. Eguchi-Ishimae M, Eguchi M, Kempski H, Greaves M. NOTCH1 mutation can be an early, prenatal genetic event in T-ALL. Blood. 2008;111:376-378.

298. Rich BE, Campos-Torres J, Tepper RI, Moreadith RW, Leder P. Cutaneous lymphoproliferation and lymphomas in interleukin 7 transgenic mice. J Exp Med. 1993;177:305-316.

299. von Freeden-Jeffry U, Vieira P, Lucian LA, McNeil T, Burdach SE, Murray R. Lymphopenia in interleukin (IL)-7 gene-deleted mice identifies IL-7 as a nonredundant cytokine. J Exp Med. 1995;181:1519-1526.

300. Roifman CM, Zhang J, Chitayat D, Sharfe N. A partial deficiency of interleukin-7R alpha is sufficient to abrogate T-cell development and cause severe combined immunodeficiency. Blood. 2000;96:2803-2807.

301. Elenius K, Salmivirta M, Inki P, Mali M, Jalkanen M. Binding of human syndecan to extracellular matrix proteins. J Biol Chem. 1990;265:17837-17843.

302. Koda JE, Rapraeger A, Bernfield M. Heparan sulfate proteoglycans from mouse mammary epithelial cells. Cell surface proteoglycan as a receptor for interstitial collagens. J Biol Chem. 1985;260:8157-8162.

303. Saunders S, Bernfield M. Cell surface proteoglycan binds mouse mammary epithelial cells to fibronectin and behaves as a receptor for interstitial matrix. J Cell Biol. 1988;106:423-430.

304. Sanderson RD, Borset M. Syndecan-1 in B lymphoid malignancies. Ann Hematol. 2002;81:125-135.

305. Borghesi LA, Yamashita Y, Kincade PW. Heparan sulfate proteoglycans mediate interleukin-7-dependent B lymphopoiesis. Blood. 1999;93:140-148.

306. Chomczynski P, Sacchi N. Single-step method of RNA isolation by acid guanidinium thiocyanate-phenol-chloroform extraction. Anal Biochem. 1987;162:156-159.

307. Salamov AA, Nishikawa T, Swindells MB. Assessing protein coding region integrity in cDNA sequencing projects. Bioinformatics. 1998;14:384-390.

308. Chen J, Jette C, Kanki JP, Aster JC, Look AT, Griffin JD. NOTCH1-induced T-cell leukemia in transgenic zebrafish. Leukemia. 2007;21:462-471.

309. Schmitt TM, Zuniga-Pflucker JC. Induction of T cell development from hematopoietic progenitor cells by delta-like-1 in vitro. Immunity. 2002;17:749-756.

310. Lo K, Smale ST. Generality of a functional initiator consensus sequence. Gene. 1996;182:13-22.

311. Reithmeier RAF. Assemby of proteins into membranes. In: Vance DF, Vance J, eds. Biochemistry of lipids, lipoproteins and membranes (ed 2nd). Amsterdam: Elsevier Science Publishers B.V.; 1991:525-578.

312. Riballo E, Kuhne M, Rief N, et al. A pathway of double-strand break rejoining dependent upon ATM, Artemis, and proteins locating to gamma-H2AX foci. Mol Cell. 2004;16:715-724.

313. Huang CY, Sharma GG, Walker LM, Bassing CH, Pandita TK, Sleckman BP. Defects in coding joint formation in vivo in developing ATM-deficient B and T lymphocytes. J Exp Med. 2007;204:1371-1381.

314. Bishop AJ, Barlow C, Wynshaw-Boris AJ, Schiestl RH. Atm deficiency causes an increased frequency of intrachromosomal homologous recombination in mice. Cancer Res. 2000;60:395-399.

315. Roehl AC, Vogt J, Mussotter T, et al. Intrachromosomal mitotic nonallelic homologous recombination is the major molecular mechanism underlying type-2 NF1 deletions. Hum Mutat. 2010;31:1163-1173.

316. Suminaga R, Takeshima Y, Yasuda K, Shiga N, Nakamura H, Matsuo M. Non-homologous recombination between Alu and LINE-1 repeats caused a 430-kb deletion in the dystrophin gene: a novel source of genomic instability. J Hum Genet. 2000;45:331-336.

317. Vardiman JW, Thiele J, Arber DA, et al. The 2008 revision of the World Health Organization (WHO) classification of myeloid neoplasms and acute leukemia: rationale and important changes. Blood. 2009;114:937-951.

318. Uyttebroeck A, Vanhentenrijk V, Hagemeijer A, et al. Is there a difference in childhood T-cell acute lymphoblastic leukaemia and T-cell lymphoblastic lymphoma? Leuk Lymphoma. 2007;48:1745-1754.

319. Reizis B, Leder P. Direct induction of T lymphocyte-specific gene expression by the mammalian Notch signaling pathway. Genes Dev. 2002;16:295-300.

320. Moellering RE, Cornejo M, Davis TN, et al. Direct inhibition of the NOTCH transcription factor complex. Nature. 2009;462:182-188.

321. Wei P, Walls M, Qiu M, et al. Evaluation of selective gamma-secretase inhibitor PF-03084014 for its antitumor efficacy and gastrointestinal safety to guide optimal clinical trial design. Mol Cancer Ther. 2010;9:1618-1628.

322. Wu Y, Cain-Hom C, Choy L, et al. Therapeutic antibody targeting of individual Notch receptors. Nature. 2010;464:1052-1057.

323. Yuan JS, Kousis PC, Suliman S, Visan I, Guidos CJ. Functions of notch signaling in the immune system: consensus and controversies. Annu Rev Immunol. 2010;28:343-365.

324. Schroeter EH, Kisslinger JA, Kopan R. Notch-1 signalling requires ligand-induced proteolytic release of intracellular domain. Nature. 1998;393:382-386.

325. Aster JC, Blacklow SC, Pear WS. Notch signalling in T-cell lymphoblastic leukaemia/lymphoma and other haematological malignancies. J Pathol. 2011;223:262-273.

326. Marks DI, Paietta EM, Moorman AV, et al. T-cell acute lymphoblastic leukemia in adults: clinical features, immunophenotype, cytogenetics, and outcome from the large randomized prospective trial (UKALL XII/ECOG 2993). Blood. 2009;114:5136-5145.

327. Jenkinson S, Koo K, Mansour MR, et al. Impact of NOTCH1/FBXW7 mutations on outcome in pediatric T-cell acute lymphoblastic leukemia patients treated on the MRC UKALL 2003 trial. Leukemia. 2012.

328. Huang EY, Gallegos AM, Richards SM, Lehar SM, Bevan MJ. Surface expression of Notch1 on thymocytes: correlation with the double-negative to double-positive transition. J Immunol. 2003;171:2296-2304.

329. Petrie HT, Pearse M, Scollay R, Shortman K. Development of immature thymocytes: initiation of CD3, CD4, and CD8 acquisition parallels down-regulation of the interleukin 2 receptor alpha chain. Eur J Immunol. 1990;20:2813-2815.

330. Penit C, Vasseur F, Papiernik M. In vivo dynamics of CD4-8- thymocytes. Proliferation, renewal and differentiation of different cell subsets studied by DNA biosynthetic labeling and surface antigen detection. Eur J Immunol. 1988;18:1343-1350.

331. Yuan JS, Tan JB, Visan I, et al. Lunatic Fringe prolongs Delta/Notch-induced self-renewal of committed alphabeta T-cell progenitors. Blood. 2011;117:1184-1195.

332. Liyanage M, Weaver Z, Barlow C, et al. Abnormal rearrangement within the alpha/delta T-cell receptor locus in lymphomas from Atm-deficient mice. Blood. 2000;96:1940-1946.

333. Mitchell DL, DiMario JX. Bimodal, reciprocal regulation of fibroblast growth factor receptor 1 promoter activity by BTEB1/KLF9 during myogenesis. Mol Biol Cell. 2010;21:2780-2787.

334. Simmen FA, Xiao R, Velarde MC, et al. Dysregulation of intestinal crypt cell proliferation and villus cell migration in mice lacking Kruppel-like factor 9. Am J Physiol Gastrointest Liver Physiol. 2007;292:G1757-1769.

335. Simmen RC, Eason RR, McQuown JR, et al. Subfertility, uterine hypoplasia, and partial progesterone resistance in mice lacking the Kruppel-like factor 9/basic transcription element-binding protein-1 (Bteb1) gene. J Biol Chem. 2004;279:29286-29294.

336. Du P, Kibbe WA, Lin SM. lumi: a pipeline for processing Illumina microarray. Bioinformatics. 2008;24:1547-1548.

337. Gidskehaug L, Anderssen E, Flatberg A, Alsberg BK. A framework for significance analysis of gene expression data using dimension reduction methods. BMC Bioinformatics. 2007;8:346.

338. Smyth GK. Linear models and empirical bayes methods for assessing differential expression in microarray experiments. Stat Appl Genet Mol Biol. 2004;3:Article3.

339. Tabrizifard S, Olaru A, Plotkin J, Fallahi-Sichani M, Livak F, Petrie HT. Analysis of transcription factor expression during discrete stages of postnatal thymocyte differentiation. J Immunol. 2004;173:1094-1102.

340. Subramanian A, Tamayo P, Mootha VK, et al. Gene set enrichment analysis: a knowledge-based approach for interpreting genome-wide expression profiles. Proc Natl Acad Sci U S A. 2005;102:15545-15550.

341. Cline MS, Smoot M, Cerami E, et al. Integration of biological networks and gene expression data using Cytoscape. Nat Protoc. 2007;2:2366-2382.

342. Hasserjian RP, Aster JC, Davi F, Weinberg DS, Sklar J. Modulated expression of notch1 during thymocyte development. Blood. 1996;88:970-976.

343. Aslam A, Mittal S, Koch F, Andrau JC, Winkler GS. The Ccr4-NOT deadenylase subunits CNOT7 and CNOT8 have overlapping roles and modulate cell proliferation. Mol Biol Cell. 2009;20:3840-3850.

344. Bagley BN, Keane TM, Maklakova VI, et al. A dominantly acting murine allele of mcm4 causes chromosomal abnormalities and promotes tumorigenesis. PLoS Genet;8:e1003034.

345. Ji SQ, Yao L, Zhang XY, Li XS, Zhou LQ. Knockdown of the nucleosome binding protein 1 inhibits the growth and invasion of clear cell renal cell carcinoma cells in vitro and in vivo. J Exp Clin Cancer Res;31:22.

346. Yao NY, Johnson A, Bowman GD, Kuriyan J, O'Donnell M. Mechanism of proliferating cell nuclear antigen clamp opening by replication factor C. J Biol Chem. 2006;281:17528-17539.

347. Yoshizawa-Sugata N, Masai H. Roles of human AND-1 in chromosome transactions in S phase. J Biol Chem. 2009;284:20718-20728.

348. Rodier G, Makris C, Coulombe P, et al. p107 inhibits G1 to S phase progression by down-regulating expression of the F-box protein Skp2. J Cell Biol. 2005;168:55-66.

349. Tenbaum SP, Papaioannou M, Reeb CA, et al. Alien inhibits E2F1 gene expression and cell proliferation. Biochim Biophys Acta. 2007;1773:1447-1454.

350. Ying M, Sang Y, Li Y, et al. KLF9, A Differentiation-Associated Transcription Factor, Suppresses Notch1 Signaling and Inhibits Glioblastoma-Initiating Stem Cells. Stem Cells. 2011;29:20-31.

351. Real PJ, Tosello V, Palomero T, et al. Gamma-secretase inhibitors reverse glucocorticoid resistance in T cell acute lymphoblastic leukemia. Nat Med. 2009;15:50-58.

352. Rowland BD, Bernards R, Peeper DS. The KLF4 tumour suppressor is a transcriptional repressor of p53 that acts as a context-dependent oncogene. Nat Cell Biol. 2005;7:1074-1082.

353. Schober SL, Kuo CT, Schluns KS, Lefrancois L, Leiden JM, Jameson SC. Expression of the transcription factor lung Kruppel-like factor is regulated by cytokines and correlates with survival of memory T cells in vitro and in vivo. J Immunol. 1999;163:3662-3667.

354. Shima N, Alcaraz A, Liachko I, et al. A viable allele of Mcm4 causes chromosome instability and mammary adenocarcinomas in mice. Nat Genet. 2007;39:93-98.

355. Simmons CD, Pabona JM, Heard ME, et al. Kruppel-like factor 9 loss-of-expression in human endometrial carcinoma links altered expression of growth-regulatory genes with aberrant proliferative response to estrogen. Biol Reprod;85:378-385.

356. Sporl F, Korge S, Jurchott K, et al. Kruppel-like factor 9 is a circadian transcription factor in human epidermis that controls proliferation of keratinocytes. Proc Natl Acad Sci U S A;109:10903-10908.

357. Imataka H, Sogawa K, Yasumoto K, et al. Two regulatory proteins that bind to the basic transcription element (BTE), a GC box sequence in the promoter region of the rat P-4501A1 gene. Embo J. 1992;11:3663-3671.

358. Roberts KG, Morin RD, Zhang J, et al. Genetic alterations activating kinase and cytokine receptor signaling in high-risk acute lymphoblastic leukemia. Cancer Cell;22:153-166.

359. Barata JT, Cardoso AA, Boussiotis VA. Interleukin-7 in T-cell acute lymphoblastic leukemia: an extrinsic factor supporting leukemogenesis? Leuk Lymphoma. 2005;46:483-495.

360. Cao Z, Sun X, Icli B, Wara AK, Feinberg MW. Role of Kruppel-like factors in leukocyte development, function, and disease. Blood. 2010;116:4404-4414.

361. McConnell BB, Yang VW. Mammalian Kruppel-like factors in health and diseases. Physiol Rev. 2010;90:1337-1381.

362. Greaves M. Cancer: The Evolutionary Legacy. London: Oxford University Press; 2000.

363. Greaves M, Maley CC. Clonal evolution in cancer. Nature. 2012;481:306-313.

364. Hanahan D, Weinberg RA. The hallmarks of cancer. Cell. 2000;100:57-70.

365. Hanahan D, Weinberg RA. Hallmarks of cancer: the next generation. Cell. 2011;144:646-674.

366. Greaves MF, Maia AT, Wiemels JL, Ford AM. Leukemia in twins: lessons in natural history. Blood. 2003;102:2321-2333.

367. Bateman CM, Colman SM, Chaplin T, et al. Acquisition of genome-wide copy number alterations in monozygotic twins with acute lymphoblastic leukemia. Blood. 2010;115:3553-3558.

368. Mullighan CG, Phillips LA, Su X, et al. Genomic analysis of the clonal origins of relapsed acute lymphoblastic leukemia. Science. 2008;322:1377-1380.

369. Clappier E, Gerby B, Sigaux F, et al. Clonal selection in xenografted human T cell acute lymphoblastic leukemia recapitulates gain of malignancy at relapse. J Exp Med. 2011;208:653-661.

370. Anderson K, Lutz C, van Delft FW, et al. Genetic variegation of clonal architecture and propagating cells in leukaemia. Nature. 2011;469:356-361.

371. Notta F, Mullighan CG, Wang JC, et al. Evolution of human BCR-ABL1 lymphoblastic leukaemia-initiating cells. Nature. 2011;469:362-367.

372. Ding L, Ley TJ, Larson DE, et al. Clonal evolution in relapsed acute myeloid leukaemia revealed by whole-genome sequencing. Nature. 2012;481:506-510.

373. Armstrong F, Brunet de la Grange P, Gerby B, et al. NOTCH is a key regulator of human T-cell acute leukemia initiating cell activity. Blood. 2009;113:1730-1740.

374. Chiu PP, Jiang H, Dick JE. Leukemia-initiating cells in human T-lymphoblastic leukemia exhibit glucocorticoid resistance. Blood. 2010;116:5268-5279.

375. Giambra V, Jenkins CR, Wang H, et al. NOTCH1 promotes T cell leukemia-initiating activity by RUNX-mediated regulation of PKC-theta and reactive oxygen species. Nat Med. 2012;18:1693-1698.

376. Teng YH, Aquino RS, Park PW. Molecular functions of syndecan-1 in disease. Matrix Biol. 2012;31:3-16.

377. Lendorf ME, Manon-Jensen T, Kronqvist P, Multhaupt HA, Couchman JR. Syndecan-1 and syndecan-4 are independent indicators in breast carcinoma. J Histochem Cytochem. 2011;59:615-629.

378. Kiviniemi J, Kallajoki M, Kujala I, et al. Altered expression of syndecan-1 in prostate cancer. Apmis. 2004;112:89-97.

379. Hashimoto Y, Skacel M, Adams JC. Association of loss of epithelial syndecan-1 with stage and local metastasis of colorectal adenocarcinomas: an immunohistochemical study of clinically annotated tumors. BMC Cancer. 2008;8:185.

380. Alexander CM, Reichsman F, Hinkes MT, et al. Syndecan-1 is required for Wnt-1-induced mammary tumorigenesis in mice. Nat Genet. 2000;25:329-332.

381. Seidel C, Borset M, Hjertner O, et al. High levels of soluble syndecan-1 in myeloma-derived bone marrow: modulation of hepatocyte growth factor activity. Blood. 2000;96:3139-3146.

382. Chari S, Winandy S. Ikaros regulates Notch target gene expression in developing thymocytes. J Immunol. 2008;181:6265-6274.

383. Good KL, Tangye SG. Decreased expression of Kruppel-like factors in memory B cells induces the rapid response typical of secondary antibody responses. Proc Natl Acad Sci U S A. 2007;104:13420-13425.

384. Guo W, Lasky JL, Chang CJ, et al. Multi-genetic events collaboratively contribute to Pten-null leukaemia stem-cell formation. Nature. 2008;453:529-533.

385. Guo Z, Dose M, Kovalovsky D, et al. Beta-catenin stabilization stalls the transition from double-positive to single-positive stage and predisposes thymocytes to malignant transformation. Blood. 2007;109:5463-5472.

386. Heffner LT, Jagannath S, Zimmerman TM, et al. BT062, an antibody-drug conjugate directed against CD138, given weekly for 3 weeks in each 4-week cycle: safety and further evidence of clinical activity. 54th ASH annual meeting and exposition. Atlanta, GA; 2012.

387. Kastner P, Chan S. Role of Ikaros in T-cell acute lymphoblastic leukemia. World J Biol Chem. 2011;2:108-114.

388. Kakinuma S, Nishimura M, Sasanuma S, et al. Spectrum of Znfn1a1 (Ikaros) inactivation and its association with loss of heterozygosity in radiogenic T-cell lymphomas in susceptible B6C3F1 mice. Radiat Res. 2002;157:331-340.